

Interactive comments on “Inter-technique validation of tropospheric slant total delays” by M. Kačmařík et al.

AUTHOR COMMENTS ON THE CHANGES IN THE MANUSCRIPT DUE TO A RESULTS MISTAKE FOUND IN THE PREVIOUS (REVIEWED) VERSION OF THE MANUSCRIPT

We found a bug in processing which influenced GNSS slant total delays from both TUO solutions (TUO_G and TUO_R) and one ROB (ROB_V) solution based on the VMF1 mapping function. We recomputed all the three affected GNSS STD solutions and consequently all the statistical comparisons presented in the paper. In the new version of the manuscript which also incorporates comments of both reviewers we provide corrected versions of figures (Figures 4, 7, 8, 10, 11, 12) and tables (Tables 4, 5, 7, 8) which were affected by the described mistake in three GNSS STD solutions. The changes are mainly visible in BIAS results in Table 4 and Figure 7, all other outputs were influenced only marginally. We also corrected manuscript text in section 7.1 (sections 7.1.3 and 7.1.4 in the new version of the manuscript) which discussed the previous wrong results of ROB_V and TUO_G/TUO_R solutions.

REVIEW NUMBER 1

In the last decade the assimilation of zenith total delays into numerical weather models became operational at many weather services. At the same time the focus of research shifted to the processing and utilization of slant total delays (STDs). The manuscript presented by Kačmařík et al. describes a comprehensive STD validation study which covers 7 different STD processing strategies and their validation with independent observations. The focus of the manuscript is on the identification of the optimal processing strategy and on the impact of post-fit residuals on the quality of STDs.

This is the most extensive and detailed study in this field which has been presented up to now and it provides a wealth of information. The results are in general well justified and of high significance for GNSS processing and for potential applications as well.

The manuscript is well written and organized. However, some points need clarification and additional information which is important for the reader to better understand different aspects of the validation study. This would require a minor revision.

General comments

Errors

The manuscript compares STD data from different sources: GNSS STDs processed in different ways, raytraced STDs from numerical weather models and STDs obtained from water vapor radiometers. As there is no reliable reference for STD observations, such comparisons provide the difference between two erroneous quantities but not the STD error, i.e. the error with respect to the truth.

At some points of the discussion the authors highlight this aspect but in some cases the standard deviation is regarded as the error of a certain STD product without proper justification. Especially when comparing GNSS STDs with and without residuals the increasing standard deviation due to the residuals is very often regarded as an increasing error. While this might be true in many cases it is not always justified by the analysis.

The manuscript might be improved if this issue is discussed in a paragraph somewhere at the beginning of the analysis and by addressing the corresponding specific comments.

We agree with your point of view. We haven't provided an extra paragraph in the beginning of the analysis but describe and discuss this topic in the beginning of section 8 and we also addressed all your specific comments in the manuscript.

Although the truth is not accessible in our as well as in similar studies, besides technique inter-comparisons, we have particularly focused on assessing variants without, with raw and cleaned residuals at the dual stations (section 8). In such case the assumption of similar residuals due to the tropospheric effects is expected at nearby located stations and slant delays should be thus zero, in theory.

Residuals

The application of residuals is presumably the most important topic in GNSS STD processing. The simple model used in equ. 1 is not sufficient to describe local atmospheric variations in case of severe weather events. Residuals could provide the directional information necessary to locate meteorological phenomena if the GNSS specific errors were below a certain threshold.

The residual term (RES) was added to Eq.1 and the text in Chapter 3 was adapted and re-ordered accordingly.

In the manuscript the application of residuals is discussed in detail but the analysis does not lead to a clear recommendation. Regarding the analysis presented in the manuscript the results are well justified.

However, the analysis is focused on two month mean values/standard deviations and presumably not the best way to analyze the impact of residuals. Most of the time atmospheric variations are rather smooth and can be described by equ. 1. Under such conditions residuals will probably add some noise to the solution and provide little extra information. In case of severe weather events rather large residuals would be necessary to complement equ. 1 and to locate e.g. convective cells. Under such conditions much larger errors of the residuals could be tolerated. This cannot be analyzed using two month means.

At some points in the manuscript it is mentioned that further studies are required to address this problem but the recommendations how to use residuals remain somewhat indefinite. The presented results could be understood much better if an assessment of the statistical analysis with respect to the application of residuals would be added.

Please, see a new version of section 8. We have identified days with high daily variations of cleaned post-fit residuals (corresponding to severe weather occurrences) and studied separately results for these days and days with low variation of post-fit residuals. Here we present Fig. 1 showing daily RMS of cleaned post-fit residuals at elevation angles of 10 and 30 ° at individual GNSS stations forming dual stations.

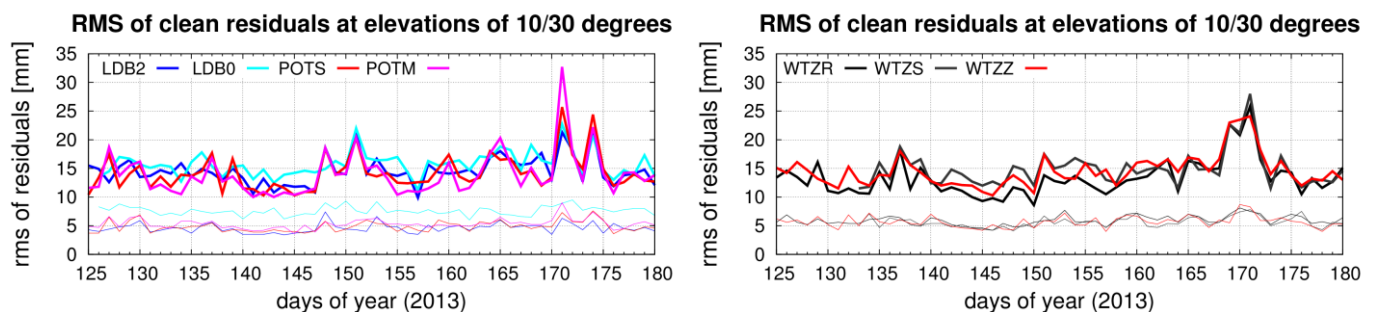


Fig. 1: RMS of clean post-fit residuals at elevation angles of 10 and 30 ° for individual days of benchmark at all GNSS stations forming dual stations

Statistics

The manuscript describes basically a statistical analysis. However, almost nothing is said about the statistical procedures used to analyze the data. At some points bias and standard deviation are used, median, median RMS, median values of biases and standard deviations, mean standard deviations, ... at others. To understand the results it is necessary to describe the statistical analysis and to explain why certain statistical methods are used for a specific analysis.

We changed Figure 9 and, currently, there are only following statistical parameters used: bias, standard deviation, median values of biases and standard deviations (made over all stations or solutions). The only exception is abstract where we state mean values. We have shortly broadened the explanation of using median values of biases and standard deviations in the Section 6.

Specific Comments

Abstract, line 18

Results show generally a very good mutual agreement among all solutions from all the techniques.

This sentence contradicts the results of the study in some way as the reader gets the impression that all solutions/techniques have almost the same high quality and it makes no difference which one is used. At the same time it would not be possible to answer the questions raised in the manuscript, i.e. which processing strategy leads to the best STD quality.

The sentence was modified – we wanted to sum up the results into a single sentence and actually we found a reasonable agreement among most of the solutions from all the techniques.

The abstract should focus more on the questions which will be answered in the manuscript and on the difficulties to come to a definite conclusion.

The last part of the abstract was significantly modified.

Page 3, equ. 1, 2

Equation 1 is essential for the discussion of residuals. Therefore it would be important to discuss the downsides of this approach. Equ. 1 is a rather simple model where all information on elevation is shifted to the mapping functions and variations with the azimuth are described by only two numbers (GN and GE). Equ. 2 describes a very smooth azimuthal variation which cannot represent the atmospheric state in case of severe weather events. Furthermore, the gradients are temporal means, usually over 1 h. In case of fast moving fronts or convective events the temporal mean can become rather misleading and can lead to an unrealistic azimuth distribution of the STDs.

Using this approach all information provided by GNSS observations is reduced to 3 numbers (ZWD, GN and GE, assuming that the Saastamoinen ZHD is used) and no directional information survives this process. If it turned out that this is the best way to model atmospheric variations the processing of STDs would be almost meaningless. It would be sufficient to provide these quantities and the user could compute any number of STDs in any direction.

For for the sake of completeness it should be defined how residuals are applied, i.e. equ. 1 + residual.

We have edited whole Section 3 including equation 1.

Page 11, section 4.4

The results presented in this section have presumably be obtained using a numerical weather model. This should be mentioned as the real situation might differ from the model state. Which model was used?

Text added in the manuscript (ALADIN-CZ NWM has been used to estimate the Hydrostatic, Wet and Hydrometeor contributions to slant delays.)

Page 13, line 6,7

... and corresponding delays in the zenith direction have been computed and mapped using mapping functions presented in Eq. 1 ...

Why do we need ZTDs to understand fig. 3? It seems that STDs are computed using the weather model and that the differences are mapped to zenith and shown in fig.3.

No new ZTDs have been computed. Only STDs have been mapped in the zenith to avoid the effect of the elevation and to look at the same order of magnitude of delays. Text modified in the manuscript.

Page 13, line 12-15

The sentence *Figure 3 confirms ...* sounds somewhat strange and should be rephrased.

Text modified in the manuscript

Page 14, line 18, 19

What is the *hydrostatic mapping function* derived from the NCEP-GFS?

We make use of GFS NCEP data to derive the hydrostatic MF. For details see below reference which we added into text.

Douša, J., Dick, G., Kačmařík, M., Brožková, R., Zus, F., Brenot, H., Stoycheva, A., Möller, G., and Kaplon, J.: Benchmark campaign and case study episode in central Europe for development and assessment of advanced GNSS tropospheric models and products, *Atmos. Meas. Tech.*, 9, 2989-3008, doi:10.5194/amt-9-2989-2016, 2016.

Page 14, line 19-22

SIWV to STD: Why are hydrostatic horizontal gradients required to convert SIWV to STD? Both observations have been taken in (almost) the same direction and the SHD in this direction should be sufficient. Li, 2015b, describes a way to estimate gradients from different SIWV observations for GNSS gradient validation. Has this also been done?

We approximate WVR STD by

$$STD = SIWV * PI + m_h * Z_h + m_g * (\cos(a) N_h + \sin(a) E_h)$$

m_h ... hydrostatic MF (from GFS NCEP, see the comment above)

Z_h ... zenith hydrostatic delay (using Saastamoinen and in-situ meteorological observations)

m_g ... gradient MF

N_h, E_h ... hydrostatic north and east gradient (from GFS NCEP, see the comment above)

Note that in general N_h & E_h are not zero. Conversely, we would approximate GPS SIWV by

$$SIWV = [STD - m_h * Z_h - m_g * (\cos(a) N_h + \sin(a) E_h)] / PI$$

To answer the second question: no, we did not compute gradients from WVR measurements.

Page 16 - 21, section 7.1

Section 7.1 is quite large and it would be very beneficial for the reader to divide it into some subsections, e.g. comparison with GFZ, comparison with/without residuals, differences of software parameters, differences depending on elevation.

The text in Section 7.1 was divided into four subsections 7.1.1 – 7.1.4.

Page 15, line 18, 19

Hence the smaller values for these settings, the smaller number of pairs found and the higher standard deviations resulted between GNSS and WVR STDs. Shouldn't it be ... **smaller** standard deviations ... ?

Yes, smaller is right, corrected in the manuscript.

Page 16, line 14

These were observed mainly as systematic errors ranging from -3.6 mm to 0.6 mm.

Fig. 4 shows differences between the GFZ solution and all other solutions. As long as the error of the GFZ solution is unknown it's not possible to attribute the differences as systematic errors.

Manuscript was modified, now the term bias is used.

Page 17, line 8, 9, discussion of pages 17 - 19

Both comparisons demonstrate systematic errors at a sub-millimetre level over all stations and solutions.

Adding residuals to the nonRES solution should lead to a somewhat different bias and a larger standard deviation, even in case of true, error free residuals. This is due to the spatial and temporal variability of the atmosphere and not necessarily an error. However, reading the discussion one gets the impression that smaller biases and standard deviations are better. This section could be improved by an evaluation of the information and potential errors provided by different solutions.

We agree and therefore modified the text of section 7.1.2 however didn't updated it to add more information in regard of the last sentence of the comment.

Page 19, line 18, 19

Surprisingly, the impact of the elevation angle cut-off (3 versus 7) resulted in a minimum mean standard deviation below 1 mm, see TUW-3 and TUW-7.

The impact of low elevation STDs below 7 depends considerably on the amount of data below 7. The small impact on bias and SDEV could be due to the small amount of data or due to the high quality of the data.

Yes, we agree with your statement. We want to add that although a cut-off elevation angle 3° was used for the TUW-3 solution, STDs from below 7° didn't enter the validation. Therefore, the difference between TUW-3 and TUW-7 solutions comes mainly from estimated horizontal gradients. We edited the manuscript in these regards.

Page 21, section 7.2

It would be very beneficial for the reader to start section 7.2 with a short summary of section 4.1 – 4.3. A short paragraph and a table giving the main parameters of the weather models and raytracers would be helpful.

We slightly modified text in the manuscript (beginning of section 4 and section 7.2). We don't want to repeat the information given in the beginning of section 4, therefore we refer the reader to go back to section 4 in the beginning of section 7 to refresh the information about NWM STD solutions.

Page 26, line 12, 13

... and it should be noted that the stability on a daily time scale was much better for GNSS STDs than for NWM ray-traced STDs.

This is presumably not a problem of the model stability but indicates that the model state deviates from the real atmospheric state for some time/region. This is the usual behavior of weather models which cannot be avoided even if STDs are assimilated.

We agree, the sentence was rewritten.

Page 30, line 2

Two sets of STDs from the same solution, but ... Which solution was used in this section?

Corrected, an explanation was given.

Page 34, line 7, 8

... that we are currently not able to remove completely all other effects due to the local troposphere.

Isn't that misleading? The ideal residual should describe the effect of the local troposphere while all GNSS specific errors should be removed.

Corrected, the sentence was rephrased.

Technical Corrections

Page 1, line 30

... part, caused by the atmospheric constituents, and the wet ... Shouldn't it be ... the **dry** atmospheric constituents ... ?

Corrected.

Page 10, line 14

$$R_d = 287.058 \text{ J}/(\text{kg K}) = 287.058 \text{ J kg}^{-1} \text{ K}^{-1}$$

Corrected.

Page 11, line 5

Contribution to hydrometeors: 17 mm to ZTD or STD?

In the zenith, corrected in the manuscript.

Page 11, fig. 1

Fig. 1 needs some improvement: It should be clearly indicated which subplot shows which quantity. The text and the color bars inside the subplots cannot be read.

Figure was modified.

Page 12, fig. 2

It's rather unusual to provide polar plots with a x and y axis. The angles (azimuth) and the radial axis (ΔSTD) should be given.

Figure was modified.

Page 16, line 8, 9

Figure 4: Comparison ... It seems that parts of the figure's caption have accidentally been copied.

Corrected

Page 16, line 15

It is particularly ... What does "It" mean?

The sentence relates to the previous one describing similarity of GFZ and GOP results.

Page 22, line 8, p. 25, l. 21, ...

side => site

No, the word side is correct. We wanted to say that the bias between POTM and POTS stations comes from GNSS data processing, not from NWM derived STDs.

Fig. 4, 6, 7, 9, 11

These plots show a large number of symbols/lines and could be improved by scaling the y axes according to the min/max values in the plots.

We adapted the y scales in figures 4, 7, 9, 11. We kept the scales in figures 5+6, 8, 10, 14 since we want to keep an identical y scale for all similar figures to make them consistently comparable with each other.

REVIEW NUMBER 2

This manuscript describes inter-comparisons of slant total delays (STDs) derived from GNSS solutions, numerical weather models (NWM), and radiometers (WVR). In comparisons between GNSS software, the authors found most of them show good agreements with each other. Moreover, they recommend no use of raw post-fit residuals whereas STDs without residuals and with cleaned residuals are better. As for NWM and WVR, the authors concluded they are not reliable due to their large errors. I roughly agree with their conclusions. However, since I have to point out some weaknesses in this manuscript, it should be published after major revisions.

Major comments 1) Residuals STD is decomposed with ZTD, gradients (G) and residuals. Since Equation 1 only represents the first two terms, the residual term should be added. Since the horizontal scales of ZTD, G, and residuals are 500, 50, and 5 km (Shoji et al. 2004), it is important to add residuals into STDs when convective activities are considered in any studies using STDs like this manuscript. From the view point of this, the authors have no chance to avoid residuals in processing STDs. In addition, residuals should be cleaned as pointed by Shoji et al. (2004). Therefore, I don't agree that "the usage of the information content from the post-fit residuals for the reconstruction of the STDs remains an open question" in this study (L5 P5). The authors should re-consider the effect of post-fit residuals in their formulation and re-organize this manuscript from the view point that they really need to investigate the effect of post-fit residuals in this study.

The residual term (RES) was added to Eq.1 and the text in Chapter 3 was adapted and re-ordered accordingly. Regarding the post-fit residuals investigation: please see following sections of the revised manuscript: 8, 9.

2) Comparison in the zenith direction. The authors compared STDs in the zenith direction using mapping functions. Since these functions were made statistically (excluding gradient on the day), I recommend the authors to use STDs only in high elevation angles (> 60 or 70 degree) for the comparisons. This is especially useful in comparison of GNSS vs WVR, because it is able to avoid errors of surface pressure gradient in calculating STDs from WVR.

For comparisons in the zenith direction we didn't use any real mapping function, we used only a simple $1/\sin(\text{ele})$ to normalize all the STDs. We didn't want to reconstruct original zenith parameters for each STD, but we wanted to compare all the variable STDs as a one unit. Mapping slant observations to the zenith direction is a standard approach in validation studies (i.e. Bender et al. (2008), Deng et al. (2011), Shang-Guan et al. (2015)) and the applying of the same mapping functions/factors for compared slants corresponds to the residuals 'normalization' with impact representing a second-order effect. We don't think that using STDs coming only from high elevation angles, as you propose, would allow us to validate the overall quality of STDs.

Regarding the GNSS vs WVR comparisons: We know that WVR measurements at low elevation angles can be of low quality, however, we didn't want to exclude them completely from the validation. Therefore, we selected a compromise of 15° elevation cut-off for these comparisons. Most of the so far presented studies used even lower elevation cut-off for WVR data (i.e. Bender et al. (2008) used 5° cut-off, Shang-Guan et al. (2015) used 7° cut-off, Braun et al. (2001) and Braun et al. (2002) used 10° cut-off, Deng et al. (2011) used 15° cut-off, Li et al. (2015a) used 20° cut-off since WVR wasn't measuring below this angle). We added dry horizontal gradients derived from NWM to WVR measurements to avoid errors of surface pressure gradients, please, see Section 5 describing the reconstruction of STDs from original SIWV WVR measurements.

3) Comparison with NWM There are three models appeared in this manuscript: ERAInterim, NCEP GFS, and ALADIN-CZ. To help the readers understand the discussion on this topic, please describe more settings on these models.

- Within these, only ALADIN is a regional model, and others are global. State their general characteristics more.

We added more information about the models to the beginning of chapter 4 together with references to other papers/relevant web pages.

- Do all of these models assimilate GNSS data for their initial conditions or not?

None of these models assimilate data from ground based stations. We added this information to manuscript (beginning of chapter 4)

- How large are their grid spacings?

The horizontal resolution for both ERA and NCEP GFS is 1°, for ALADIN-CZ it is 4.7 km (see the beginning of section 4).

- ERA-Interim is the ECMWF re-analysis data produced 6 hourly. I guess GFS is 6 hourly operational analysis data at NCEP. What is ALADIN-CZ?

With regards to ERA and NCEP: the assumption is correct. ALADIN-CZ is also 6 hourly operational analysis with forecasts for 0, 1, 2, 3, 4, 5, 6 hours. Information added to manuscript.

- Does ALADIN-CZ have large domain enough to produce STDs? I concern that STDs at low elevation angles might penetrate the lateral boundary of the model and need special treatment like STDs over the top of the model.

There is no problem in ALADIN-CZ domain which is roughly 4,000*3,000 km, see figure 3 in Douša et al. (2016).

- ALADIN-CZ may be a cloud-permitting model (this depends on its resolution) with explicit cloud microphysics. In this case, it is possible to calculate STDs with hydrometer effect. Is this right? If yes, I suggest to do this (see the major comment 5).

This was done and is described in section 4.4.

P7 section 4 There are two error sources in this comparison; STD solutions and NWMs. I suggest the authors to employ single STD solution with three NWMs and then compare the results with observed STDs. This makes error sources reduced single (only NWM) and discussion much easier (section 7.2).

We agree with the suggestion, therefore the Figure 9 was adopted and now is showing results of NWM versus GNSS GFZ solution. We rewrote the text in the chapter with the description of this figure.

4) Figures and discussion Although there are many graphs appeared in this manuscript, some of them are not appropriate for discussion. For instance, though Figure 12 displays 30 lines in 12 panels, the authors made a discussion only in single paragraph (P30 L10). Another example. Although the authors showed small number of figures in connection with GNSS versus NWM comparison, they discussed many points (stations) without figures in section 7.2. I recommend to re-organize discussion and figures.

Our goal was to balance the already significant length of the paper while giving as much as possible information - therefore for some of the results we haven't provided figures/tables. However, we try to rectify it in this document and we provide additional figures (Fig. 2, Fig. 3) to prove our statements from the text. They can be found in the text below where we address specific comments.

5) Assessment of components in the atmosphere Although the discussion on the effect of each component of the atmosphere (section 4.4) is important, the authors did not show any conclusion. I suggest to examine the same effect using NWMs additionally and illustrate useful information.

We struggle to understand this major comment. In section 4.4 we present results from NWM ALADIN-CZ.

Minor comments

P1 L21: “between GNSS a NWM” Reword to “between GNSS and NWM”.

Corrected

P1 L29: “along his path” Reword to “along the path”

Corrected

P4 L8: “was operating only” Reword to “was operated only” (?)

Corrected

P6 L91: “three variants of the solution” I don’t think that it is worth to examine “nonRES” case in this paper. See my major comment.

We don’t think we should completely skip “nonRES” solutions from the validation. It allowed us to evaluate and quantify the impact of post-fit residuals.

P8 L4: “mix ratio of liquid” mixing ratio of liquid

Corrected

P10 L24: “The contribution of water – neglected in the total delay.” As I mentioned in my major comments, I suggest the author to examine these contributions.

We examined these contributions in section 4.4. ALA/BIRA solution considered (added) these impacts in its STDs, ALA/WUELS solution did not.

P11 Figure 1 Enlarge the land names.

Figure modified with increase of the size of the name of the stations (see attachment)

P12 L4: “Figure 2 shows simulated STDs” P12 L9: “The respective differences of STD. . . are presented in Figure 2.” These are different. I guess the latter is correct. The differences were defined between each observation and their minimum, which was observed at a certain azimuth. This definition provides a kink in the graph at the minimum azimuth and then leads to miss-understandings. I suggest that the differences are made between each observation and its average.

Yes, this is right.

There is not the land name (POTS) in the body

Now POTS is visible in Fig. 1

P12 Figure 2 It was difficult for me to understand what x- and y-axis labels (Difference of slant delays (mm)) represented (actually, these are not labels for x- and y-axis). Improve locations these labels appear.

Figure improved.

P13 Figure 3 This was also made between observations and their minimum. See comment above.

Yes, right.

P13 L8: “These values” When were these observed? I guess the observed time were different for each contribution.

Minimal values obtained during the whole period of the benchmark campaign (text added into manuscript).

P13 L10+1: “the variation range of “ The standard deviation and average are better to illustrate such variation statistically. Raw variations may include outliers.

Because we look at severe weather situation, this is interesting for use to know the variation range, this is an indicator of the severity of the meteorological events. We are not sure if we understand your comment well.

P14 L7: “GPS” Is there any reason to use GPS specifying the US navigation system?

Yes, since the WVR is able to track only GPS satellites, not GLONASS or any other GNSS.

P20 L25: “Note also that ROB_V is consistent with TUO_G.” I feel that this sentence is not fear. The authors should list TUO_G at the same sentence (L23).

Read, please, our comments in the beginning of the document regarding a mistake in ROB_V and TUO_G (TUO_R) solutions. Whole paragraph of manuscript including this sentence was edited (deleted).

P22 L16: “orography representation” I guess grid spacings of these three models were different and ALADIN-CZ adopted the smallest. This means the topography of ALADINCZ is the most similar to real one. Please show modelled topography of each model and/or modelled altitude in comparison with real one.

We present a table with differences in heights between GNSS and NWM models ERA-Interim and ALADIN-CZ for all individual GNSS reference stations. We interpolated the NWM heights from four neighboring grid points. For NCEP GFS model it is not possible to provide differences in height since only pressure level fields were used to estimate the STDs and no surface layer field.

GNSS station	GNSS – ERA-Interim [m]	GNSS – ALADIN-CZ [m]
GOPE	169.6	177.7
KIBG	674.0	328.4
LDB2	81.0	60.5
POTS	65.6	75.5
SAAL	754.3	274.6
WTZR	187.7	127.5

From these altitude differences, we expect to find the largest discrepancies between the GNSS and NWM derived STDs at the station KIBG and SAAL and indeed this is what we see in Fig. 8. The reason is that the representative error and the interpolation/extrapolation error (in the ray-tracing algorithm the refractivity from the surrounding grid points is interpolated/extrapolated to the desired location) are largest at these stations. We are not confident with the ALADIN-CZ STD simulations for KIBG and SAAL. The reason is because the hydrostatic and the wet component are not well simulated. This can be due to a problem of ALADIN-CZ for simulating small-scale structures at the good locations (ERA-interim simulates structures with a larger scale). Then this can explain strong deviation/anisotropy between STD observed and simulations.

P22 L17: “ranging from -3 mm to +7 mm” It is quite difficult to measure these values from Fig. 8, because there are no scale auxiliary lines for the y axis. Please add the lines not only to Fig. 8 but also other similar figures needed.

Done, Figs 4 – 11, 14 were modified.

P22 L30: “The probable reason . . . negative effect of underestimated delays.” There is no evidence for this discussion. The authors should show any figures or numbers.

We edited the text in the manuscript to add a link to chapter 7.2.2 and we also provide here Fig. showing comparison between GNSS GFZ solution and all four NWM based STD solutions including ALA/WUELS for station KIBG where GNSS GFZ – ALA/WUELS reach 330 mm of absolute bias and 270 mm of absolute standard deviation.

P24 L1: “Chyba! Nenalezen zdroj,” Remove these Czech.

Corrected.

P24 section 7.2.2 The authors should reorganize and polish this section, because evidences for discussion in this section are missed by (not presented) or no figures. I would like to point out that one of major error sources in comparison between real and modelled STDs is super refraction in the actual atmosphere. Please examine this point.

Below, we provide two figures (Fig. , Fig.) which are variants of Figure 9 from the manuscript showing comparisons between GNSS GFZ solution and NWM STD solutions in the slant direction. Please note that both these figures use different y axis scales than Figure 9 included in the manuscript and show results for different stations.. Fig. proves our discussion regarding poor quality of ALA/WUELS STD solution visible mainly at low elevation angles. Fig. show results for station WTZZ and support our statements regarding sudden increases and decreases of standard deviation values at various elevation angles at stations WTZR, WTZS and WTZZ occurring mainly in case of ALA/BIRA solution. Plots for WTZR and WTZS stations show completely the same behavior (not presented here).

To answer the super refraction issue: We consider ground-based stations and restrict ourselves to elevation angles above 3° . We do not find any hint in literature that super refraction (the N-gradient exceeds a critical value) is a problem with such set up (ground-based station and elevation angles well above 3°).

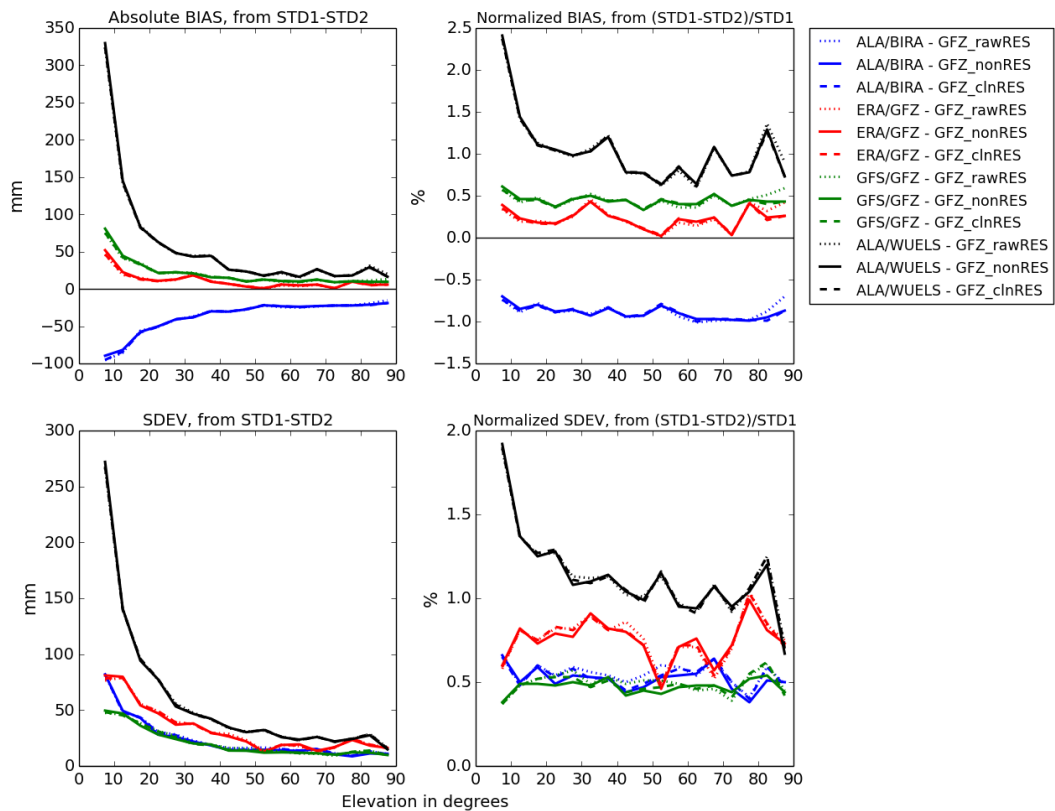


Fig. 2: Comparison of NWM-based solutions (ALA/BIRA, ERA/GFZ, GFS/GFZ, ALA/WUELS) against GNSS GFZ solution at station KIBG, in the slant direction.

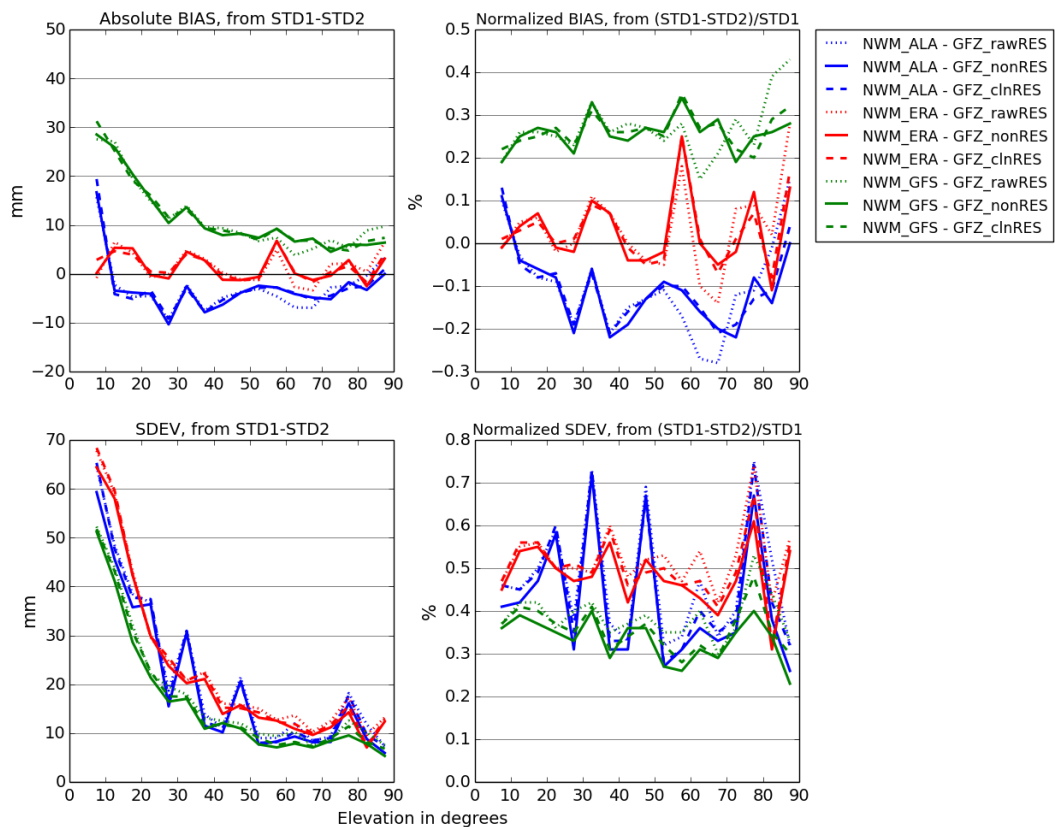


Fig. 3: Comparison of NWM-based solutions (ALA/BIRA, ERA/GFZ and GFS/GFZ) against GNSS GFZ solution at station WTZZ, in the slant direction.

P29 This paragraph is not well discussed, because, for instance, there is no figures in the sentence “The biases stay very stable “ (L4). It is recommended to show numbers and/or figures in discussion, otherwise, the readers would have to be frustrated to see tables.

The sentence is related to Tables 7 and 8 which are introduced just in the previous sentence. Therefore we don't think it is necessary to reference them again.

P30 This paragraph should be enhanced, because Figure 12 contains much information whereas the discussion is poor.

Please, read the revised Section 8 with the dual stations results – the description of mentioned figure is now in part 8.1.

P31 Conclusions If the authors illustrate discussion sections in connection with these conclusive remarks, it is happy for the readers to see discussion with evidences.

We have rewritten the conclusion chapter as well as provided extra results in this document (see figures above).

P32 L2: "for STDs to the zenith direction" It is better to use STDs at high elevation angles instead of mapped STDs.

Please, see our reply to your Major comment number 2.

P32 L13: "The impact was" I don't understand what "the impact" illustrates.

It meant the impact of adding post-fit residuals to STDs, the manuscript was corrected.

P32 L17-18: "The origin was identified as " I did not see any related discussion with this conclusion.

See Fig. in this document and our reactions to your comment for P22 L30 and P24 section 7.2.2.

P32 L18-19: "Their values varied at all . . . 15 degrees" Is there any discussion on this conclusion?

There is a short discussion in the section 7.2.2, we rephrased the sentence in the conclusion.

P33 L15: "hardly as reliable as in needed" Needed for what? State clearly.

The sentence was rephrased.

Please also note the supplement to this comment:

<http://www.atmos-meas-tech-discuss.net/amt-2016-372/amt-2016-372-RC1-supplement.pdf>

We found the supplement to be completely the same as the provided review and, hopefully, we answered all the comments/questions.

Inter-technique validation of tropospheric slant total delays

Michal Kačmařík¹, Jan Douša², Galina Dick³, Florian Zus³, Hugues Brenot⁴, Gregor Möller⁵, Eric Pottiaux⁶, Jan Kaplon⁷, Paweł Hordyniec⁷, Pavel Václavovic², Laurent Morel⁸

5 ¹ Institute of Geoinformatics, Technical University of Ostrava, Ostrava, ~~The~~-Czech Republic

² Geodetic Observatory Pecný, Research Institute of Geodesy, Topography and Cartography, Zdíby, ~~The~~-Czech Republic

³ Helmholtz Centre Potsdam - GFZ German Research Centre for Geosciences, Potsdam, Germany

⁴ Royal Belgian Institute for Space Aeronomy, Brussels, Belgium

⁵ Department of Geodesy and Geoinformation, Vienna University of Technology, Vienna, Austria

10 ⁶ Royal Observatory of Belgium, Brussels, Belgium

⁷ Institute of Geodesy and Geoinformatics, Wrocław University of Environmental and Life Sciences, Wrocław, Poland

⁸ GeF Laboratory, ESGT – CNAM, Le Mans, France

Correspondence to: M. Kačmařík (michal.kacmarik@vsb.cz)

Abstract. An extensive validation of line-of-sight tropospheric Slant Total Delays (STD) from Global Navigation Satellite
15 Systems (GNSS), ray-tracing in Numerical Weather Prediction Models (NWM) fields and microwave Water Vapour
Radiometer (WVR) is presented. Ten GNSS reference stations, including collocated sites, and almost two months of data from
2013, including severe weather events, entered the comparison. Seven institutions delivered their STDs based on GNSS
observations processed using five software and eleven strategies enabling to compare rather different solutions and to assess
the impact of several aspects of the processing strategy. STDs from NWM ray-tracing came from three institutions using three
20 different NWM models and ray-tracing software. Inter-techniques evaluations Results showdemonstrated a generally a very
good mutual agreement among all of various GNSS STD solutions from compared to a#NWM and WVR STDs the techniques.
The mean bias ~~(over all stations) between among the~~ GNSS solutions not considering selected as reference, which did not use
post-fit residuals in STDs, and all other GNSS solutions without post-fit residuals is was -0.6 mm for STDs scaled in the zenith
direction, and the ~~corresponding~~ mean standard deviation was 3.7 mm. Standard deviations of comparisons between GNSS
25 and NWM ray-tracing solutions were typically 10 mm +/- 2 mm (scaled in the zenith direction), depending on the NWM
model and the GNSS particular station-considered. When eComparing GNSS versus WVR STDs reached, standard deviations
reached of 12 mm +/- 2 mm, as also scaled in the zenith direction. Moreover, the influenceImpacts of adding raw GNSS post-
fit residuals, as well asand cleaned residuals screened out of systematic effects on optimal reconstructing of GNSS STDs was
particularly evaluated at inter-technique comparison and for GNSS at collocated sites, to STDs was studied to. The use of ~~it~~
30 was found that adding raw post-fit residuals is not generally recommended as they might contain strong systematic effects as
demonstrated in case of station LDB0. Simplified STDs reconstructed only from estimated GNSS tropospheric parameters,
i.e. without applying post-fit residuals, performed the best in all the comparisons, however, it obviously missed part of
tropospheric signals due to non-linear temporal and spatial variations in the troposphere. Although the post-fit residuals cleaned
from visible systematic errors generally showed a slightly worse performance, they contained significant tropospheric signal
35 on top of the simplified model. They are thus recommended for the reconstructing STDs, particularly during a high variability

~~in the troposphere. Cleaned residuals showed also a stable performance during ordinary days while containing promising information about the troposphere at low elevation angles, always led to lower quality of GNSS STDs while the situation was not that straightforward after the post-fit residuals cleaning.~~

1 Introduction

- 5 Tropospheric Slant Total Delay (STD) represents the total delay that undergoes the GNSS radio-signal due to the neutral atmosphere along ~~his~~the path from a satellite to a ground receiver antenna. This total delay can be separated into the hydrostatic part, caused by the dry atmospheric constituents, and the wet part caused specifically by water vapour. By quantifying the total delay, and by separating the hydrostatic and wet parts, it is possible to retrieve the amount of water vapour in the atmosphere along the path followed by the GNSS signal.
- 10 During the processing of GNSS observations only the total delay in the zenith direction (Zenith Total Delay, ZTD) above the GNSS antenna can be estimated for each epoch or for a time interval. ZTDs from GNSS reference stations are operationally assimilated into Numerical Weather Models (NWM) for almost a decade (Benitt and Jupp, 2012; Mahfouf et al., 2015). In Europe, this activity is coordinated mainly in the framework of the EUMETNET EIG GNSS Water Vapour Programme (E-GVAP, 2005-2017, Phase I-III, <http://egvap.dmi.dk>). Many recent studies demonstrated a positive impact of the ZTD or
- 15 Integrated Water Vapour (IWV) assimilation on precipitation weather forecasts, especially of the short-time ones (Vedel and Huang, 2004; Guerova et al., 2006; Shoji et al., 2009; Guerova et al., 2016). On the other hand, continuous developments in NWM forecasting and nowcasting tools, as well as increasing needs for better predictions of severe weather events, stress the demand of high-quality humidity observations with high spatial and high temporal resolutions. While ZTDs provide information in zenith directions above GNSS stations, linear horizontal tropospheric gradients give information about the first-
- 20 order spatial asymmetry around the station. Besides, Slant Tropospheric Delays (STDs) can provide additional details about the horizontal asymmetry in the troposphere, more specifically in the directions from a receiver to all observed GNSS satellites. With the increasing number of GNSS systems and satellites, the atmosphere scanning will be more complete, hence gaining even more interest. Bauer et al. (2011) showed a positive impact of STD assimilation into the Mesoscale Model 5 (MM5) and Kawabata et al. (2013) demonstrated a significant advantage of assimilating STDs into a high-resolution model in case of
- 25 forecasting local heavy rainfall event against the scenario of assimilating ZTDs only. Also, Shoji et al. (2014) and Brenot et al. (2013) showed promising techniques for prediction of severe weather events using advanced GNSS tropospheric products such as horizontal gradients and STDs. The GNSS tomography technique aiming at the three-dimensional reconstruction of the water vapour field (Flores et al., 2001) uses STDs as input data as well. Obviously, the quality of the tomography depends on both the accuracy of the STDs (Bender et al., 2009) and the observation geometry (Bender et al., 2011).
- 30 Validation of GNSS slant delays with independent measurements is not a new research topic. GNSS slant delays were validated against WVR measurements in Braun et al. (2001), Braun et al. (2002) and Gradinarsky (2002). First attempts to derive slant delays from NWM fields and to compare them with GNSS STDs were carried out by De Haan et al. (2002) and Ha et al.

(2002). Additional effort in evaluation of GNSS slant delays using WVR and NWM data was done at GFZ Potsdam during last years. Bender et al. (2008) showed an existing high correlation within the three sources (GPS, WVR, NWM) of slant wet delays and tried to quantify the effect of removing multipath from GPS post-fit residuals using a stacking method what was also done by Kačmařík et. al (2012). Deng et al. (2011) validated tropospheric slant path delays derived from single- and dual-frequency GPS receivers with NWM and WVR data. Shang-Guan et al. (2015) compared GPS versus WVR slant IWV values (SIWV) using a 184-day long dataset. They also analysed the influence of the elevation angle setting and the meteorological parameters (used for the conversion to IWV) on the comparison results. More recently, a validation of multi-GNSS slant total delays retrieved in real-time from GPS, GLONASS, Galileo and BeiDou constellation was presented by Li et al. (2015a) using WVR and NWM as independent techniques for the assessment. Using multiple GNSS constellations brought a visible advantage, not only in terms of number of available slants, but also in their higher accuracy and robustness.

Nevertheless, most of the so-far presented studies were limited to only a single strategy for obtaining GNSS STDs, and usually restricted to a limited set of stations and/or a relatively short time period. The main purpose of this study is an extensive comparison of various solutions from GNSS processing, NWM ray-tracing and WVR measurements using one common dataset, and also comparing results from collocated stations. The GNSS solutions evaluated in this work used five different software and eleven strategies, and exploited the GNSS4SWEC benchmark dataset (Douša et al., 2016). Then, the paper studies the impact of various approaches on STD estimates and aims at finding the most suitable strategy for estimating the GNSS-based STDs ~~with the highest precision possible~~.

Section 2 briefly introduces the validation study dataset, and Section 3 describes the process of retrieving GNSS STDs including an overview of the different GNSS solutions. Section 4 provides a description of STDs generated from NWMs, and Section 5 summarizes WVR principals and WVR-based STD solutions. Section 6 introduces the methodology used in the validation of STDs, and Sections 7 and 8 study the results achieved at single GNSS reference stations and at closely collocated stations, respectively.

2 Experiment description

The presented work has been carried out in the context of the EU COST Action ES1206 "Advanced Global Navigation Satellite Systems tropospheric products for monitoring severe weather events and climate (GNSS4SWEC)" (http://www.cost.eu/COST_Actions/essem/ES1206, 2013-2017). Three mutually cooperating Working Groups (WG) have been established to cover the proposed topics: 1) WG1: Advanced GNSS processing techniques, 2) WG2: GNSS for severe weather monitoring, and 3) WG2: GNSS for climate monitoring. Validation of STDs belongs mainly under WG1, which is besides other topics oriented toward the development of new advanced tropospheric products. The idea of preparing a common benchmark dataset, which could serve efficiently for most planned activities, was designed in the beginning of the project, and the data were collected, cleaned, documented, reference products generated and assessed (Douša et al., 2016). The selected geographical area is situated in central Europe (Austria, Germany, the Czech Republic, Poland) where severe weather events,

including extensive floods on Danube, Moldau and Elbe rivers, occurred between May and June 2013. The benchmark dataset gathers observations from 430 GNSS reference stations, 610 meteorological synoptic stations, 21 radiosonde launching sites, 2 Water Vapour Radiometers (WVR), 2 meteorological radars, and output fields from the ALADIN-CZ Numerical Weather Prediction (NWP) model over a period of 56 days. ZTDs and horizontal tropospheric gradients from the reference GNSS and NWM-derived tropospheric products were already evaluated, and all resulted in very good agreements (Douša et al., 2016). All STDs used in this paper were computed by exploiting the benchmark dataset.

From the complete benchmark dataset, we selected a subset of 10 GNSS reference stations situated at six different locations (Table 1). The selection was based on the following requirements: 1) long-term quality of observations and its stability, 2) availability of another GNSS reference station in the site vicinity, 3) availability of another instrument capable of STD measurements in the site vicinity, and 4) the location of the station w.r.t. its altitude and the weather events which occurred during the evaluation period. The subset also includes collocated (dual) GNSS stations playing an important role in the validation. The collocated stations observed GNSS satellites with the same azimuth and elevation angles, so that they should theoretically deliver the same or very similar tropospheric parameters – ZTD, linear horizontal gradients and slant delays. Post-fit residuals of carrier-phase observations at the collocated stations should represent common effects due to the local tropospheric anisotropy, while systematic differences could remain due to instrumentation and environmental effects such as antenna and receiver characteristics, and multipath. Only STDs from the WVR at Potsdam, collocated with the GNSS stations POTM and POTS, were available for this study because the second WVR, located at Lindenberg and collocated with the GNSS stations LDB0 and LDB2, was operated only in the zenith direction during the period of the study.

3 Slant Total Delay retrievals from GNSS observations

The tropospheric Slant Total Delay (STD) cannot be estimated directly from GNSS data since the total number of unknown parameters in the solution would be higher than the number of observations. Instead, the total delays in the zenith direction above the GNSS station (i.e. ZTD) are adjusted, ~~and together with,~~ optionally, ~~along with the~~ total tropospheric linear horizontal gradients (G) to account for the first-order asymmetry of the local troposphere. The estimates are valid for individual processing epochs whenever using a stochastic approach, or for a given time interval when modelling the troposphere with a deterministic process, e.g. by a piece-wise constant or linear models.

In practice, the ZTD is decomposed into an a priori model, usually by introducing the Zenith Hydrostatic Delay (ZHD, see Saastamoinen, 1972), and the estimated corrections, representing (mainly) the Zenith Wet Delay (ZWD). Similarly, the STD is decomposed ~~based onto~~ the ZHD , ZWD , ~~and~~ G ~~and post-fit residuals (RES)~~ as described in Eq. (1) (Teke et al., 2014), where ele is the elevation angle and azi is the azimuth angle in degrees. The STD value is given in meters.

$$STD(ele, azi) = ZHD \cdot mf_h(ele) + ZWD \cdot mf_w(ele) + G(ele, azi) + RES \quad (1)$$

The elevation angle dependency of STD is described by the mapping functions, separately for the hydrostatic (mf_h) and the wet (mf_w) components. Nowadays, the Vienna Mapping Function (VMF1, see Böhm et al., 2006a) - or VMF1 like concepts - is commonly used in GNSS data processing. Also, the empirical mapping function 'Global Mapping Function' (GMF, see Böhm et al., 2006b) is popular since it is consistent with VMF1 and easier to implement (independent on external data needing updates). Both, the VMF1 and the GMF are applicable down to 3° elevation angles.

The first-order horizontally asymmetric delay $G(ele, azi)$ in Eq. (1) reflects local changes in temperature and particularly in water vapour. MacMillan (1995) proposed a model describing the gradient delay as a function of the elevation and azimuth angles:

$$G(ele, azi) = mf_g \cdot (G_N \cdot \cos(azi) + G_E \cdot \sin(azi)) \quad (2)$$

where $mf_g(ele) = mf_h(ele) \cdot \cot(ele)$. Chen and Herring (1997) replaced the elevation dependent term $mf_h(ele) \cdot \cot(ele)$ by the gradient mapping function $mf_g(ele) = 1/(\sin(ele) \cdot \tan(ele) + C)$, with $C = 0.0032$, nowadays commonly used as standard in GNSS data processing (Herring 1992). Typical range for G_N and G_E is from 0 mm to below 1--2 mm, however, gradients can reach up to 7 mm during a significant extreme weather events. The gradient of 1 mm corresponds to about 55 mm slant delay correction when projected to 7° elevation angle using the gradient mapping function.

Additionally, the observation post-fit residuals RES were stored since they might contain un-modelled tropospheric effects not covered by the estimated tropospheric parameters. Such remaining effects are supposed to be mainly caused mainly by higher spatial and temporal variations of the humidity in the troposphere or its significant horizontal asymmetry in the troposphere. Obviously, unfortunately, residuals contain also other un-modelled effects like such as multipath, errors in antenna phase centre variations or satellite clock errors can superimpose any tropospheric asymmetry information. For eliminating or of such systematic effects, such as multipath and antenna phase centre variations further cleaning of the post-fit residuals was applied done by generating elevation/azimuth-dependent residuals correction maps as described by Shoji et al. (2004). For each solution and each station, we thus computed the mean values of the post-fit residuals in 1×1 degree bins were computed overusing the whole benchmark period while. R-residuals exceeding ±3 times the standard deviation were excluded from the computation of the mean. Computed means were then subtracted from the original post-fit residuals to generate the variant solutions introducing using cleaned residuals.

For the analysis of GNSS L1 and L2 carrier-phase observations, a the least-squares adjustment or a Kalman-filter approach was applied to estimate the ZWDs and the two horizontal gradient components G_N and G_E at each GNSS site (Table 1) and for a specific validity period. Afterwards, Eq. (1) was used to compute STDs for each satellite in view. Whenever zero-differenced (ZD) post-fit residuals were available for any solution, three variants of the solution are presented in the paper: 1) solution without residuals (nonRES), 2) solution with raw residuals (rawRES), and 3) solution with cleaned residuals (clnRES). For the analysis of GNSS L1 and L2 carrier phase observations, a least squares adjustment or a Kalman filter approach was applied

to estimate the ZWDs and the two horizontal gradient components G_N and G_E at each GNSS site (Table 1) and for a specific validity period. Afterwards, Eq. (1) was used to compute STDs for each satellite in view. In addition, the observation post-fit residuals were stored since they might contain un-modelled tropospheric effects not covered by the estimated tropospheric parameters. These remaining effects are supposed to be mainly caused by high spatial and temporal variations of the humidity in the troposphere. Unfortunately, other un-modelled effects like multipath or satellite clock errors can superimpose any tropospheric asymmetry information. Hence, the usage of the information content from the post-fit residuals for the reconstruction of the STDs remains an open question and it is further analysed in Sections 7 and 8.

Seven institutions delivered their STD solutions for this validation study, namely Ecole Supérieure des Géomètres et Topographes (ESGT CNAM), Geodetic Observatory Pecny (GOP, RIGTC), Helmholtz Centre Potsdam - German Research Centre for Geosciences (GFZ), Royal Observatory of Belgium (ROB), Technical University of Ostrava (TUO), Vienna University of Technology (TUW), and Wrocław University of Environmental and Life Sciences (WUELS). Principal information about individual solutions are given in Table 2 with a few specific notes important for the interpretation of the results.

GOP delivered two solutions based on the Precise Point Positioning (PPP) technique (Zumberge et al., 1997) and using the in-house developed application Tefnut (Douša and Václavovic, 2014) derived from the G-Nut core library (Václavovic et al., 2013). Considering all available GNSS solutions, only GOP used a stochastic modelling approach to estimate ~~the-all~~ parameters. Additionally, GOP provided two solutions: 1) GOP_F using Kalman filter (forward filter only), i.e. capable of providing ZTD, tropospheric gradients and STDs in real time, and 2) GOP_S applying the backward smoothing algorithm (Václavovic and Douša, 2015) on top of the Kalman filter in order to improve the quality of all estimated parameters during the batch processing interval and for avoiding effects such as the PPP convergence or re-convergence.

Some institutions delivered also two STD solutions ~~in such a way that these solutions only~~ which differ in a single processing setting. The aim was to evaluate their impact on STDs: a) TUO_G and TUO_R exploit GPS-only and GPS+GLONASS observations respectively, b) TUW_3 and TUW_7 apply an elevation cut-off angle of 3 and 7 degrees respectively, and c) ROB_G and ROB_V use the GMF and VMF1 mapping functions respectively. Additionally, ROB solutions are the only ones based on the processing of double-difference (DD) observations and providing ~~zero-differenced-(ZD)~~ carrier-phase post-fit residuals converted from the original DD residuals using the technique described in Alber et al. (2000). For other DD solutions, variants without adding residuals were compared only.

In total, we ~~compared-validated~~ eleven solutions computed with five different GNSS processing software. Five of the solutions used GPS and GLONASS observations and six solutions used GPS-only observations; five of them are based on double-difference observations and six of them are computed using zero-difference data in PPP analysis. More information about TUW solutions can be found in Möller et al. (2016), about GFZ in Bender et al. (2009, 2011), Deng et al. (2011) and about CNAM in Morel et al. (2014). For ROB, TUO and WUE solutions we refer the reader to Dach et al. (2015).

~~Whenever ZD post-fit residuals were available for any solution, three variants of the solution are presented in the paper: 1) solution without residuals (nonRES), 2) solution with raw residuals (rawRES), and 3) solution with cleaned residuals (cmRES).~~

The cleaning of the post-fit residuals used to eliminate systematic effects such as multipath and antenna phase centre variations was done via generating time /azimuth /zenith dependent residuals correction maps as described by Shoji et al. (2004). For each solution and each station, the mean of the post-fit residuals in 1×1 degree bins were computed over the whole benchmark period while residuals exceeding ± 3 times the standard deviation were excluded from the computation of mean. Computed means were then subtracted from the original post-fit residuals to generate the variant introducing cleaned residuals.

4 Computation of Slant Total Delay from Numerical Weather Prediction model

Simulating STDs in NWP models consists in integrating the atmospheric refractivity through the path followed by GNSS signals. STDs have been simulated using three different NWMs: ALADIN-CZ (4.7 km-resolution limited-area hydrostatic model, operational analysis in 6h interval with forecasts for 0, 1, 2, 3, 5, 6 h, <http://www.umr-cnrm.fr/aladin/>), ERA-Interim (1° horizontal resolution, 6h reanalysis), and NCEP-GFS (1° horizontal resolution, 6h operational analysis, <https://www.ncdc.noaa.gov/data-access/model-data/model-datasets/global-forecast-system-gfs>). None of these NWM assimilates data from ground GNSS stations. For more details information about the models, see Douša et al. (2016) and specifically Trojáková (2016) for ALADIN-CZ model and Dee et al. (2011) for ERA-Interim. First, STD solutions using the ERA-Interim and NCEP-GFS models were delivered by GFZ Potsdam using acronym ERA/GFZ and GFS/GFZ, respectively.

Only a short introduction is provided in Section 4.1 since the GFZ tool for an accurate and ultra-fast NWM ray-ray-tracing has been described in other papers cited below. Two STD solutions were then delivered for the ALADIN-CZ model: a) the ALA/BIRA, which was generated at Royal Belgian Institute for Space Aeronomy (BIRA), described in Section 4.2, and b) the ALA/WUELS, which was delivered by Wrocław University of Environmental and Life Sciences, described in Section 4.3.

4.1 Description of ERA-Interim STD solution (ERA/GFZ) and NCEP-GPS STD solution (GFS/GFZ)

The ERA-Interim and NCEP-GFS STD solutions by GFZ are based on 'assembled' STDs. At first, for the considered station and epoch, a set of ray-traced STDs (various elevation and azimuth angles) is computed using technique described in Zus et al. (2014). Secondly, from this set of ray-traced STDs, the tropospheric parameters (i.e. zenith delays, mapping function coefficients, first- and higher-order gradient components) are determined. Finally, for the required azimuth and elevation angle the STD is 'assembled' using the tropospheric parameters. For a detailed description of the tropospheric parameter determination the reader is referred to Douša et al. (2016). The differences between the 'assembled' and ray-traced STDs are sufficiently small in particular for elevation angles above 10° (Zus et al., 2016). In essence, the largest uncertainty in the 'assembled' (and ray-traced) STDs remains the uncertainty of the underlying NWM refractivity field. This uncertainty is estimated to be about 8-10 mm close to the zenith increasing to about 8-10 cm at an elevation angle of 5° (Zus et al., 2012). Similar uncertainty of around 8 mm for the zenith direction was also found for ALADIN-CZ model in Douša et al. (2016).

4.2 Description of ALADIN-CZ STD solution from BIRA (ALA/BIRA)

To compute STDs from ALADIN-CZ, a simplified strategy has been used to model the curve path followed by GNSS signals through the neutral atmosphere, as suggested by Saastamoinen (1972). The delays simulated with this strategy show small differences in comparison to straight line simulations (differences of about 4 mm, 5 mm and 10 mm respectively at 15°, 10° and 5°-elevation). Simulations have computed STDs down to 3°-elevation, however, under an elevation of 15°, a proper ray tracing strategy, as mentioned in Section 4.1, should be preferably applied.

For each latitude-longitude grid point and each level of ALADIN-CZ model, the NWP outputs considered to compute STDs are: geopotential height (*geopotH* in m), pressure (*P* in Pa), temperature (*T* in K), partial pressure of water vapour (*e* in Pa), mixing ratio of liquid and solid water (in kg/kg). The ground pressure of each column is also retrieved. The geopotential height is converted to the altitude above the geoid:

$$h_{geoid} = (g_0 * R_e * geopotH) / (g * R_e - g_0 * geopotH) \quad (3)$$

where g_0 is a standard gravity acceleration (mean value of 9.80665 m/s^2 from the World Meteorological Organization, WMO); $R_e = 6378137 / (1.006803 - 0.006706 * \sin^2(lat))$ is the radius of the ellipsoid in meter for the latitude (*lat* in degrees); g is the gravity acceleration (in m/s^2) of the considered location given as:

$$g = 9.7803267714 * (1. + 0.00193185138639 * \sin^2(lat)) / \sqrt{1. - 0.00669437999013 * \sin^2(lat)} \quad (4)$$

Then, the height above the geoid is converted to height above the WGS84 ellipsoid (in m) with the use of the EGM96 (Earth Gravitational Model, Lemoine et al., 1998) undulation. Note that for the region of the benchmark campaign the difference between geoid and WGS84 altitude is about 47 m.

Using the hypsometric equation, the ground pressure and the pressure of each level are considered to estimate the altitude for the different levels. In total ALADIN-CZ outputs provide 87 levels up to an altitude of about 55 km. However, to assess STDs from ALADIN-CZ, the integration was stopped at 15 km since the contribution of water vapour above this altitude is negligible.

An adaptive step is considered (100 m, 200 m, 250 m, 500 m, 1000 m, respectively for vertical altitudes between 0-1 km, 1-3 km, 3-5 km, 5-10 km, 10-15 km). Bi-linear interpolations of ALADIN-CZ parameters at the altitude of the GNSS station and for each step of the integration were proceeded. Note that there is no station selected for the validation located below the first layer of ALADIN-CZ.

The expression of simulated STDs from ALADIN-CZ is the summation of these four contributions:

$$STD = SHD_{int} + SWD_{int} + SHMD_{int} + STD_{ext} \quad (5)$$

where SHD_{int} , SWD_{int} and $SHMD_{int}$ are respectively the inside-model integration contribution of the hydrostatic, wet and hydrometeor delays, and STD_{ext} is the external model contribution (over 15 km).

$$SHD_{int} = 10^{-6} \sum_{k=1}^{k=k_{top}} k_1 \frac{P_i}{T v_i} \Delta S_i \quad (6)$$

5

$$SWD_{int} = 10^{-6} \sum_{k=1}^{k=k_{top}} \left(k'_2 \frac{e_i}{T_i} + k_3 \frac{e_i}{T_i^2} \right) \Delta S_i \quad (7)$$

with $k'_2 = k_2 - k_1 * R_d / R_w$ where k_1 (in K/Pa), k_2 (in K/Pa), k_3 (in K²/Pa) are the empirical refractivity coefficients of Bevis et al. (1994), R_d and R_w the gas constants respectively for dry air and water vapour (in J/kmol K), and T_v is the virtual temperature (in K). For the estimation of the hydrometeor contribution inside the model, as presented in Eq. (8), (N_{lw}, M_{lw}) and (N_{ice}, M_{ice}) are (atmospheric refractivity, mass content per unit of air volume) of the liquid and ice water, respectively.

$$SHMD_{int} = 10^{-6} \sum_{k=1}^{k=k_{top}} (N_{lw} + N_{ice}) \Delta S_i = \sum_{k=1}^{k=k_{top}} (\alpha_{lw} M_{lw} + \alpha_{ice} M_{ice}) \Delta S_i \quad (8)$$

15 The estimation of coefficients $\alpha_w \sim 1.45$ and $\alpha_{ice} \sim 0.69$ is presented in Brenot et al. (2006). The ALADIN-CZ model provides mixing ratios of cloud water (liquid components) and pristine ice (solid water components). The mass content per unit of air volume is obtained using the associated mixing ratio, pressure, water vapour partial pressure and temperature.

STD_{ext} is obtained with the hydrostatic formulation (Saastamoinen, 1972) mapped with mf_h (see Eq. 1) and using the elevation, latitude and pressure of the last step of the integration (i.e. at 15 km). Note that the wet contribution over 15 km is neglected since it is practically zero. The estimation of STD_{ext} (about 0.21 m) provides sufficiently accurate modelling for the hydrostatic contribution over 15 km (as shown by the sensitivity test from Brenot et al., 2006).

20

4.3 Description of ALADIN-CZ solution from WUELS (ALA/WUELS)

The ray-traced tropospheric delays for WUELS solution are based on piece-wise bent-2d model propagation. Thus, it prevents to know the exact trajectory in advance in contrary to straight-line model and needs to be solved iteratively based on preceding ray refractive index. Similar examples are given by Böhm and Schuh (2003) or Hobiger et al. (2008). We assume the ray-path does not leave the plane of constant azimuth for a given elevation angle to a satellite. The out-of-plane contribution to the delay is thus neglected making the propagation two-dimensional, hence 2d. The real ray-path is then approximated by a finite number of linear ray-pieces in WGS84 coordinates using Euler formula for Earth radius

30

$$R = (\cos^2 A / M + \sin^2 A / N)^{-1} \quad (9)$$

where A is the azimuth angle between a satellite and a receiver, M and N are radii of curvature along meridian and prime vertical, respectively. We follow height-dependent increments as presented in Rocken et al. (2001): 10 m, 20 m, 50 m, 100 m, 500 m respectively for geometric altitudes between 0-2 km, 2-6 km, 6-16 km, 16-36 km, and above 36 km which require meteorological parameters to be vertically interpolated in order to obtain finer resolution. Both P and e are interpolated exponentially from two nearest layers, while the temperature change is considered linear. Horizontally, we find the four nearest nodes for each ray to perform weighted mean interpolation, where the weighting function equals to the inverse squared distance. The reference hybrid-level of the ALADIN-CZ model is determined by surface geopotential which is converted to geopotential meters by dividing the geopotential values by g_0 . Meteorological parameters are expressed on pressure levels which represent standard vertical coordinate. The hypsometric equation is used to calculate geometric thickness between consecutive isobaric surfaces

$$dz = R_d * T_m / g_0 * \ln(P_1 / P_2) \quad (10)$$

where $R_d = 287.058 \text{ J/K} \cdot \text{kg}^{-1}$ is the gas constant for dry air, T_m is the mean virtual temperature of the layer between P_1 and P_2 pressure levels in Kelvin. The conversion from ALADIN-CZ vertical coordinate system to geometric altitudes is then consistent with the BIRA approach described in Section 4.2. In WUELS solution, the signal tracking is performed exploiting a full model vertical resolution up to the uppermost ALADIN-CZ layer at 55 km. Above the top layer, we adopt the U.S. Standard Atmosphere (1976) to provide supplementary meteorological data up to 86 km. For each ray-path coordinates, the refractive index is calculated as a function of P (in hPa), e (in hPa) and T (in K) with empirically derived “best available” coefficients k given by Rueger (2002).

$$N = (n - 1) \times 10^6 = k_1 * (P - e) / T + k_2 * e / T + k_3 * e / T^2 \quad (11)$$

The contribution of water droplets and ice crystals in the atmosphere is neglected in the total delay. All tropospheric delays are traced with respect to vacuum elevation angles. The electromagnetic delay is calculated for a given chord length (s) using the mean refractive index n between two consecutive rays yielding the total delay in meters

$$STD = \sum s_i (n_i - 1) \times 10^6 \quad (12)$$

which can be separated on hydrostatic and wet part using respective refractive indices. Additionally, to the radio path length, the accumulated bending effect (*bend*) along the ray path is added to the hydrostatic mapping function which, together with the wet mapping function, can be calculated as follows:

$$bend = \sum (s_i - \cos(ele_i - ele_k) s_i) \quad (13)$$

$$mf_h = (SHD + bend) / ZHD \quad (14)$$

$$mf_w = SWD / ZWD \quad (15)$$

where ele_i is the elevation angle for a given model layer and ele_k is the outgoing elevation angle at uppermost altitude.

4.4 Assessment of the Hydrostatic, Wet and Hydrometeor Contributions to the Slant delays

5 ALADIN-CZ NWM has been used to estimate the Hydrostatic, Wet and Hydrometeor contributions to slant delays. During the whole period of the benchmark campaign, the maximum contribution of hydrometeors reached 17 mm at the zenith during the extreme weather events on 20-23 June (Douša et al., 2016). The 2D fields of ZTD, ZHD, ZWD, and ZHMD (zenith hydrometeor delays) are presented in Figure 1. They illustrate the large-scale convection with the presence of hydrometeors along the convergence line associated with a strong contrast of dry and wet air masses. The contribution of hydrometeors to
 10 ZTD reached up to 7 mm (as scaled in the zenith direction) for the stations POTS and POTM at 15:00 UTC on 23 June 2013 (see Figure 1d). According to satellite trajectories at this time for the station POTS, a maximum SHMD of 25.6 mm is observed for a satellite at 22°-elevation angle.

Figure 2 shows simulated differential STDs for a cone with a 10° elevation angle during the severe weather condition of the 23rd of June 2013, and mapped in the zenith direction (at 90°) using the mapping functions of Eq. (1): mf_h for SHD and mf_w for
 15 SWD and SHMD. For this 10°-cone, the minimum present values of total, hydrostatic, wet and hydrometeors delays simulated at 15:00 UTC on 23 June, are given as STD_{min}, SHD_{min}, SWD_{min} and SHMD_{min} in Figure 2. The respective differences of STD, SHD, SWD and SHMD and corresponding minimum values simulated at 15:00 UTC are presented in Figure 2. The anisotropic variation of total, hydrostatic, wet and hydrometeor delays can be visualised on a skyplot. As a confirmation of Figure 1b and 1d, Figure 2 shows weak hydrostatic anisotropy. This anisotropy (up to 5.8 mm) is almost the same as the
 20 hydrometeors one (up to 6 mm). The area within the red curve is larger than the purple area (hydrostatic anisotropy), meaning that the total effect of the hydrometeor anisotropy is slightly larger than the one from the hydrostatic component. Note that Figure 2 shows the anisotropies simulated at 10° and mapped at 90° (giving an idea of the variations in the zenith direction). The largest anisotropy is clearly induced by water vapour (values up to 20 mm in the south-east direction of POTS, also shown in Figure 1c). With mean hydrostatic and hydrometeor anisotropies oriented in the opposite direction of the wet one, Figure 2
 25 presents a total anisotropy with weaker values (up to 12 mm) than the wet anisotropy.

To complement the snapshot of Figure 2 the time-evolutions of SHD, SWD, SHMD, and STD in the direction of all observed GNSS satellites for the station POTS are presented in Figure 3. Slant delays have been simulated in the direction of observed satellites (hydrostatic, wet, hydrometeor and total contributions) and, to avoid the effect of the elevation and to look at the
 30 same order of magnitude of delays, corresponding delays in the zenith direction have been computed and mapped using mapping functions presented in Eq. 1 (mf_h for SHD and mf_w for SWD and SHMD). These values (STD_{min} = 2310.6 mm, SHD_{min} = 2240.8 mm, SWD_{min} = 43.1 mm and SHMD_{min} = 0 mm) obtained during the whole period of the benchmark campaign, have been subtracted from their corresponding values simulated in direction of satellites. Then, the differences have been mapped back at 90°. For day of year (DOY) 174 (i.e. 23rd of June 2013), we can see a contribution of hydrometeors up to 10 mm.

Looking at the whole period of the benchmark campaign, the variation range of STD, SHD and SWD (mapped at 90°) are 275 mm, 80 mm and 230 mm, respectively. Figure 3 illustrates the interest of GNSS delay observations for meteorology (detection of variation of water vapour represented by the wet delay, but also detection of heterogeneities from hydrostatic delays and occasionally from hydrometeors in specific severe weather cases), ~~confirms the interest of GNSS delay observations for meteorology and the detection of variation of water vapour, pointing the importance of simulating slant total delays (that take into account mainly the variation from wet delay, but also from hydrostatic delays and occasionally from hydrometeors in specific severe weather cases)~~. Note that there is no data available for POTS station between DOY 121 and 125 and DOY 160 and 163. For this reason, we have not simulated the slant delays for this period, as shown by the gaps in Figure 3. The simplified strategy used to simulate curve slant paths gives some inaccurate simulations of slant delays for elevations between 3° and 5°, shown by isolated values in Figure 3. Such inaccuracies could be avoided by using a ray-tracing algorithm. For a comprehensive overview on ray-tracing algorithms and comparisons the reader is referred to Nafisi et al. (2012).

5 Water Vapour Radiometer Measurements

During the benchmark period, the WVR located at GFZ Potsdam operated in a mode scanning the atmosphere at selected elevation and azimuth angles. The instrument is situated on the same roof as the GNSS reference stations POTM and POTS. All three devices are within ten meters from each other. The HATPRO WVR from Radiometer Physics was set up to scan the atmosphere to extract profiles of atmospheric temperature, water vapour and liquid water using frequencies between 22.24 and 27.84 GHz and a window channel at 31.4 GHz. The WVR is switching between ‘zenith mode’ when it is measuring Integrated Water Vapour (IWV) and ‘slant mode’ when it is tracking GPS satellites using an in-built GPS receiver. In the latter case, Slant Integrated Water Vapour (SIWV) values are delivered for the direction of satellites. Since the instrument can track only one satellite at one moment the number of observations is quite limited compared to slants from GNSS which are simultaneously observed from several GNSS satellites.

Our study focuses on the comparison of STDs, not SIWV. It was thus necessary to convert the WVR SIWV into STDs. Firstly, WVR observations with rain flag and Atmospheric Liquid Water (ALW) values exceeding 1 kg*m⁻² were rejected. Both rain and high values of ALW can significantly distort the quality of WVR measurements. Secondly, SIWV values were converted into Slant Wet Delays (SWD) using the Askne and Nordius (1987) formula and the refractivity constants from Bevis et al. (1994). ZHD values were computed with the precise model given by Saastamoinen (1972). For the described conversions, we used values of the atmospheric pressure and temperature measured in situ of the GNSS reference station POTS. A hydrostatic correction for the altitude difference between the meteorological station and the WVR position was applied to the atmospheric pressure values. ZHD values were mapped to elevation angles of the WVR using the hydrostatic mapping function derived from the NCEP-GFS ([Douša et al., 2016](#)). In order to convert accurately SIWV to STDs, we took into account the influence of the hydrostatic horizontal gradients (see e.g. Li et al., 2015b). We used the hydrostatic horizontal gradients derived from

the NCEP-GFS for that purpose. Finally, SHD and SWD values were summed up to deliver STDs. The described conversion of WVR SIWVs to STDs aimed at minimum distorting the accuracy of original WVR observations.

6 Methodology of STD comparisons

We provide the specificities of each type of technique comparisons in this section. Since NWM outputs are restricted to the time resolution of their predictions (typically one, three or six hours) and since WVR is able to track only one satellite at one moment, all three sources provide different numbers of STDs per day. Therefore, three different comparisons are presented: 1) results for GNSS versus GNSS comparisons, 2) results for GNSS versus NWM comparisons, and 3) results for GNSS versus WVR comparisons. Section 7 presents the validation at individual stations and Section 8 inter-compare results obtained at GNSS dual stations. All the given results are obtained over the whole benchmark period. No outlier detection and removal procedure was applied during the statistics computation within the study.

Two variants of the comparisons are ~~always~~ presented: ‘ZENITH’ and ‘SLANT’. ‘ZENITH’ stands for original STDs mapped back to zenith direction using $1/\sin(e)$ formula. ~~Such This~~ mapping aimed at normalizing STD ~~differences~~ for their evaluation ~~as in a whole single~~ unit. The ‘SLANT’ type of comparison denotes an evaluation of STDs at their actual elevation angles. To be more specific, slant delays were grouped into individual elevation bins of 5 degrees, i.e. for example all slants with an elevation angle between 10 and 15 degrees were evaluated as a single unit. There was one exception regarding the size of a bin since the lowest one contained slants from 7° to 10° elevation angle, 7° being the lowest elevation angle common to all GNSS STD solutions. This cut-off angle was thus used in all GNSS versus GNSS and GNSS versus NWM comparisons.

Presented values of biases and standard deviations were ~~always~~ computed directly from all STDs within the processed benchmark campaign period, therefore they are not based on any kind of daily or other averaging. In some tables, only median values of bias and standard deviation over all GNSS STD solutions (Tables ~~75~~, ~~9-7~~ and ~~108~~) or over all processed stations (Tables 3 and 4) are given to consolidate the presentation of validation results. Median was used as a parameter minimally affected by outliers.

6.1 GNSS versus GNSS comparisons

In the case of individual inter-GNSS solutions validation, the situation was straightforward and no interpolation nor specific hypothesis was necessary: the comparisons were done on a direct point-to-point basis of observations coming from identical azimuth and elevation directions.

6.2 GNSS versus WVR comparisons

To find pairs of STDs observations between WVR and GNSS, the following rules were used: 1) the time difference between both observations had to be shorter than 120 s, and 2) the difference between both azimuth and elevation angles had to be smaller than 2.5° and 0.25° , respectively. From these criteria, the maximum difference in elevation angle has the largest impact

on the number of observation pairs found. Hence the smaller values for these settings, the smaller number of pairs found and the ~~higher~~ smaller standard deviations resulted between GNSS and WVR STDs. As an illustration, a change from 0.35° to 0.25° led to the decrease of the number of STD pairs between the GNSS GFZ solution and the WVR at station POTS from 63,703 to 48,583 pairs; the standard deviation of the projected STD differences in the zenith direction then decreased from 14.6 to 11.7 mm too. Since the bias practically remained unchanged (-6.1 mm versus -5.9 mm), the applied selection procedure mainly influenced the stability of the comparison between WVR and other sources of slant delays. When comparing GNSS versus WVR STDs, a cut-off elevation angle was set to 15 degrees to exclude low-elevation angle observations from WVR as their quality could be further degraded by a ground radiation or other local environment conditions.

6.3 GNSS versus NWM comparisons

Given the very small distances between collocated antennas and the coarse resolution of the global NWM models, STDs from NWM ray-tracing using the ERA-Interim and the NCEP GFS models were derived only for one of the collocated stations. The same set of NWM-derived STDs was then used for the validation of the results at the collocated receivers.

7 Results at individual stations

7.1 GNSS versus GNSS

The total STD pairs available for this part of the validation is roughly 1.7 million, and varies from 140,987 to 206,320 according to the station.

7.1.1 Evaluation of all GNSS solutions versus the reference GNSS solution

Individual GNSS solutions were first compared to the GFZ solution in the zenith direction (ZENITH). We chose the ‘GFZ’ solution as the reference because GFZ Potsdam has long-term experience in producing GPS slant delays and because the GFZ near real-time solution for German GNSS reference stations is already being operationally delivered to the Deutscher Wetterdienst - The German Meteorological Service for NWM assimilation testing purposes (Bender et al., 2016). Figure 4 shows all the solutions using STDs calculated from the estimated ZTD and horizontal gradient parameters, i.e. without adding post-fit residuals. Adding raw or clean residuals, applied consistently to both compared and reference solutions, provided very similar graphs (not displayed). Colours in Figure 4 indicate the processing software used in individual solutions. Medians of all solutions (dotted lines in each bin) are displayed for each station in order to highlight differences among the stations. These were observed mainly as ~~systematic errors~~ biases ranging from -3.6 mm to 0.6 mm. The better agreement between GOP and GFZ solutions could be attributed to a similar strategy of both solutions compared to others. It is particularly visible for LDB0 and POTM stations where median values over all solutions differ by -2.3 mm and -3.6 mm, respectively. The reason for the divergent behaviour at the two stations has not been identified although site metadata were cross-checked carefully. A significant difference can also be noticed for TUV_3 and TUV_7 at the station KIBG where these solutions used individual

antenna calibration files while all others solution used type mean calibration (Schmid et al., 2016). On the other hand, plots with standard deviations show agreements within 3-5 mm among all the stations and all solutions. The only exception is the GOP_F solution representing a simulated real-time analysis applying only a Kalman filter (not backward smoothing) and providing results by a factor of 2 worse compared to the others in terms of precision.

5 7.1.2 Impact of post-fit residuals

All individual GNSS STD solutions were ~~then~~ compared independently using none (nonRES), raw (rawRES) and clean (clnRES) residuals. The comparison aimed at assessing the impact of different strategies for reconstructing GNSS STDs. Figure 5 displays biases and standard deviations for all solutions when comparing STDs with and without raw residuals. Similarly, Figure 6 shows results for STDs with and without clean residuals. Both comparisons demonstrate ~~systematic errors~~ ~~biases~~ at a sub-millimetre level over all stations and solutions. Smaller biases are however observed in the latter case (clnRES) which ~~indicates demonstrates~~ the ~~impact presence~~ of station-specific systematic errors ~~in raw residuals (over all days of the benchmark) when~~ projected into zenith directions. Although the decrease of biases is visible for all solutions, several solutions (GFZ, GOP, WUE) resulted ~~with almost~~ ~~with~~ zero ~~biases values~~ over all the stations. It could be attributed to ~~a better easier possibility of removing removal of~~ systematic effects in PPP as absolute residuals are accessible directly. This is in contrast to ~~the double-difference solutions using double-difference observations (by ROB) which need to with ZD residuals~~ ~~residuals from double-difference ones using representing~~ relative information ~~in original values only~~. Interestingly, the TUW PPP solutions seem to perform similarly to the ROB DD solution in this case.

Comparing standard deviations in both figures demonstrates that the impact of ~~adding cleaning~~ residuals ~~on the precision led to the standard deviations reduced by the factor of 1.2-1.5 overall stations and solutions, namely reaching of the size reached from 2.5 mm to 4.5 mm, while adding for clean residuals compared to 3.0-6.5 mm resulting from raw residuals resulted in increased discrepancies between 3.0 mm and 6.5 mm.~~ The station-specific behaviour is more obvious for the latter rather than for the former; and, generally, the relative performance over all stations is in a good agreement among different solutions ~~applying clean residuals, see~~ Figure 6. In particular, LDB0 and LDB2 stations show ~~a worse quality in performance which was observed already in Figure 4 higher discrepancies for raw residuals, see~~ Figure 5, ~~while their~~ standard deviations were ~~however also~~ significantly reduced after cleaning the residuals ~~and~~ ~~becoming~~ more homogeneous with other stations. In this context it should be noted that the station LDB0 is missing in both ROB solutions since it has been excluded from the network solution during the pre-processing phase due to a lower quality of observations. Besides the GOP_F ~~demonstrating simulated specific real-time solution, showing about 25 % worse standard deviations compared to other solutions in~~ Figure 6, we can ~~also observe by a 12 % worse performance that of the GOP_S solution using forward filtering and backward smoother performs worse provides higher differences by about 25% compared to the other solutions. This Both~~ can be attributed to the stochastic model ~~applied in the GOP software using with the epoch-wise parameter estimation, and and partly also to potential remaining deficiencies in implementations of all applied necessary GNSS models. The latter is considered because the as the only in-house software was the only one has been~~ developed from scratch recently and, in contrast to ~~all~~ others, could not have

been extensively used in a variety of applications. Finally, there are rather small differences observed due to the applied strategy, namely forward versus backward filtering, GPS versus GPS+GLO and the cut-off 3 versus 7 degrees for elevation angles (statistically compared for STDs above the elevation ~~angle~~-cut-off angle of 7 degrees).

Table 3 summarizes statistics related to the figures providing medians and standard deviations over all stations. Notably, ~~systematic errors/biases~~ of STDs (over all stations) expressed in the zenith direction are negligible in all solutions, i.e. not affected by adding raw or clean residuals. The impact of adding raw residuals to the estimated model can be characterized by the median RMS of 3.9 mm (~~see the first two data columns in the table~~) which may vary ~~strongly~~ for different stations, e.g. as evident for stations LDB0 and LDB2 in Figure 5 and Figure 6. Adding In this comparison, the use of cleaned residuals reached shows an overall the impact of 2.8 mm (~~see the middle two data data columns in the table~~) corresponding to a the mean ~~decrease/reduction~~ of 29 %; compared to raw residuals and but up to 50 % for individual problematic stations; such as LDB0 and LDB2, it could reach up to 50 %. This The comparison can be is also understood as the impact of removing systematic errors from the residuals or, in other words, as a degradation of STDs quality when applying uncleaned residuals due to the contamination by ~~these~~ systematic errors. From this reason, While estimating STDs, we it should would not thus not be recommended to adding uncleaned (raw) raw residuals, but cleaned only, when providing STDs from GNSS. However, this ~~comparison does not suggest any preference for~~ either for using purely the estimated model (~~no without residuals~~) or a preference of adding clean residuals to reconstruct STDs. Both approaches still comprise of various errors due to approximations, local environmental effects, instrumentation effects or processing-applied models. Additionally, the impact of cleaning the post-fit residuals for the reconstruction of STDs can be characterized by a median standard deviation SDEV of 2.6 mm when projected into the zenith direction, roughly 25 mm at the elevation of 6 degrees, which is estimahen calculated from differences between STDs using raw and clean residuals STDs over all solutions and stations (last data columns); ~~see the last two data columns in the table~~.

7.1.3 Evaluation of ZTD processing settings

Individual GNSS solutions provided also variants using the same software and strategy, but with modified settings. This allows us to assess its impact on the estimated parameters, see Table 4. Consequently, we evaluated STDs calculated without residuals ~~expecting~~ the impact (mainly) on estimated ZTDs and horizontal gradients. Biases reached a sub-millimetre level and were almost insignificant with a ~~single~~-slight exception of using GMF versus VMF1 mapping function resulting in a positive bias of +1.20.94±0.28 mm over all days and stations. Studied effects were sorted ~~then~~ by the magnitude of ~~their~~ standard deviations. Surprisingly, the The impact of the elevation angle cut-off (3 ° versus 7 °) resulted in a minimum mean median of standard deviation below 1 mm, see TUV_3 and TUV_7. In this regard, it is necessary to mention that the difference between those ~~two solutions comes mainly from estimated horizontal tropospheric gradients since no STDs below 7 ° entered the STD validation. The impact of cut-off angle is also dependable on number and quality of observations below 7 ° which were used in TUV_3 solution and their quality.~~ The use of mapping functions based on climatology (GMF) or meteorological (VMF1) data resulted in a slightly larger impact, at the level of 2 mm, which is similar as the impact found for using single (GPS) or

dual (GPS+GLO) GNSS constellations. The use of different temporal resolutions of ZTDs and gradients could not be avoided among various contributions due to limited capabilities of handling high number of parameters. An assessment of the temporal resolution ~~will be~~ also influenced by applying relative constrains in deterministic approach or setting a noise level in stochastic process. Anyway, we compared two solutions (ROB_V and TUO_R) using the Bernese software and DD method with the same settings, but different temporal resolutions of ZTDs and gradients. The results show discrepancies at a level of 3 mm which could be partly explained by different sampling, ~~h-~~ However, we assume also contributions from specific differences in strategies such as data pre-processing. Last but not least, the impact of using Kalman filter for simulating real-time solution compared to the back-smoother (offline) solutions resulted in the ~~lowest discrepancies agreement represented by standard deviation~~ of 4.8 mm ~~in terms of the standard deviation calculated from differences.~~

7.1.4 Evaluation in the slant direction

Figure 7 provides an evaluation of the STDs at their original elevation angles for the station POTS. Four individual panels show bias (top left), normalized bias (NBIAS, top right), standard deviation (bottom left), and normalized standard deviation (NSDEV, bottom right). Normalized bias and normalized standard deviation were computed to see the dependence of relative errors in STDs at different elevations. For its computation, absolute differences of STDs from two solutions were divided by the STD values from the reference solution. For example, when the solution from GFZ (taken here as the reference) was compared against TUO, the standard deviation was computed from all valid absolute differences given as

$$diff_absolute = STD_{GFZ}^i - STD_{TUO}^i \quad (16)$$

and normalized standard deviation from all valid relative differences given as

$$diff_relative = (STD_{GFZ}^i - STD_{TUO}^i) / STD_{GFZ}^i \quad (17)$$

Since STDs are reconstructed mainly from ZTDs and horizontal gradients, any small differences between the two solutions in the zenith direction should become much larger after mapping down to lower elevations. Therefore, higher values of bias and standard deviation are expected with the decreasing of elevation angle. Indeed, we found that the agreement among individual solutions compared to the GFZ STDs is rather stable above the elevation angle of 30 degrees. Corresponding biases of individual elevation bins are ~~almost constantly~~ within ± 4 mm and standard deviations are slowly increasing up to 10 mm at 30 degrees. ~~With elevation angles decreasing below 30 degrees the biases slightly increase for some solutions. However, both increases significantly for bins below 30 degrees which is mainly pronounced for standard deviations following an exponential decay up to 50 mm at 7 degrees. Biases are also more dependent on solutions and stations, and for example it strongly deviates in the case of ROB_V and ROB_G solutions from the others. Both perform contrary to each other below 30 degrees in particular case of the station POTS while both use the Bernese GNSS Software and the same strategy, but different mapping function only. ROB_V reached mean offsets up to +17 mm for the lowest elevation angles while ROB_G gave mean negative offsets down to -12 mm. Note also that ROB_V is consistent with TUO_G. Since STDs from ROB_V at higher elevations bins are also negative compared to GFZ, it compensated the extreme behaviour at the lowest elevation angles and the overall offset in the zenith direction becomes negative too. The difference between ROB_G and ROB_V biases at low elevations are thus~~

not so apparent in the zenith statistics, but still visible at the level of 1 mm (Figure 4). The positive bias of GMF versus VMF1—visible in Table 4—can be explained as the effect prevailing in the modelling observations at the elevation angles below 30 degrees. Similarly, overall biases in the ROB_V solution compared to ROB_G are found at low elevation angles for all other stations though the situation is not always as significant as for the station POTS. It should be also noted that the conclusion is independent of adding or not any residuals.

In terms of standard deviation, the presumption about the dependency of statistics on the elevation angle is clearly visible in the increasing errors with the decreasing elevation angles (Figure 7)- while following an exponential decay up to 45 mm at 7 degrees. Normalized standard deviation remains almost constant over all elevation angles indicating a very consistent relative performance of STDs among all the solutions. A similar behaviour is present at all stations although the absolute values can be higher for some stations or solutions, namely GOP_F for LDB0 and WTZZ with standard deviations reaching up to 72 mm.

7.2 GNSS versus NWM

STDs from four individual NWM ray-tracing solutions delivered by three different institutions entered the validation (see sections 4.1 - 4.3 for more information). Even the time resolution of NWM is not continuous (only NWM-based results given at 00, 06, 12, and 18 UTC were used), the comparison with GNSS STDs measurements can be used to estimate the quality of the weather prediction. On the other hand, when the meteorological situation is well simulated by NWM, it is relevant for this study to compare model with GNSS observations.~~Only NWM based results given at 00, 06, 12, and 18 UTC were used.~~ To ensure the consistency of the comparison, only epochs for which STD values were available in all GNSS solutions were considered, i.e. if a single STD value was missing in any GNSS solution, then the STD values at the same epoch were also removed from all other GNSS solutions. This selection of observations and the low time resolution of the NWM models (six hours) led to a restricted set of STDs available for the validation consisting of 9,866 of observations in total.

7.2.1 Evaluation of all GNSS solutions without residuals in the zenith direction

Figure 8 presents the comparison of individual NWM STDs and GNSS STDs (without residuals) expressed in the zenith direction. From top to bottom, plots show biases (left) and standard deviations (right) for ALA/BIRA, ERA/GFZ, GFS/GFZ and ALA/WUELS. For most stations, the bias varies between -5 mm and +3 mm for the ALA/BIRA solution, with all GNSS solutions performing similarly. Slightly higher biases and more variability between GNSS solutions are observed at the station POTM. This behaviour is ~~to-accounted~~ed at the side of to the GNSS solutions, since POTM and POTS are collocated and the ALA/BIRA provide the same STDs for the validation at both stations. If we exclude both GOP solutions and the GFZ solution the range of biases at station POTM is very similar to range at station POTS. The difference in height of those two stations is 0.5 m. The station POTS is equipped with a choke ring antenna while the station POTM is not. ~~It,~~ which indicates large multipath effects (see Figure 12) his could causing the slightly higher range of biases ~~for-for~~ individual solutions ~~which occurred~~ at station POTM. Significant biases of approximately -20 mm are present at two Austrian stations, KIBG and SAAL, and being similar for all GNSS solutions. Both stations are situated in the mountainous area south-west of Salzburg city. Since

the same biases do not occur at GNSS versus ERA/GFZ nor GNSS versus GFS/GFZ comparisons, they are most likely due to a deficiency of the ALADIN-CZ orography representation. Note that ALA/BIRA and ALA/WUELS STDs show an unexpected opposite behaviour for KIBG and SAAL stations (Figure 8), which is related to the difference in the strategy used. This is possibly due to the estimation of the altitude of parameters, their interpolations, and the difference in the step of integration. Except at those two stations, similar biases as for ALA/BIRA can be also found for the GNSS versus ERA/GFZ comparison, ranging from -3 mm to +7 mm (+11 mm at POTM). Although the bias characteristics for GFS/GFZ are practically identical to those obtained for ERA/GFZ, the results for the NCEP GFS model are shifted by approximately +5 mm, resulting into biases ranging from +3 mm to +12 mm (+17 mm at POTM). The origin of this systematic deviation was identified in ZWD values estimated from the GFS model (Douša et al., 2016), and understood as the effect of the lower vertical resolution of NCEP GFS model compared to other NWMs, leading to larger errors in vertical interpolations.

Standard deviations between GNSS STDs and ALA/BIRA, ERA/GFZ and GFS/GFZ solutions are usually around 10 mm when projected into the zenith. Generally, they are higher than the comparison of individual GNSS solutions presented in Section 7.1 and they are also more station dependent. Degradations can be observed at mountainous stations KIBG and SALL for the ERA/GFZ, GFS/GFZ, and ALA/BIRA STDs, reaching standard deviations up to 18 mm in case of the ERA-Interim NWM.

ALA/WUELS solution performed differently compared to all other NWM solutions. It is biased against GNSS solutions, with biases ranging from +9 mm to +25 mm and highest values observed at stations KIBG and SAAL. Standard deviation values are also much higher, by about a factor of 2.5 worse compared to values obtained from the GNSS versus GFS/GFZ comparison. The probable reason for this is that signal tracking was performed for vacuum elevation angles. As we discuss in the following sub-chapter ~~The-this~~ impact is especially visible at low elevation ray-paths at which the signal has to travel through the troposphere for a longer time, enhancing the negative effect of underestimated delays.

~~Finally, Evaluation of the influence of raw and cleaned post-fit residuals on slant total delays~~ ~~Chyba! Nenalezen zdroj odkazů.~~ Comparisons between the three versions of GNSS solutions (nonRES, clnRES, rawRES) and the ALA/BIRA, ERA/GFZ, and GFS/GFZ NWM solutions were done to test the influence of post-fit residuals on GNSS STDs. The ALA/WUELS solution was excluded from this comparison because of the lower quality of its STDs. All GNSS solutions without post-fit residuals reached slightly lower standard deviation values than the solutions which included either raw or cleaned post-fit residuals, while differences in biases were negligible (not displayed). An average increase of standard deviation was 4.5 % for clean residuals and 8.3 % for raw residuals. Indeed, because of their low horizontal and time resolution, the used NWP models can barely capture the very fine-scale tropospheric structures which are supposed to be included in the GNSS residuals. As a consequence, this comparison does not allow to conclude clearly on the potential benefits of ~~cleaned~~-post-fit residuals in the reconstruction of the GNSS STDs.

7.2.2 Evaluation in the slant direction

Statistics from the comparison of ALA/BIRA, ERA/GFZ and GFS/GFZ against all three versions of GNSS GFZ solutions expressed at original elevation angles of slant delays are presented for the station POTS in Figure 9. ~~Full lines display the median over all GNSS solutions and dashed lines represent minimum and maximum ranges.~~ Significantly higher biases can be found at the lowest elevation bin in all three solutions and at all stations (not displayed). At some stations, sudden increases of bias at individual elevation bins were observed. They happened at any ~~kind of~~ elevation angle (different for each ~~3 comparisons~~ NWM STD solution) and ~~we~~ are particularly visible in terms of normalized bias. -These sudden increases of the bias might ~~found its~~ origin either in the fact that the model sometimes cannot render the tropospheric structures at their exact locations (unexpected location of high/low values of water vapour partial pressure), or because models running at these resolutions have a tendency to smooth out such tropospheric heterogeneities. Comparing with a model running at convective-permitting scale (e.g. 1 to 4 km) would help to sort out if the origin of such behaviours is to account on the NWP model STD side or on the GNSS STD side.

For all stations, standard deviations present the shape with significantly higher values at elevations below thirty degrees followed by more a gentle decrease towards the zenith direction. An exception was found at stations WTZR, WTZS and WTZZ where a rather smooth shape of the curve is disrupted with sudden ~~increases and decreases of~~ changes of standard deviation at particular bins over all elevation angles. This implies mainly for GNSS versus ALA/BIRA solution. GNSS versus ERA/GFZ and GNSS versus GFS/GFZ results show such ~~increases and decreases~~ changes low less frequently and with ~~a~~ lower magnitude by a factor of two or three. Normalized standard deviations vary at all elevation angles for all validated stations without distinct common characteristics. ~~The V~~ values range between 0.2 % and 0.9 % with the highest values ~~usually~~ occurring usually at high elevation angles.

Results from the GNSS versus ALA/WUELS solutions (not ~~presented~~ displayed) show enormous increase of both absolute and normalized bias and standard deviations at low elevation angles below 25 degrees at all stations. It ~~even~~ reached biases up to 350 mm and standard deviations up to 300 mm at some stations. Statistical parameters became more stable above 25 degrees, with occasional disturbances similar to those observed in other NWM-based solutions.

7.2.3 Summary of results for GNSS versus NWM

A summary of the GNSS versus NWM validation is presented in Table 5. For each reference station a median of bias and a median of standard deviation in the zenith direction between all GNSS solutions and a particular NWM-based solution are given. If we consider ALA/BIRA and ERA/GFZ only, without the two mountainous stations KIBG and SAAL, absolute biases between NWM and GNSS solutions stay mostly below 3 mm, which represents a very good agreement between these independent sources used for retrieving slant delays. Standard deviations generally range from 8 mm to 12 mm in the zenith projection, with the exception of ALA/WUELS showing lower precision by a factor of 2.5.

In this paper, statistics stems from the complete benchmark period, and it should be noted that the ~~stability-daily variation on a daily time scale was much better for~~ of GNSS STDs ~~was much lower~~ than ~~for~~ of NWM ray-traced STDs. Significantly higher values of biases and standard deviations were observed at particular days for NWM solutions. A detail evaluation of daily statistics with a respect to the extreme weather conditions is one of the topics that we will study in future.

5 7.3 GNSS versus WVR

Figure 10 compares GNSS and WVR solutions at stations POTM and POTS, in the zenith direction. The number of slant observations which entered the comparison was 32,794 at station POTM and 36,070 at station POTS. Two remarks can be done on the evaluation of biases. Firstly, an overall bias of about 4 mm between the stations POTM and POTS, ~~identified visible~~ for all GNSS solutions ~~already~~ in Figure 8, indicates a common issue with the GNSS data processing at the station POTM. ~~It, was~~ particularly ~~diverging-increased~~ for GOP_F, GOP_S and GFZ ~~PPP~~ solutions. Secondly, a bias of about 5.5 mm in the zenith direction can be found between WVR and GNSS solutions ~~even~~ at station POTS. This bias roughly corresponds to 1 kg/m² of Integrated Water Vapour (IWV), what can be addressed as the achievable accuracy of any technique, ~~however, WVR accuracy is more dependent on a proper instrument calibration-~~.

Values of standard deviation, resulting mostly in 12 mm, are higher than ~~what was those~~ observed in ~~any~~ GNSS versus GNSS comparisons (Section 7.1). ~~It is als and e~~ slightly higher than ~~from the~~ GNSS versus NWM comparisons (Section 7.2). A cut-off elevation angle of 15- ~~degrees~~ was used for the comparison ~~of GNSS versus with~~ WVR STDs ~~instead of, 7 ° used in contrast to the validations in~~ of other ~~sources (7 °) validations~~. ~~Consequently, the largest differences in STD values found at very low elevation angles did not enter this validation-~~ Additionally, it has to be noted that the results can be partly influenced with the settings applied for finding pairs between GNSS and WVR STDs (Section 6). STDs from WVR can thus originate from slightly different azimuth/elevation angles and times than the GNSS ones. All GNSS solutions perform ~~very~~ similarly against WVR, ~~with exception of the~~ GOP_F ~~as expected~~ due to ~~applying a the~~ real-time ~~capable methodology strategy applied~~. ~~The GNSS versus WVR validation at the station POTS using original elevation angles is displayed in Figure 11. Although some differences between GNSS solutions are visible, all of them performed in a very similar manner. The decrease of values of four statistical parameters strongly follows the increase of elevation angle and, generally, it is steeper than statistics dependency of GNSS versus NWM. It indicates that slant delays from WVR below 40 ° becomes generally unreliable which is particularly clear from~~ ~~Although some differences between solutions are visible, all of them performed very similarly. High values of the normalized biases and standard deviations at lower elevation angles indicate difficulties for the WVR to provide high quality observations at low elevations. A sudden increase of the values is visible observed at elevations of elevations between 55–60 degrees most likely originating from WVR observations which has not been understood yet.~~

Generally, standard deviations for all solutions using cleaned residuals (resp. raw residuals) are in average 1.7 % (resp. 3.8 %) higher than for the solutions without residuals. ~~Although the d~~ Differences between solutions variants are smaller ~~due to an overall higher uncertainty of WVR observations, however, the situation results is are~~ in a good agreement with ~~those results~~ obtained for GNSS versus NWM comparisons presented in Section ~~7.4~~7.1.

Cleaning of post fit residuals proved to be valuable, however, the difference between versions of solutions with no residuals and cleaned residuals are too small to allow a decision if residuals should be avoided at all or if the cleaning filter still needs improvements to better benefits the STD reconstruction. Therefore, more investigation around the post fit residuals cleaning needs to be done.

5 ~~The GNSS versus WVR validation at the station POTS using original elevation angles is displayed in Figure 11. The decrease of values of four statistical parameters strongly follows the increase of elevation angle. Although some differences between solutions are visible, all of them performed very similarly. High values of the normalized standard deviation at lower elevation angles indicate difficulties for the WVR to provide high quality observations at low elevations. A sudden increase of the values is visible at elevations between 55–60 degrees most likely originating from WVR observations which has not been understood yet.~~

8 Results Validation of results at dual-located stations

Always two erroneous techniques for STD retrievals have been compared in previous sections (GNSS vs. NWM, GNSS vs. WVR) without knowing the true reference. The errors stem from the observation noise on one hand and, from the processing models including the model for adjusted parameters on the other hand. From this perspective, the higher standard deviations for GNSS STD solutions applying clean residuals compared to those using adjusted GNSS parameters only (without residuals) do not necessarily mean the lower quality of the former. GNSS and NWM models with limited temporal and spatial approximations are not able to represent true signal tropospheric delays between a receiver and all visible satellites. The simplifications certainly result in better agreement of STDs without residuals in Eq.1, however, hardly represent the true tropospheric path delays, deviating particularly during the events with high spatio-temporal variations in the troposphere.

20 For this reasons, we assessed all GNSS solutions at the collocated (dual) stations as for such constellation we are able to provide troposphere-free differences of STDs to evaluate noise of GNSS STD retrievals. We particularly focused on days with a high variability in the troposphere selected from the benchmark period. Dual stations were available in the benchmark campaign at three different locations in Germany. The first two sites collocate twin GNSS reference stations (LDB0+LDB2 and POTM+POTS), the third location collocate three individual reference stations (WTZR+WTZS+WTZZ). Nevertheless, in the case of Wettzell, only results for WTZR+WTZS are presented due to their similarity with the two other combinations at the same place. Characteristics of the stations are summarized in Table 6. ~~This comparison aims at validating the (internal) accuracy of STDs based on the presumption that STDs from collocated receivers should be very similar from the atmospheric point of view. Results are presented hereafter for each location.~~

8.1 Slant residuals and slant delay differences

30 STD validations in this paper were done for two months of the benchmark during which heavy rain events occurred for some days, particularly May 30 – June 43, June 9-11 and June 21-26, all causing severe flooding in Central Europe. During normal

weather conditions, the tropospheric variation is reasonably smooth, meaning it can be well represented by GNSS STDs reconstructed from ZTDs and horizontal gradients. However, during high temporal or spatial variabilities in the troposphere, post-fit residuals certainly contain tropospheric signals which were not modelled. If they surpass the observation noise and other residual errors from GNSS models, cleaned residuals should be considered in the GNSS STD model as described in Eq.1.

5 In order to initially address optimal STD modelling under different weather conditions within the benchmark, we tried to identify days with a high variability in the troposphere. Daily standard deviations of cleaned post-fit residuals were computed individually for each day of the benchmark, for every station and GNSS solution for 1-degree elevation angle bins. We studied their daily variations considering the GNSS model applied. If cleaned post-fit residuals consist of the noise of observations only, the variation in time should be negligible. However, the days showing significantly higher values, correlated at all

10 collocated stations, indicate highly variable tropospheric conditions.

Three such days were identified at LDB0, LDB2, POTM and POTS stations (May 31, June 20, June 23) and two days at WTZR and WTZS stations (June 19, June 20). They all very well correspond to the days initiating heavy precipitations in the domain, Douša et al. (2016). Typical differences between raw and clean residuals are displayed in Figure 12 for all elevations during the normal day (June 19, DOY 170) and the day with high variability in the troposphere (DOY 171, June 20) for LDB0, LDB2,

15 POTM and POTS stations using GFZ solution. Obviously, the variability of clean residuals (black dots) and their 2-sigma envelopes are higher by a factor of 2two for the day of year 171 compared to 170. The variability is clearly visible over all elevations, but the increase is slightly higher at low elevations. The plots for these four stations clearly demonstrates the different quality of GNSS observations, particularly related to a multipath effect displayed by 2-sigma envelop (green curves). Low multipath is common to the stations using choke ring antennas, in our case POTS and LDB2, however, LDB2 still suffer

20 from unknown systematic effects at 35-55 ° elevations. Very high multipath effect was observed particularly at LDB0 station over all elevations. Variability of 2-sigma envelopes of clean residuals (red curves) indicates a higher sensitivity of clean residuals to the weather conditions compared to station selection and observation quality, thus suggesting a significant contribution from the troposphere to the cleaned residuals. In the same context, raw residuals show much higher sensitivity to the observation quality compared to different weather conditions, which is particularly true in case of LDB0 and LDB2 stations.

25 Elevation-dependent differences of STDs using clean residuals (black dots) are displayed in Figure 13 for the same days as in Figure 12, selecting GFZ solution and station pairs WTZS–WTZR and LDB0–LDB2. Additionally, 2-sigma envelopes are plotted for differences without residuals (red curves), clean residuals (green curves) and raw residuals (blue curves).

Firstly, we can notice that STD differences are more or less similar for both days, i.e. no significantly different between days with normal and high variations in the troposphere which is found common to other days of the benchmark. It suggests that

30 increased residuals in Figure 12 for DOY 171 contain strong contributions from the tropospheric effect that could not have been assimilated into ZTDs and tropospheric horizontal gradients. Alternative explanation suggests a possible contribution of satellites-specific errors common to both receivers, thus easily eliminated in STD differences at the dual stations. However, systematic errors at satellites are well absorbed by initial phase ambiguities in PPP and short-term or random errors, e.g. such as due to satellite clocks, are in this study eliminated by the use of final products, i.e. stable enough to avoid observed day-to-

day variability in cleaned residuals. The DOY 171 thus shows the situation when cleaned residuals contain a tropospheric signal that should be added to the STD retrievals. In the case of GFZ, the contribution from residuals is particularly important due to local troposphere variation in time when using model of piece-wise constant function with 15 minutes time resolution for ZTD and 60 minutes for horizontal gradients. It is not so obvious in case of a stochastic process using for epoch-wise estimates of all tropospheric parameters. However, the uncertainty of estimated parameters is then higher compared to the deterministic model, which is more difficult to separate errors in estimated parameter and errors due to insufficiency of the linearized tropospheric model in time.

Secondly, we can see that envelopes of differences using raw residuals are always the largest ones. Raw residuals vary more with the elevation angle, which is particularly visible for differences LDB0–LDB2. Obviously, it is due to the large systematic errors at LDB0 station and additional contribution from LDB2 errors observed at 35-55 ° elevations. The 2-sigma envelopes of STD differences with clean residuals smoothly follows the 2-sigma envelop of STDs differences without residuals, keeping the difference within ±15 mm over all elevations. It indicates a stable and reliable usage of clean residuals under any conditions. On the other hand, applying raw residuals at problematic sites may seriously degrade STDs as observed at LDB0 station. Finally, we can consider that error contribution from both stations to STD differences at dual stations is equal, i.e.

$$\delta_{STD_dif}^2 = 2 \delta_{STD_res}^2 \quad (18)$$

with $\delta_{STD_dif}^2$ variance calculated from cleaned STD differences at specific elevations when using the same processing strategy at both dual stations and, with $\delta_{STD_res}^2$ characterizing the variance over errors in GNSS STD retrievals corresponding to the observation elevation angle and the applied strategy. Although we can notice some differences in $\delta_{STD_dif}^2$ in collocations, partly due to differences in contributions from both stations, the relative performance of differences from STDs with clean residuals (green curves) and without residuals (red curves) for different days remains similar. Uncertainties of the simplified STDs at low elevations surpass additional uncertainties due to applying clean residuals (green curves vs red curves). According to the magnitude of clean residuals at these elevations (Figure 12), the small uncertainties from calculated differences indicate the presence of tropospheric signals in the residuals at low elevations, roughly below 30 degrees. It seems to be almost independently from the weather conditions and is supposed to represent mainly unmodelled horizontal asymmetry in the troposphere. However, further study on detail impact of residuals on GNSS STDs modelling during severe weather conditions requires longer data set which will be subject of our upcoming study.

Figure 14 displays results for comparison of individual dual stations in the slant directions calculated from all days of the benchmark. The same statistics and plots (not displayed) were prepared also for days identified with ‘severe’ weather conditions, but only minor differences were observed. Strong variations are observed mainly in normalized biases over all elevation angles for the solutions using raw post-fit residuals (rawRES) regardless weather conditions type. These are clearly related to local effects such as multipath or modelling instrumented related effects instrumentation (phase centre offsets and variations) and disappears after the using the cleaned residuals, cleaning as obvious from the solutions using cleaned residuals (cInRES). The standard deviations and normalized standard deviations at all stations are clearly the lowest for variants

~~not without~~ using post-fit residuals (nonRES), ~~a slightly little worse higher when~~ using ~~cleaned~~ residuals, and ~~by much significantly worse higher~~ when using raw residuals, i.e. corresponding to above performed inter-technique validations.

8.2 Differences in zenith direction

Table 7 and Table 8 show the statistics expressed in the zenith direction for observations ~~at~~ ranging at elevation angles from 7
5 to 15 and from 15 to 90 degrees, respectively. Median values computed over all GNSS solutions for which residuals were available are presented. Results for the identified days with high daily tropospheric variation are given in the upper part of the table – days are stated in the previous section. In the bottom part results for selected days with low daily variation of post-fit residuals are presented. These days were the same for all collocated stations: May 25, May 30, June 6 (DOY 145, 150, 157).
~~The b~~Biases ~~remains stay~~ very stable regardless the severe weather occurrence and if post-fit residuals are used or not. The
10 lowest ~~values of~~ standard deviations are can be always found related for to the solutions without using post-fit residuals ~~(nonRES), indicating that the residuals are still strongly site specific, i.e. not only representing the effect due to the local asymmetry in the water vapour distribution around the GNSS station. Additionally, by cleaning the systematic portion in residuals, we are not able to remove all instrumentation, multipath or other local effects sufficiently. Anyway, using raw post fit residuals from GNSS analysis without additional cleaning should always be avoided.~~ Interestingly, comparing the
15 statistics for STDs evaluated separately from for ranges of 7-15 and 15-90 elevation degree ~~ranges~~, ~~the~~ standard deviations are smaller in high elevations compared to low elevations for variant ~~not without~~ using residuals, ~~while these are and in the opposite way vice versa for higher for low elevations when using either variants using either~~ cleaned or raw residuals. This can be interpreted as the standard GNSS tropospheric model (ZTD and horizontal gradients) represents ~~very~~ well observations at elevations above 15 degrees, but suffers by the modelling deficiencies mainly at low elevations. These statistics also supports
20 the above statement that cleaned residuals are valuable particularly for reconstructing low-elevation STDs regardless the weather conditions as they certainly contain non-negligible tropospheric signal from high-order horizontal asymmetry. The negative effect of adding cleaned or raw residuals is then more pronounced in the statistics for STDs at high elevations. During the days with high variation of residuals, the all standard deviations the SDEV values are almost always usually a little bit higher than during the days with low variation, however, there is no difference between these two regarding the above described above
25 general mentioned behaviour patterns.

9 Conclusions

~~In this paper, w~~We presented results of validating tropospheric slant total delays obtained from GNSS data processing with those obtained from NWM ray-tracing, WVR measurements and collocated GNSS stations, ~~focusing on in search of~~ the optimal method for estimating GNSS STDs. Ten GNSS reference stations were selected, exploiting data from ~~the~~ a 56-day
30 COST ES1206 B benchmark campaign period. Eleven GNSS solutions, four NWM-based solutions and one WVR-based dataset entered this validation study. Eight out of eleven GNSS solutions delivered STDs in three variants: 1) without post-fit

residuals, 2) with raw post-fit residuals, and 3) with cleaned post-fit residuals. The comparisons were carried out into two scenarios, firstly for STDs at their true elevation angles, and secondly, for STD differences mapped into the zenith direction using a common simple mapping function of $1/\sin(e)$, e being the elevation angle.

All GNSS solutions without residuals were compared against the GNSS solution without residuals provided by GFZ Potsdam, which was selected as the reference. Almost all solutions were in a very good mutual agreement although many different software, strategies and settings were used. Absolute biases between GFZ and other solutions were within ± 3 mm for all individual stations and standard deviations were ranging from 3 mm to 5 mm in the zenith direction. An exception was the GOP_F solution—designed for a real time demonstration capability—with standard deviations around 7 mm. Comparisons of variants of individual STD solutions without residuals, with raw and with cleaned residuals were used to study the impact of different strategies for optimally retrieving STDs from GNSS (i.e. including a maximum of relevant information relative to the asymmetry of the local troposphere). The impact of cleaning residuals led to the standard deviations reduced by the factor of 1.2-1.5 over all stations and solutions, namely reaching 2.5-4.5 mm in the zenith direction for clean residuals compared to 3.0-6.5 mm resulting from raw residuals, the latter. The impact of adding cleaned residuals reached 2.5—4.5 mm in the zenith direction, while using raw residuals instead resulted in increased discrepancies at the level of 3.0—6.5 mm, also being highly with a pronounced station dependency dependent. The impact of adding raw or cleaned residuals was practically negligible in terms of systematic errors biases which remaining remained all the time around within ± 0.1 mm for raw residuals and less than ± 0.1 mm for cleaned residuals, thus fully negligible.

GNSS STDs were then validated against STDs obtained from NWM ray tracing. Biases and standard deviation values between GNSS and NWM solutions strongly depend ed on applied ray-tracing method, NWM source and individual station location. Significantly worse results, by a factor of 2.5 in terms of standard deviation, were shown observed for the ALA/WUELS solution. The originating in was identified as mainly a deficiency in of the the applied ray-tracing methodology. Generally, Biases biases in the zenith direction remained usually were below ± 3 mm for other solutions ALA/BIRA and ERA/GFZ solutions, while with the exception of a positive bias of around 65 mm was observed for GFS/NWM GFS solution NWM model. Standard deviations for all GNSS versus NWM STD comparisons were similar at the level of with a small oscillation around 10 mm, when excluding the ALA/WUELS solution. Contrary to the GNSS versus GNSS comparisons, no Normalized standard deviation values showed pronounced did not variability remain stable throughout with the all elevation angles as in the case of GNSS versus GNSS comparisons.

Using the simulation of delays from ALADIN-CZ weather model, we illustrated the impact of the hydrostatic, wet and hydrometeors contributions to zenith and slant delays. These showed strong horizontal variations allowing relevant characterisation of mesoscale meteorological situations. Visualising the slant anisotropic variation of total, hydrostatic, wet and hydrometeor delays in a common sky plot illustrated a weak hydrostatic anisotropy (up to 5.8 mm) which was almost the same as the hydrometeors one (up to 6 mm). The largest anisotropy was induced by water vapour (up to 20 mm), but the total anisotropy was much weaker (12 mm) due to the compensation of mean hydrostatic and hydrometeor anisotropies oriented in

~~the opposite direction. Their values varied at all elevation angles and over all stations reaching often the lowest values at elevation angles below 15 degrees.~~

~~GNSS STD solutions from stations POTM and POTS were validated against collocated WVR observations pointed to GNSS satellites. A positive bias of about 5.5 mm was and 10 mm was found for the WVR instrument when it was compared to GNSS STDs from for POTS and POTM station, respectively. Standard deviations for from comparisons of GNSS versus WVR comparisons STDs reached about 12 mm in the zenith direction, and were higher than thus the higher compare with to NWM solutions. Normalized standard deviations revealed a strong elevation dependency indicating the WVR observations lack the quality at low elevations, particularly below 40 degrees. GNSS STDs without post fit residuals agreed slightly better than their versions including either raw or cleaned residuals.~~

~~STDs from collocated GNSS reference stations using the same solution were confronted in order to validate the impact of post-fit residuals. For this purpose, Collocated GNSS stations at three different locations were evaluated used to evaluate the quality of GNSS STD retrievals applying statistics over troposphere-free STD differences from theoretical point of view. We could observe strong systematic errors in raw residuals at any elevation angles, particularly at stations without the choke ring antenna, such as LDB0 and POTM. We found a strong elevation dependency of bias when using raw residuals which almost vanished when cleaning the residuals from visible systematic errors. It suggests not recommending use of raw residuals, at least without any information about possible systematic errors. Although the simplified STDs reconstructed from the estimated GNSS tropospheric parameters performed the best in all the comparisons, it obviously missed part of tropospheric signals due to non-linear temporal and spatial variations in the troposphere. Identifying low and high variability in the troposphere during all days in the benchmark, we showed that residuals contain significant tropospheric signals in addition to the simplified model, particularly during highly variable troposphere. Additionally, we also identified tropospheric signals at low elevations due to a non-linear horizontal asymmetry in cleaned residuals regardless of the station selection and the quality of its observations. From such finding, we recommend the use of cleaned residuals for an optimal STD retrievals from GNSS, at least for low elevation angles and during a high variability in the troposphere. We also haven't seen any obvious degradation of STD retrievals in other conditions.~~

~~The better inter-solution and inter-technique agreements of STDs without residuals compared to those using clean residuals are attributed to the too simple tropospheric model resulting in smooth and robust STDs and, consequently, not containing all interesting signals from the troposphere. STDs from all solutions without including post fit residuals reached always the lowest standard deviations compared to the solutions with post fit residuals. We found a strong elevation dependency of bias for the variant using raw residuals and the discrepancies were observed generally larger for higher than smaller elevation angles. This strong elevation dependency almost vanished for the variant using cleaned residuals.~~

~~Based on this validation study, we do not recommend adding raw post fit residuals into STDs since residuals still contain systematic effects which surpass the tropospheric information content. As already mentioned in Bender et al. (2008) and Kačmařík et al. (2012), cleaning post fit residuals improves the situation considerably the agreement between GNSS and WVR STDs compared to using only raw residuals. However, similarly to what was found by Kačmařík et al. (2012), variants of~~

~~GNSS STD solutions generated without post-fit residuals still reached better agreement with NWM and WVR solutions than those with cleaned residuals indicating probably that we are currently not able to remove completely all other effects due to obtain only the local troposphere information. The use of clean residuals for STD retrievals could be therefore recommended only after improving the strategy to screen and remove all undesirable effects what is a matter of a further study. On the other hand, most of the majority of evaluated the GNSS solutions used deterministic models with rather long validity of one hour or less for the estimating-estimated tropospheric parameters horizontal gradients, which assumes that the first order asymmetry in the troposphere can be at least partly captured by them, although often averaged by potentially low temporal resolution compared to their real dynamics. for which the residuals are important to overcome modelling deficiencies of low-resolution parameter estimates in time. Our future study will be focused on the evaluation of GNSS STDs estimated using a stochastic process easily applicable in real-time and, on a long-term evaluation of azimuthal-dependency of post-fit residuals under specific-severe weather conditions.~~

~~It has to be also noted that used WVR and NWM STDs have their own limitations and part of the difference originates just from the fact that different techniques sense by essence differently the local asymmetry of the troposphere. Unless the NWM model is run at a convection-permitting scale with proper physics models inside and with a quick update cycle and the WVR is correctly calibrated and delivers observations exactly in the direction of GNSS satellites at desired epochs, STDs from those two techniques can be hardly as reliable as is needed.~~

~~Last but not least, we should discuss an additional complexity of the GNSS processing when using cleaned post-fit residuals to reconstruct the STDs. In addition to the standard GNSS data processing, i.e. the estimation of ZTD/ZWD and horizontal gradient parameters, information about azimuth/elevation angles for all observations and corresponding residuals need to be stored along with all solutions. The cleaning of systematic effects (e.g. multipath, environmental effects and antenna phase centre variations) requires statistical information about the residuals over tens of days in order to provide reliable stacking maps characterizing them properly. All that lead to additional complexities and increased computation load when targeting operational provision of STDs (including cleaned residuals) for weather forecasting.~~

Acknowledgement

This study has been organised within the E.U. COST Action ES1206 (GNSS4SWEC). The authors thank all the institutions that provided data for the benchmark campaign (~~Douša et al., 2016~~) on which the validation was based on. Namely we want to thank S. Heise (GFZ) for providing the WVR data. The GFS data were provided by the National Centers for Environmental Prediction (www.ncep.noaa.gov). The ERA-interim data were provided by the European Centre for Medium-Range Weather Forecasts (<http://www.ecmwf.int/en/forecasts/datasets>). M. Kačmařík, J. Douša and P. Václavovic acknowledge the support from the Czech Ministry of Education, Youth and Sports (project no. LD14102). E. Pottiaux (ROB) and H. Brenot (BIRA) acknowledge the support from the Solar-Terrestrial Centre of Excellence (STCE). J. Kapłon and P. Hordyniec (WUELS) acknowledge the support of Polish National Science Centre (project no. UMO-2013/11/D/ST10/03473) for financial support

and Wrocław Center of Networking and Supercomputing (<http://www.wcss.wroc.pl>) for computational grant using Matlab Software License No: 101979.

References

- Alber, Ch., Ware, R., Rocken, Ch., Braun, J.: Obtaining single path phase delays from GPS double differences, *Geophysical Research Letters*, Vol. 27, pp. 2661-2664, doi: 10.1029/2000gl011525, 2000.
- 5
- Askne, J., and Nordius, H.: Estimation of Tropospheric Delay for Microwaves from Surface Weather Data, *Radio Science*, 22 (3), 379–386, doi: 10.1029/rs022i003p00379, 1987.
- Atmosphere, US Standard. NASA TM-X 74335. National Oceanic and Atmospheric Administration. National Aeronautics and Space Administration and United States Air Force, 1976.
- 10
- Bauer, H.-S., Wulfmeyer, V., Schwitalla, T., Zus, F. and Grzeschik, M.: Operational assimilation of GPS slant path delay measurements into the MM5 4DVAR system, *Tellus A*, 63, 2, doi: 10.1111/j.1600-0870.2010.00489.x, 2011.
- Bender, M., Dick, G., Wickert, J., Schmidt, T., Shong, S., Gendt, G., Ge, M. and Rothacher, M.: Validation of GPS slant delays using water vapour radiometers and weather models, *Meteorologische Zeitschrift*, Vol. 6, No. 17, pp. 807-812, doi: 10.1127/0941-2948/2008/0341, 2008.
- 15
- Bender, M., Dick, G., Wickert, J., Ramatschi, M., Ge, M., Gendt, G., Rothacher, M., Raabe, A. and Tetzlaff, G.: Estimates of the information provided by GPS slant data observed in Germany regarding tomographic applications, *J. Geophys. Res.*, 114, D06303, doi:10.1029/2008JD011008, 2009.
- Bender, M., Stosius, R., Zus, F., Dick, G., Wickert, J. and Raabe, A.: GNSS water vapour tomography: Expected improvements by combining GPS, GLONASS and Galileo observations, *Advances in Space Research*, 47(5), 886–897, doi: 10.1016/j.asr.2010.09.011, 2011.
- 20
- Bender, M., Stephan, K., Schraff, Ch., Reich, H., Rhodin, A., Potthast, R.: GPS Slant Delay Assimilation for Convective Scale NWP, Fifth International Symposium on Data Assimilation (ISDA), University of Reading, UK, July 18-22, 2016.
- Bennitt, E. and Jupp, A.: Operational Assimilation of GPS Zenith Total Delay Observations into the Met Office Numerical Weather Prediction Models, *Monthly Weather Review*, 140(8), pp. 2706-2719, doi: 10.1175/MWR-D-11-00156.1, 2012.
- 25
- Bevis, M., Businger, S., Chiswell, S., Herring, T., Anthes, R., Rocken, C. and Ware, R.: GPS Meteorology: Mapping Zenith Wet Delays onto Precipitable Water, *Journal of Applied Meteorology*, 33, 379–386, doi: 10.1175/1520-0450(1994)033<0379:gmmzwd>2.0.co;2, 1994.

- Böhm, J., Werl, B., and Schuh, H.: Troposphere mapping functions for GPS and very long baseline interferometry from European Centre for Medium-Range Weather Forecasts operational analysis data, *J. Geophys. Res.*, 111, B02406, doi:10.1029/2005JB003629, 2006a.
- Böhm, J., Niell, A., Tregoning, P., and Schuh, H.: Global MappingFunction (GMF): A new empirical mapping function based on numerical weather model data, *Geophys. Res. Lett.*, 33, L07304, doi:10.1029/2005GL025546, 2006b.
- Böhm, J. and Schuh, H.: Vienna mapping functions. In Proc. 16th Working Meeting on European VLBI for Geodesy and Astrometry, pp. 131-143, Leipzig, Germany, Verlag des Bundesamtes für Kartographie und Geodäsie, 2003.
- Braun, J., Rocken, Ch. and Ware, R.: Validation of line-of-sight water vapour measurements with GPS, *Radio Science*, Vol. 36, Num. 3, pp. 459-472, doi: 10.1029/2000rs002353, 2001.
- 10 Braun, J., Rocken, Ch. and Liljergen, J.: Comparisons of Line-of-Sight Water Vapor Observations Using the Global Positioning System and a Pointing Microwave Radiometer, *Journal of Atmospheric and Oceanic Technology*, Vol. 20, pp. 606-612, doi: 10.1175/1520-0426(2003)20<606:colosw>2.0.co;2, 2002.
- Brenot, H.: Potential of ground-based GPS measurements for the study of Mediterranean heavy rains. PhD of the French State, <http://tel.archives-ouvertes.fr/tel-00012085>, 2006.
- 15 Brenot, H., Neméghaire, J., Delobbe, L., Clerbaux, N., De Meutter, P., Deckmyn, A., Delcloo, A., Frappez, L. and Van Roozendael, M.: Preliminary signs of the initiation of deep convection by GNSS, *Atmos. Chem. Phys.*, 13, 5425–5449, doi:10.5194/acp-13-5425-2013, 2013.
- Chen, G., and Herring, T. A.: Effects of atmospheric azimuthal asymmetry on the analysis of space geodetic data, *J. Geophys. Res.*, 102(B9), 20489–20502, doi:10.1029/97JB01739, 1997.
- 20 Dach, R., Lutz, S., Walser, P., and Fridez, P. (Eds): Bernese GNSS Software Version 5.2. User manual, Astronomical Institute, University of Bern, Bern Open Publishing, doi: 10.7892/boris.72297, ISBN: 978-3-906813-05-9, 2015.
- [Dee, D. P., Uppala, S. M., Simmons, A. J. et al.: The ERA-Interim reanalysis: Configuration and performance of the data assimilation system, *Q. J. Roy. Meteor. Soc.*, 137, 553–597, doi: 10.1002/qj.828, 2011.](#)
- Deng, Z., Bender, M., Zus, F., Ge, M., Dick, G., Ramatschi, M., Wickert, J., Löhnert, U. and Schön, S.: Validation of tropospheric slant path delays derived from single and dual frequency GPS receivers, *Radio Science*, 46, RS6007, doi:10.1029/2011RS004687, 2011.
- 25 Douša, J. and Václavovic, P.: Real-time zenith tropospheric delays in support of numerical weather prediction applications. *Advances in Space Research*, 53(9):1347-1358, doi:10.1016/j.asr.2014.02.021, 2014.

- Douša, J., Dick, G., Kačmařík, M., Brožková, R., Zus, F., Brenot, H., Stoycheva, A., Möller, G. and Kaplon, J.: Benchmark campaign and case study episode in Central Europe for development and assessment of advanced GNSS tropospheric models and products, *Atmospheric Measurement Techniques*, 9, pp. 2989-3008, doi:10.5194/amt-9-2989-2016, 2016.
- De Haan, S., Marel, van der H., and Barlag, S.: Comparison of GPS slant delay measurements to a numerical model: case study of a cold front passage, *Physics and Chemistry of the Earth*, Vol. 27, pp. 317-322, doi: 10.1016/s1474-7065(02)00006-2, 2002.
- Flores, A., Rius, A., Vilá-Guearou, J. and Escudero, A.: Spatio-temporal tomography of the lower troposphere using GPS signals, *Phys. Chem. Earth (A)*, Vol. 26, No. 6-8, 405-411, doi: 10.1016/s1464-1895(01)00074-6, 2001.
- Gradinarsky, L. P.: Sensing Atmospheric Water Vapor Using Radio Waves, Ph.D. thesis, School of Electrical Engineering, Chalmers University of Technology, Göteborg, Sweden, 2002.
- Guerova, G., Bettems, J. M., Brockmann, E. and Matzler, C.: Assimilation of COST 716 Near-Real Time GPS data in the nonhydrostatic limited area model used at MeteoSwiss, *Meteorology and Atmospheric Physics*, vol. 91, Issue 1-4, pp. 149-164, doi: 10.1007/s00703-005-0110-6, 2006.
- Guerova, G., Jones, J., Dousa, J., Dick, G., de Haan, S., Pottiaux, E., Bock, O., Pacione, R., Elgered, G., Vedel, H., and Bender, M.: Review of the state-of-the-art and future prospects of the ground-based GNSS meteorology in Europe, *Atmos. Meas. Tech. Discuss.*, doi:10.5194/amt-2016-125, in review, 2016.
- Ha, S.-Y, Kuo, Y.-H., Guo, Y.-R., Rocken, C., and Van Hove, T.: Comparison of GPS slant wet delay measurements with model simulations during the passage of a squall line, *Geophysical Research Letters*, Vol. 29(23), 28/1-4, doi: 10.1029/2002gl015891, 2002.
- ~~Herring T. A.: Modelling atmospheric delays in the analysis of space geodetic data, In: de Munck, J. C., Spoelstra, T. A. T. (eds), Proceedings of the symposium refraction of transatmospheric signals in geodesy. The Netherlands, The Hague, 157-164, 1992.~~
- Hobiger, T., Ichikawa, R., Koyama, Y. and Kondo, T.: Fast and accurate ray-tracing algorithms for real-time space geodetic applications using numerical weather models. *Journal of Geophysical Research: Atmospheres*, 113(D20), doi: 10.1029/2008jd010503, 2008.
- Kačmařík, M., Douša, J. and Zapletal, J.: Comparison of GPS slant wet delays acquired by different techniques, *Acta geodynamica et geomaterialia*, Vol. 9, No. 4(168), pp. 427-433, 2012.
- Kawabata, T., Shoji, Y., Seko, H. and Saito, K.: A Numerical Study on a Mesoscale Convective System over a Subtropical Island with 4D-Var Assimilation of GPS Slant Total Delays, *Journal of the Meteorological Society of Japan*, Vol. 91, No. 5, pp. 705-721, doi:10.2151/jmsj.2013-510, 2013.

- Lemoine, F. G., Kenyon, S. C., Factor, J. K., Trimmer, R. G., Pavlis, N. K., Chinn, D. S., Cox, C. M., Klosko, S. M., Luthcke, S. B., Torrence, M. H., Wang, Y. M., Williamson, R. G., Pavlis, E. C., Rapp, R. H. and Olson T. R.: The development of the joint NASA GSFC and the National Imagery and Mapping Agency (NIMA) geopotential model EGM96, NASA/TP—1998–206861, doi: 10.1007/978-3-662-03482-8_62, 1998.
- 5 Li, X., Zus, F., Lu, C., Dick, G., Ning, T., Ge, M., Wickert, J. and Schuh, H.: Retrieving of atmospheric parameters from multi-GNSS in real time: Validation with water vapor radiometer and numerical weather model, *J. Geophys. Res. Atmos.*, 120, doi:10.1002/2015JD023454, 2015a.
- Li, X., Zus, F., Lu, C., Ning, T., Dick, G., Ge, M., Wickert, J. and Schuh, H.: Retrieving high-resolution tropospheric gradients from multiconstellation GNSS observations. *Geophysical Research Letters*, 42, 4173-4181, doi:10.1002/2015GL063856,
10 2015b.
- MacMillan, D. S.: Atmospheric gradients from very long baseline interferometry observations. *Geophys. Res. Lett.*, 22, 1041–1044, doi:10.1029/95GL00887, 1995.
- Mahfouf, J.-F., Ahmed, F., Moll, P. and Teferle, F. N.: Assimilation of zenith total delays in the AROME France convective scale model: a recent assessment, *Tellus A*, 67, 26106, doi:10.3402/tellusa.v67.26106, 2015.
- 15 Möller, G., Wittmann, C., Yan, X., Umnig, E., Joldzic, N. and Weber, R.: 3D ground based GNSS atmospheric tomography, Final Report GNSS-ATom, Austrian Research Promotion Agency (FFG), 9th call, project number 940098, 2016.
- Morel, L., Pottiaux, E., Durand, F., Fund, F., Boniface, K., de Oliveira, P.-S. and Van Baelen, J.: Validity and behaviour of tropospheric gradients estimated by GPS in Corsica. *Adv. Space Res.*, <http://dx.doi.org/10.1016/j.asr.2014.10.004>, 2014.
- Nafisi, V., Urquhart, L., Santos, M. and Nievinski, F., Böhm, J., Wijaya, D., Schuh, H., Ardalan, A., Hobiger, T., Ichikawa,
20 R., Zus, F., Wickert, J. and Gegout, P.: Comparison of ray-tracing packages for troposphere delays, *IEEE Transactions on Geoscience and Remote Sensing*, 50, 469–481, doi:10.1109/TGRS.2011.2160952, 2012.
- Rocken C., Sokolovskiy, S., Johnson, J.M., Hunt, D.: Improved Mapping of Tropospheric Delays, *Journal of Atmospheric and Oceanic Technology*, Vol. 18, pages 1205-1213, doi: 10.1175/1520-0426(2001)018<1205:imotd>2.0.co;2, 2001.
- Rueger, J. M.: Refractive index formulae for radio waves, FIG XXII International Congress, USA, April 19-26, 2002.
- 25 Saastamoinen, J.: Atmospheric Correction for the Troposphere and Stratosphere in Radio ranging of satellites, *Geophys. Monogr. Ser.*, 15, 247–251, doi: 10.1029/gm015p0247, 1972.
- Schmid, R., Dach, R., Collilieux, X., Jäggi, A., Schmitz, M., and Dilssner, F.: Absolute IGS antenna phase center model igs08.atx: status and potential improvements, *Journal of Geodesy*, Vol. 90, 343-364, doi:10.1007/s00190-015-0876-3, 2016.
- Shang-Guan, M., Heise, S., Bender, M., Dick, G., Ramatschi, M. and Wickert, J.: Validation of GPS atmospheric water vapor
30 with WVR data in satellite tracking mode, *Ann. Geophys.*, 33, 55–61, doi:10.5194/angeo-33-55-2015, 2015.

- Shoji, J. Nakamura, H., Iwabuchi, T., Aonashi, K., Seko, H., Mishima, K., Itagaki, A., Ichikawa, R. and Ohtani, R.: Tsukuba GPS dense net campaign observation: Improvement in GPS analysis of slant path delay by stacking one-way postfit phase residuals, *Journal of the Meteorological Society of Japan*, 82, No. 1B, 301–314, doi: 10.2151/jmsj.2004.301, 2004.
- Shoji, Y., Kunii, M. and Saito, K.: Assimilation of Nationwide and Global GPS PWV Data for a Heavy Rain Event on 28 July 2008 in Hokuriku and Kinki, Japan, *Scientific Online Letters on the Atmosphere*, Vol. 5, pp. 45-48, doi:10.2151/sola.2009-012, 2009.
- Shoji, Y., Yamauchi, H., Mashiko, W. and Sato, E.: Estimation of Local-scale Precipitable Water Vapor Distribution Around Each GNSS Station Using Slant Path Delay, *SOLA*, Vol. 10, 29–33, doi:10.2151/sola.2014-007, 2014.
- Trojáková, A.: The NWP activities at CHMI, Joint 26th ALADIN Workshop & HIRLAM All Staff Meeting 2016, Lisbon, Portugal, April 4-8, 2016.
- ~~Teke, K., Böhm, J., Nilsson, T., Schuh, H., Steigenberger, P., Dach, R., Heinkelmann, R., Willis, P., Haas, R., Garcia Espada, S., Hobiger, T., Ichikawa, R., and Shimizu, S.: Multi-technique comparison of troposphere zenith delays and gradients during CONT08, *Journal of Geodesy*, 85, 7, pp. 395–413, doi: 10.1007/s00190-010-0434-y, 2011.~~
- Václavovic, P., Douša, J. and Györi, G.: G-Nut software library - state of development and first results, *Acta Geodyn. Geomater*, Vol. 10, No. 4 (172), pp 431-436, doi:10.13168/AGG.2013.0042, 2013.
- Václavovic, P. and Douša, J.: Backward smoothing for precise GNSS applications, *Advances in Space Research*, 56(8):627-1634, doi:10.1016/j.asr.2015.07.020, 2015.
- Vedel, H. and Huang, X.: Impact of Ground Based GPS Data on Numerical Weather Prediction, *Journal of the Meteorological Society of Japan*, Vol. 82, No. 1B, pp. 459-472, doi: 10.2151/jmsj.2004.459, 2004.
- Zumberge, J. F., Heflin, M. B., Jefferson, D. C., Watkins, M. M., and Webb, F. H.: Precise point positioning for the efficient and robust analysis of GPS data from large networks, *J. Geophys. Res.*, 102(B3), 5005–5017, doi:10.1029/96JB03860, 1997.
- Zus, F., Bender, M., Deng, Z., Dick, G., Heise, S., Shang-Guan, M. and Wickert, J.: A methodology to compute GPS slant total delays in a numerical weather model, *Radio Sci.*, 47, RS2018, doi:10.1029/2011RS004853, 2012.
- Zus, F., Dick, G., Heise, S., Douša, J., and Wickert, J., The rapid and precise computation of GPS slant total delays and mapping factors utilizing a numerical weather model, *Radio Science*, Vol. 49(3), pp. 207-216, doi: 10.1002/2013rs005280, 2014.
- Zus, F., Douša, J., Dick, G. and Wickert, J.: Station specific NWM based tropo parameters for the Benchmark campaign, ES1206-GNSS4WEC COST Workshop, Iceland, March 8-10, 2016.

Table 1: Characteristics of 10 GNSS reference stations.

Name	Latitude [°]	Longitude [°]	Height [m]	Network	Dual station	Receiver	Antenna
GOPE	49.914	14.786	593	IGS, EPN		TPS NET-G3	TPSCR.G3 TPSH
KIBG	47.449	12.309	877			TPS GB-1000	TPSCR3_GGD CONE
LDB0	52.210	14.118	160		LDB2	JAVAD TRE_G2T	JAV_GRANT-G3T NONE
LDB2	52.209	14.121	160		LDB0	JPS LEGACY	LEIAR25.R4 LEIT
POTM	52.379	13.066	145		POTS	JAVAD TRE_G3TH	JAV_GRANT-G3T NONE
POTS	52.379	13.066	144	IGS, EPN	POTM	JAVAD TRE_G3TH DELTA	JAV_RINGANT_G3T NONE
SAAL	47.426	12.832	796			TPS GB-1000	TPSCR3_GGD CONE
WTZR	49.144	12.879	666	IGS, EPN	WTZS, WTZZ	LEICA GRX1200+GNSS	LEIAR25.R3 LEIT
WTZS	49.145	12.895	663	IGS	WTZR, WTZZ	SEPT POLARX2	LEIAR25.R3 LEIT
WTZZ	49.144	12.879	666	IGS	WTZR, WTZS	JAVAD TRE_G3TH DELTA	LEIAR25.R3 LEIT

Table 2: Information about individual GNSS-based STD solutions used in the validation.

Solution Name	Institution	Strategy	Software	GNSS	Elev. cut-off	Mapping function	Products	ZTD/gradients interval	ZD post-fit residuals
CNAM	ESGT CNAM	DD	GAMIT	GPS	3°	VMF1	IGS final	1h / 1h	NO
GFZ	GFZ Potsdam	PPP	EPOS 8	GPS	7°	GMF	GFZ	15min / 1h	YES
GOP_F	GO Pecný	PPP	G-Nut/Tefnut	GPS	7°	GMF	IGS final	2.5min / 2.5min	YES
GOP_S	GO Pecný	PPP	G-Nut/Tefnut	GPS	7°	GMF	IGS final	2.5min / 2.5min	YES
ROB_G	ROB	DD	Bernese 5.2	GPS+GLO	3°	GMF	CODE final	15min / 1h	YES
ROB_V	ROB	DD	Bernese 5.2	GPS+GLO	3°	VMF1	CODE final	15min / 1h	YES
TUO_R	TU Ostrava	DD	Bernese 5.2	GPS+GLO	3°	VMF1	CODE final	1h / 3h	NO
TUO_G	TU Ostrava	DD	Bernese 5.2	GPS	3°	VMF1	CODE final	1h / 3h	NO
TUW_3	TU Vienna	PPP	NAPEOS	GPS+GLO	3°	GMF	ESA final	30min / 1h	YES
TUW_7	TU Vienna	PPP	NAPEOS	GPS+GLO	7°	GMF	ESA final	30min / 1h	YES
WUE	WUELS	PPP	Bernese 5.2	GPS	3°	VMF1	CODE final	2.5min / 1h	YES

Table 3: Statistics from comparisons of individual GNSS STDs (projected in the zenith direction) while using none, raw and clean residuals; median values of biases and standard deviations (SDEV) calculated over all stations with an exception of LDB0 station are given.

Solution	nonRES – rawRES		nonRES – clnRES		rawRES – clnRES	
	Bias [mm]	SDEV [mm]	Bias [mm]	SDEV [mm]	Bias [mm]	SDEV [mm]
GFZ	+0.02 ± 0.03	3.88 ± 0.51	-0.01 ± 0.01	2.77 ± 0.19	-0.01 ± 0.03	2.73 ± 0.67
GOP_F	-0.00 ± 0.02	4.69 ± 0.41	+0.00 ± 0.01	3.43 ± 0.19	-0.01 ± 0.01	3.14 ± 0.50
GOP_S	-0.00 ± 0.01	4.39 ± 0.42	-0.01 ± 0.00	3.12 ± 0.16	-0.01 ± 0.01	2.99 ± 0.53
ROB_G	+0.02 ± 0.05	3.59 ± 0.66	+0.02 ± 0.02	2.66 ± 0.30	+0.00 ± 0.04	2.37 ± 0.67
ROB_V	+0.01 ± 0.05	3.58 ± 0.67	+0.02 ± 0.02	2.66 ± 0.30	+0.01 ± 0.04	2.37 ± 0.67
TUW_3	+0.03 ± 0.06	3.90 ± 0.75	-0.01 ± 0.04	2.85 ± 0.35	-0.02 ± 0.06	2.63 ± 0.78
TUW_7	+0.04 ± 0.05	3.89 ± 0.75	-0.01 ± 0.04	2.80 ± 0.35	-0.02 ± 0.04	2.60 ± 0.78
WUE	+0.02 ± 0.04	3.64 ± 0.49	+0.00 ± 0.01	2.54 ± 0.19	-0.02 ± 0.04	2.50 ± 0.66

Table 4: Impact of selected strategy modifications assessed via comparing individual STDs solution variants. Median values of biases and standard deviations (SDEV) calculated over all stations with an exception of LDB0 station using the estimated model only (without residuals) are given.

<u>Compared solutions</u>	<u>Remarks on solution differences</u>		<u>Bias [mm]</u>	<u>SDEV [mm]</u>
<u>TUW_3 – TUW_7</u>	<u>Elevation angle cut-off:</u>	<u>3° versus 7°</u>	<u>+0.46 ± 0.69</u>	<u>0.98 ± 0.45</u>
<u>ROB_G – ROB_V</u>	<u>Mapping function:</u>	<u>GMF versus VMF1</u>	<u>+1.20 ± 0.20</u>	<u>1.91 ± 0.27</u>
<u>TUO_G – TUO_R</u>	<u>GNSS observations:</u>	<u>GPS versus GPS+GLO</u>	<u>+0.66 ± 0.37</u>	<u>2.01 ± 0.47</u>
<u>ROB_V – TUO_R</u>	<u>ZTD/gradient resolution:</u>	<u>15min/1h versus 1h/3h</u>	<u>-0.19 ± 0.34</u>	<u>3.10 ± 0.40</u>
<u>GOP_F – GOP_S</u>	<u>Processing strategy:</u>	<u>Kalman filter versus backward smoothing</u>	<u>-0.60 ± 0.55</u>	<u>4.81 ± 0.79</u>

<u>Compared solutions</u>	<u>Remarks on solution differences</u>		<u>Bias [mm]</u>	<u>SDEV [mm]</u>
<u>TUW_3 – TUW_7</u>	<u>Elevation angle cut-off:</u>	<u>3° versus 7°</u>	<u>+0.46 ± 0.69</u>	<u>0.98 ± 0.45</u>
<u>ROB_G – ROB_V</u>	<u>Mapping function:</u>	<u>GMF versus VMF1</u>	<u>+0.94 ± 0.28</u>	<u>1.90 ± 0.27</u>
<u>TUO_G – TUO_R</u>	<u>GNSS observations:</u>	<u>GPS versus GPS+GLO</u>	<u>+0.18 ± 0.32</u>	<u>1.95 ± 0.37</u>
<u>ROB_V – TUO_R</u>	<u>ZTD/gradient resolution:</u>	<u>15min/1h versus 1h/3h</u>	<u>+0.28 ± 0.18</u>	<u>3.24 ± 0.30</u>
<u>GOP_F – GOP_S</u>	<u>Processing strategy:</u>	<u>Kalman filter versus backward smoothing</u>	<u>-0.60 ± 0.55</u>	<u>4.81 ± 0.79</u>

Table 5: Medians of bias and standard deviation values of differences between all GNSS solutions and a particular NWM-based solution at each reference station, expressed in the zenith direction.

Station	Bias (mm)				Standard deviation (mm)			
	ALA/BIRA	ERA/GFZ	GFS/GFZ	ALA/WUELS	ALA/BIRA	ERA/GFZ	GFS/GFZ	ALA/WUELS
GOPE	-0.0	-2.9	-8.3	11.1	-8.4	10.3	-7.2	22.4
KIBG	-19.2	-5.0	-9.7	22.6	11.7	17.7	11.0	26.7
LDB0	-1.1	-1.6	-6.4	11.5	10.0	10.4	-8.9	26.2
LDB2	-1.5	-1.0	-6.2	15.1	-9.2	10.1	-8.7	25.4
POTM	-2.8	-5.7	12.0	18.4	-8.0	10.6	-9.4	26.2
POTS	-1.9	-1.3	-7.4	12.4	-7.7	10.3	-9.2	25.8
SAAL	-19.9	-7.3	11.1	23.8	12.6	17.7	11.7	22.9
WTZR	-4.6	-1.5	-4.9	10.4	10.8	11.7	-8.5	22.9
WTZS	-3.1	-0.5	-4.7	11.2	11.4	12.1	-8.5	23.6
WTZZ	-2.4	-0.9	-5.9	11.6	11.4	12.1	-9.1	23.7

Station	Bias (mm)				Standard deviation (mm)			
	ALA/BIRA	ERA/GFZ	GFS/GFZ	ALA/WUELS	ALA/BIRA	ERA/GFZ	GFS/GFZ	ALA/WUELS
<u>GOPE</u>	<u>0.3</u>	<u>3.3</u>	<u>8.6</u>	<u>11.5</u>	<u>8.3</u>	<u>10.3</u>	<u>7.1</u>	<u>22.4</u>
<u>KIBG</u>	<u>-19.3</u>	<u>4.9</u>	<u>9.6</u>	<u>22.5</u>	<u>11.6</u>	<u>17.8</u>	<u>11.0</u>	<u>26.7</u>
<u>LDB0</u>	<u>-2.0</u>	<u>0.7</u>	<u>5.5</u>	<u>10.6</u>	<u>9.9</u>	<u>10.3</u>	<u>8.5</u>	<u>26.2</u>
<u>LDB2</u>	<u>-1.6</u>	<u>0.9</u>	<u>6.1</u>	<u>15.1</u>	<u>9.1</u>	<u>10.1</u>	<u>8.6</u>	<u>25.4</u>
<u>POTM</u>	<u>3.4</u>	<u>6.3</u>	<u>12.5</u>	<u>18.9</u>	<u>8.0</u>	<u>10.6</u>	<u>9.4</u>	<u>26.2</u>
<u>POTS</u>	<u>-1.7</u>	<u>1.4</u>	<u>7.6</u>	<u>12.5</u>	<u>7.7</u>	<u>10.3</u>	<u>9.2</u>	<u>25.8</u>
<u>SAAL</u>	<u>-19.4</u>	<u>7.8</u>	<u>11.7</u>	<u>24.3</u>	<u>12.7</u>	<u>17.9</u>	<u>11.8</u>	<u>22.9</u>
<u>WTZR</u>	<u>-4.8</u>	<u>-1.5</u>	<u>4.9</u>	<u>10.2</u>	<u>11.0</u>	<u>11.8</u>	<u>8.5</u>	<u>23.1</u>
<u>WTZS</u>	<u>-3.5</u>	<u>-0.9</u>	<u>4.2</u>	<u>10.8</u>	<u>11.4</u>	<u>12.3</u>	<u>8.7</u>	<u>23.7</u>
<u>WTZZ</u>	<u>-2.1</u>	<u>0.9</u>	<u>6.0</u>	<u>11.6</u>	<u>11.3</u>	<u>12.0</u>	<u>8.9</u>	<u>23.7</u>

Table 6: Characteristics of individual dual stations.

Dual station	Location	Horizontal distance (m)	Vertical distance (m)	Identical type of receiver	Identical type of antenna	Pairs of observations
LDB0+LDB2	Lindenberg	177	0.6	NO	NO	143,005
POTM+POTS	Potsdam	2.5	-0.5	NO	NO	180,636
WTZR+WTZS	Wetzell	69	2.6	NO	YES	84,443

Table 7: Comparison of GNSS STDs from the elevation angles ranging from 7 to 15 degrees at three dual stations; results for days with high daily variability of cleaned post-fit residuals, results for days with low daily variability of post-fit residuals in the bottom part; median values of biases and standard deviations (SDEV) calculated over all GNSS STD solutions are given; statistics are expressed in the zenith direction.

	<u>nonRES</u>		<u>clnRES</u>		<u>rawRES</u>	
	<u>Bias</u> <u>[mm]</u>	<u>SDEV</u> <u>[mm]</u>	<u>Bias</u> <u>[mm]</u>	<u>SDEV</u> <u>[mm]</u>	<u>Bias</u> <u>[mm]</u>	<u>SDEV</u> <u>[mm]</u>
<u>LDB0+LDB2</u>	<u>-1.60</u>	<u>3.47</u>	<u>-1.58</u>	<u>4.43</u>	<u>-1.57</u>	<u>5.35</u>
<u>POTM+POTS</u>	<u>-6.00</u>	<u>1.91</u>	<u>-5.98</u>	<u>3.20</u>	<u>-6.67</u>	<u>4.00</u>
<u>WTZR+WTZS</u>	<u>-0.11</u>	<u>2.13</u>	<u>-0.09</u>	<u>3.34</u>	<u>-0.05</u>	<u>3.87</u>

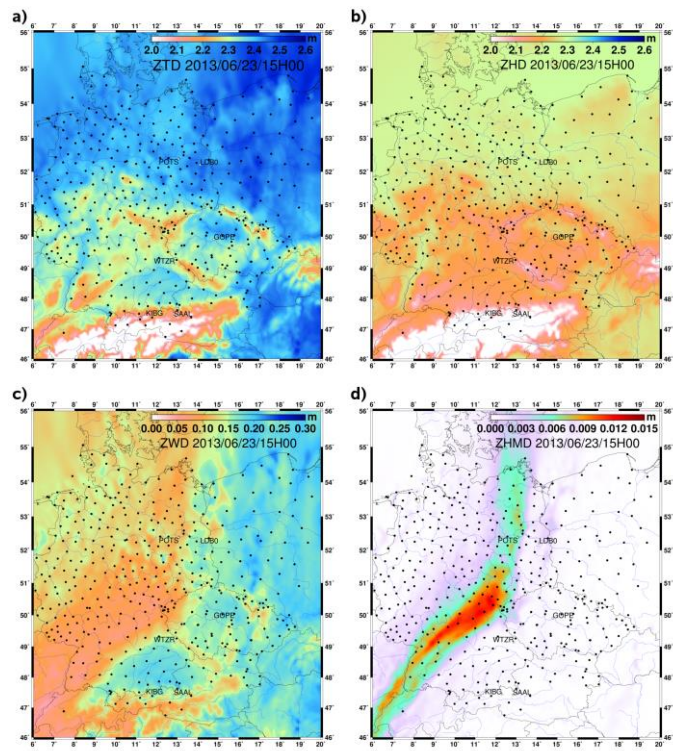
5

	<u>nonRES</u>		<u>clnRES</u>		<u>rawRES</u>	
	<u>Bias</u> <u>[mm]</u>	<u>SDEV</u> <u>[mm]</u>	<u>Bias</u> <u>[mm]</u>	<u>SDEV</u> <u>[mm]</u>	<u>Bias</u> <u>[mm]</u>	<u>SDEV</u> <u>[mm]</u>
<u>Days with high variability of post-fit residuals</u>						
<u>LDB0+LDB2</u>	<u>-1.56</u>	<u>4.63</u>	<u>-1.44</u>	<u>5.51</u>	<u>-1.52</u>	<u>5.89</u>
<u>POTM+POTS</u>	<u>-5.24</u>	<u>1.89</u>	<u>-5.16</u>	<u>3.47</u>	<u>-5.91</u>	<u>4.24</u>
<u>WTZR+WTZS</u>	<u>-0.24</u>	<u>2.31</u>	<u>-0.06</u>	<u>3.25</u>	<u>-0.03</u>	<u>3.77</u>
<u>Days with low variability of post-fit residuals</u>						
<u>LDB0+LDB2</u>	<u>-0.52</u>	<u>3.06</u>	<u>-0.52</u>	<u>4.23</u>	<u>-0.59</u>	<u>5.05</u>
<u>POTM+POTS</u>	<u>-4.97</u>	<u>1.87</u>	<u>-5.03</u>	<u>3.00</u>	<u>-5.79</u>	<u>3.87</u>
<u>WTZR+WTZS</u>	<u>-0.01</u>	<u>1.87</u>	<u>-0.05</u>	<u>3.22</u>	<u>-0.09</u>	<u>3.82</u>

Table 8: Comparison of GNSS STDs from the elevation angles ranging from 15 to 90 degrees at three dual stations; results for days with high daily variability of cleaned post-fit residuals, results for days with low daily variability of post-fit residuals in the bottom part; median values of biases and standard deviations (SDEV) calculated over all GNSS STD solutions are given; statistics are expressed in the zenith direction.

-	<u>nonRES</u>		<u>elnRES</u>		<u>rawRES</u>	
	<u>Bias [mm]</u>	<u>SDEV [mm]</u>	<u>Bias [mm]</u>	<u>SDEV [mm]</u>	<u>Bias [mm]</u>	<u>SDEV [mm]</u>
<u>LDB0+LDB2</u>	<u>-0.56</u>	<u>3.11</u>	<u>-0.55</u>	<u>5.17</u>	<u>-0.46</u>	<u>7.97</u>
<u>POTM+POTS</u>	<u>-6.14</u>	<u>1.68</u>	<u>-6.13</u>	<u>3.26</u>	<u>-6.08</u>	<u>4.54</u>
<u>WTZR+WTZS</u>	<u>-0.22</u>	<u>1.96</u>	<u>-0.21</u>	<u>3.93</u>	<u>-0.22</u>	<u>5.17</u>

-	<u>nonRES</u>		<u>elnRES</u>		<u>rawRES</u>	
	<u>Bias [mm]</u>	<u>SDEV [mm]</u>	<u>Bias [mm]</u>	<u>SDEV [mm]</u>	<u>Bias [mm]</u>	<u>SDEV [mm]</u>
<u>Days with high variability of post-fit residuals</u>						
<u>LDB0+LDB2</u>	<u>-0.92</u>	<u>4.19</u>	<u>-0.88</u>	<u>6.13</u>	<u>-0.88</u>	<u>8.87</u>
<u>POTM+POTS</u>	<u>-5.28</u>	<u>1.68</u>	<u>-5.30</u>	<u>3.39</u>	<u>-5.30</u>	<u>4.64</u>
<u>WTZR+WTZS</u>	<u>-0.53</u>	<u>2.29</u>	<u>-0.56</u>	<u>4.12</u>	<u>-0.49</u>	<u>5.21</u>
<u>Days with low variability of post-fit residuals</u>						
<u>LDB0+LDB2</u>	<u>-0.07</u>	<u>2.59</u>	<u>-0.07</u>	<u>4.93</u>	<u>0.04</u>	<u>7.83</u>
<u>POTM+POTS</u>	<u>-4.96</u>	<u>1.82</u>	<u>-4.92</u>	<u>3.30</u>	<u>-4.93</u>	<u>4.65</u>
<u>WTZR+WTZS</u>	<u>-0.01</u>	<u>1.74</u>	<u>-0.05</u>	<u>3.77</u>	<u>0.02</u>	<u>5.07</u>



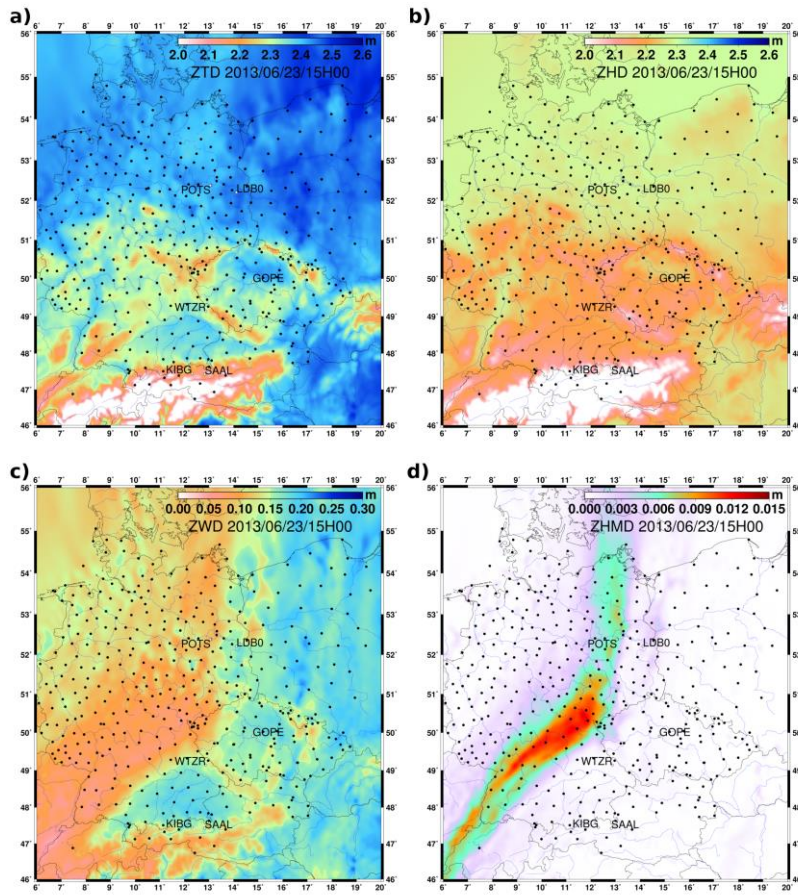


Figure 1: Simulation of ZTD, ZHD, ZWD and ZHMD at 15:00 UTC on 23 June 2013. Each black dot represents a GNSS station included in the benchmark dataset. For stations included in this STD validation study their names are given.

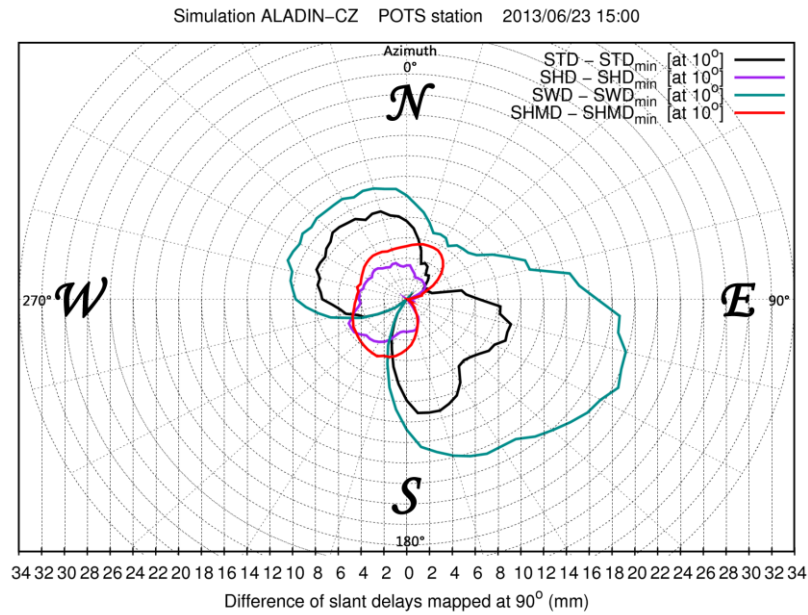
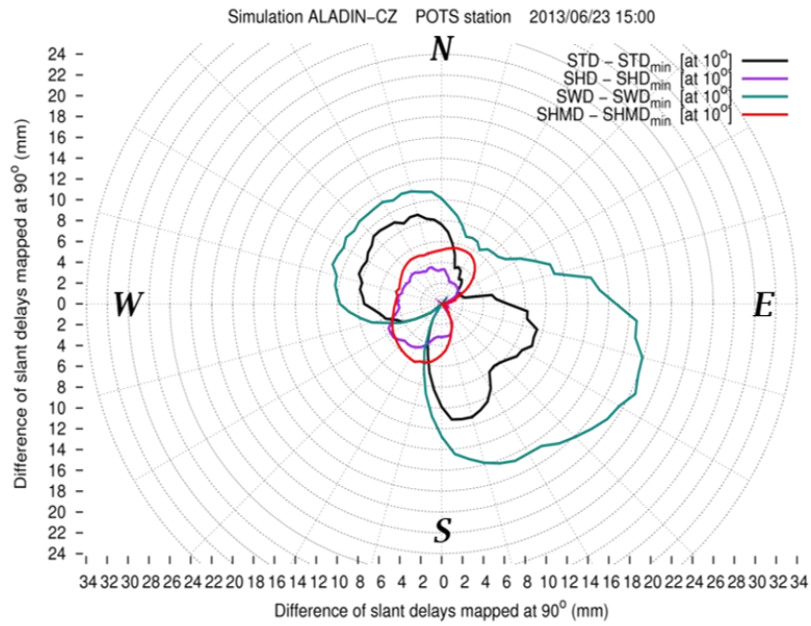


Figure 2: Skyplot of differential slant delays simulated at 10° and mapped at 90° , for a 360° azimuthal range (at 15:00 UTC on 23 June 2013). For total, hydrostatic, wet and hydrometeors delays, a differential slant delay is the difference between a slant delay simulated and the respective minimum value (obtained considering slant delays simulated at 10° elevation along all the azimuthal directions).

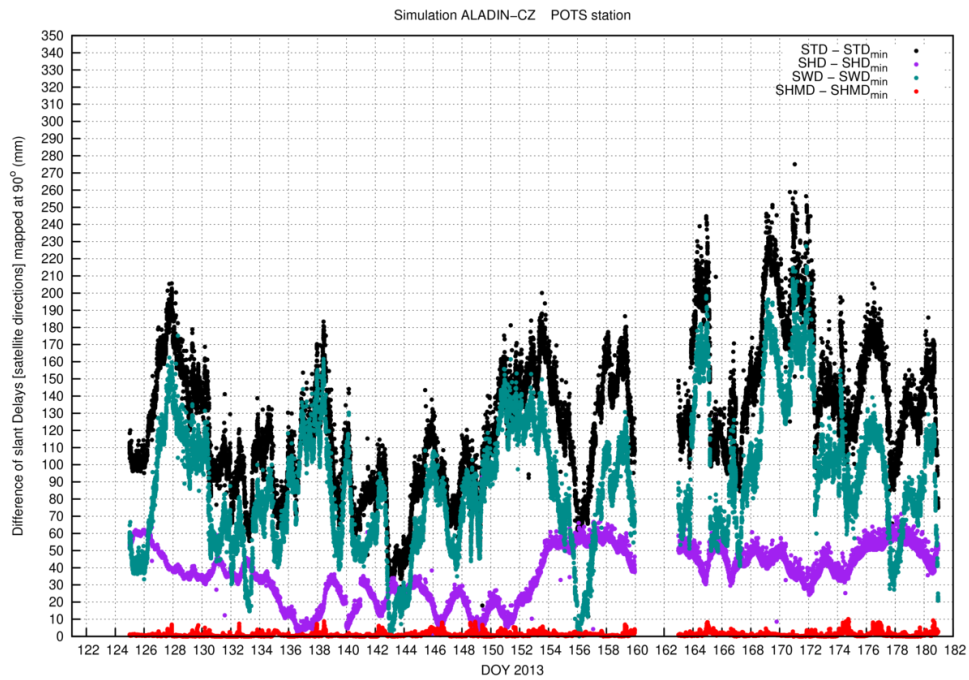


Figure 3: Time-series of slant delays (STD, SHD, SWD, and SHMD) differences (in direction of all GNSS visible satellites, then mapped in the zenith direction) during the whole period of the benchmark campaign for the station POTS.

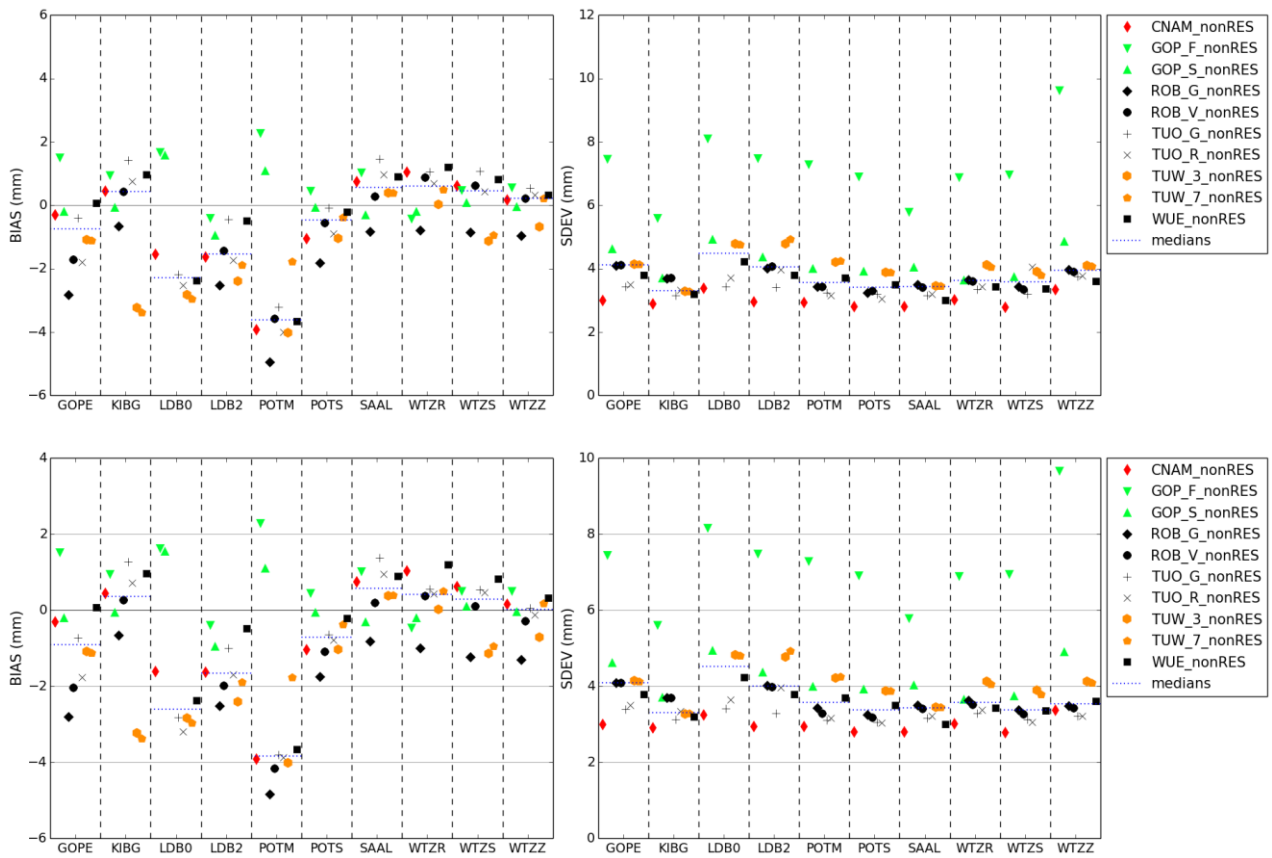


Figure 4: Comparison of individual GNSS STD solutions against GFZ solution, all without using residuals (nonRES) and projected in the zenith direction: bias (left) and standard deviation (right). The median value of all solutions at each station is represented by the dotted blue line in each bin.

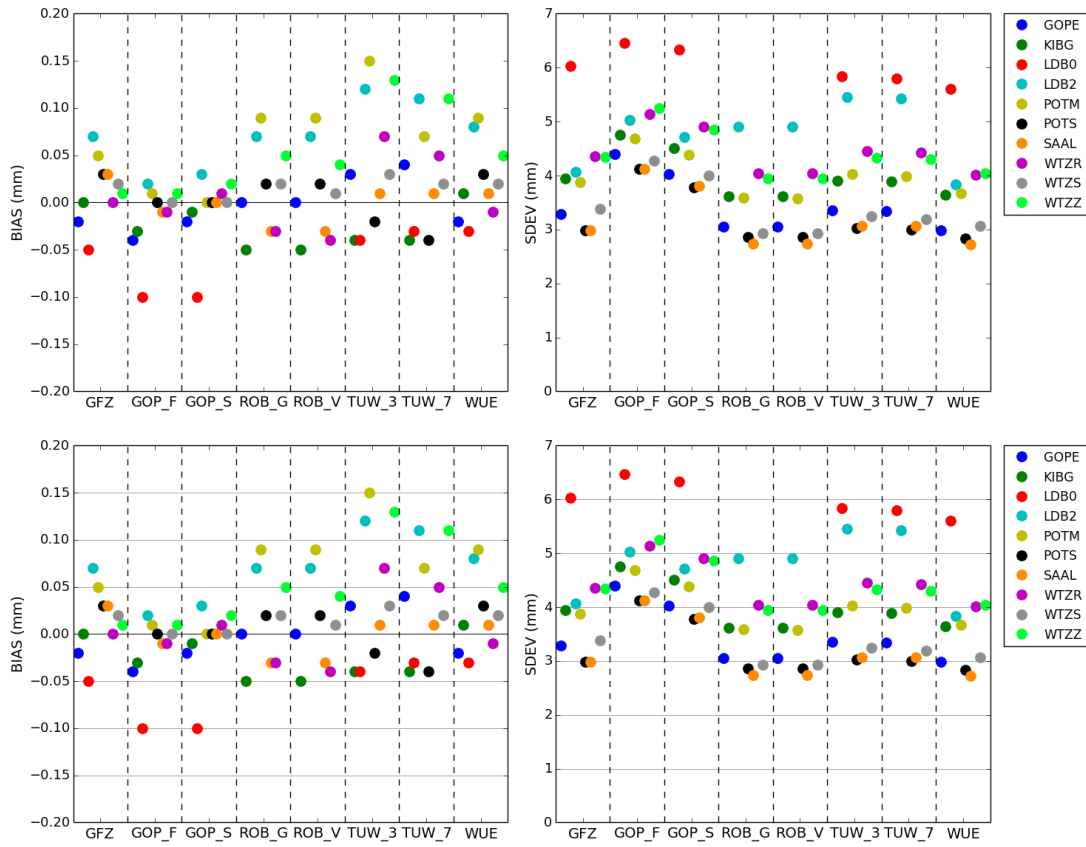


Figure 5: Comparison of individual GNSS STD solutions without residuals (nonRES) and with raw residuals (rawRES); statistics are projected in the zenith direction: bias (left) and standard deviation (right).

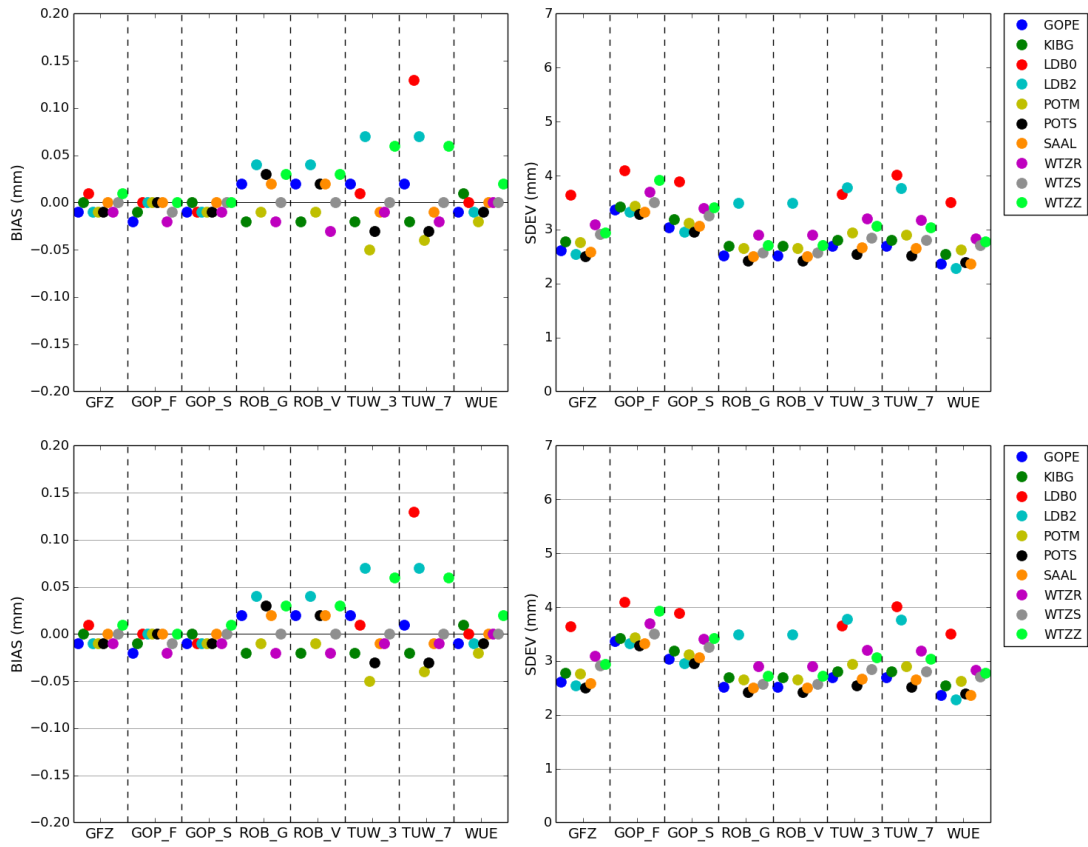


Figure 6: Comparison of individual GNSS STD solutions without residuals (nonRES) and with clean residuals (clnRES); statistics are projected in the zenith direction: bias (left) and standard deviation (right).

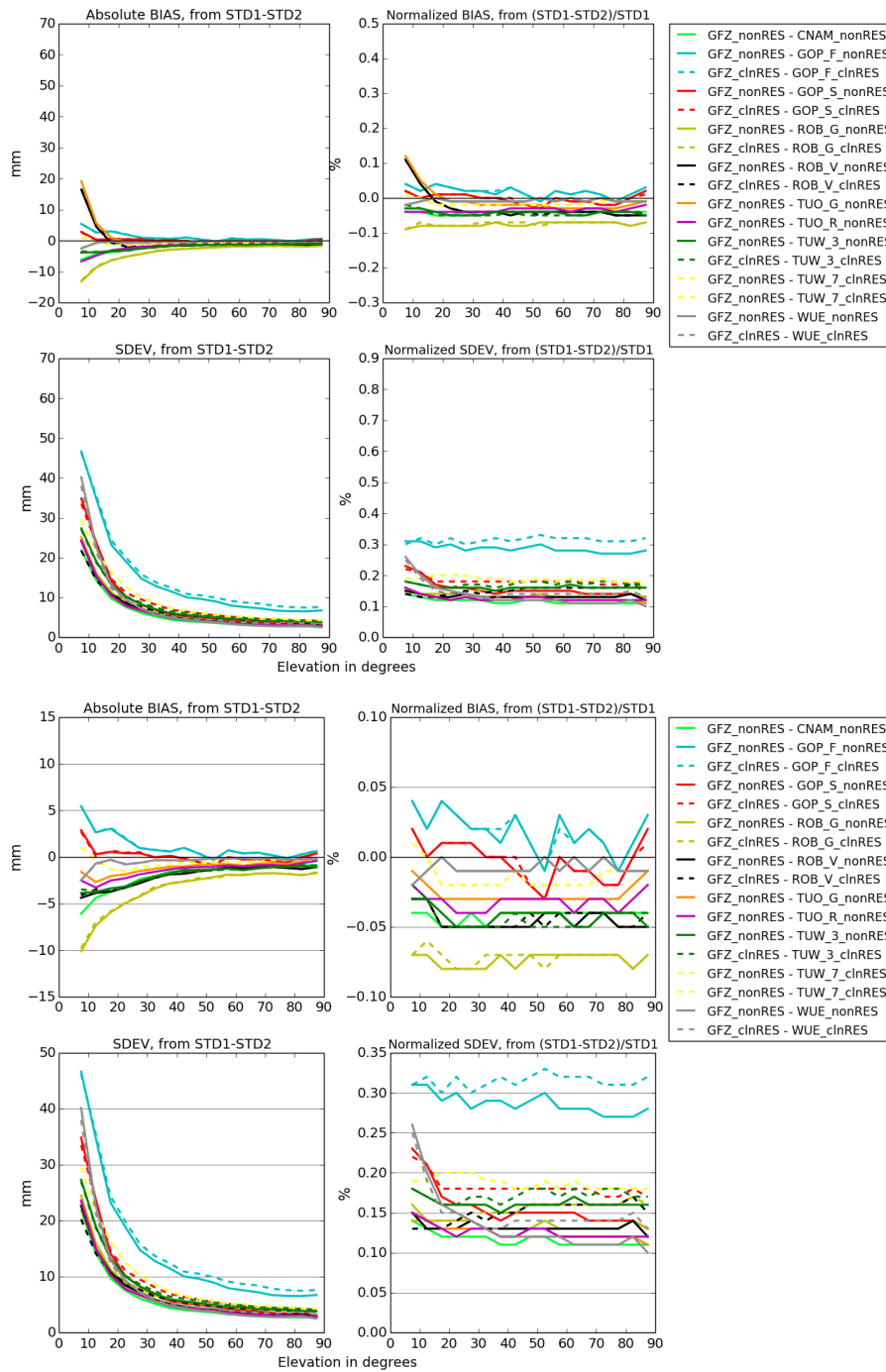
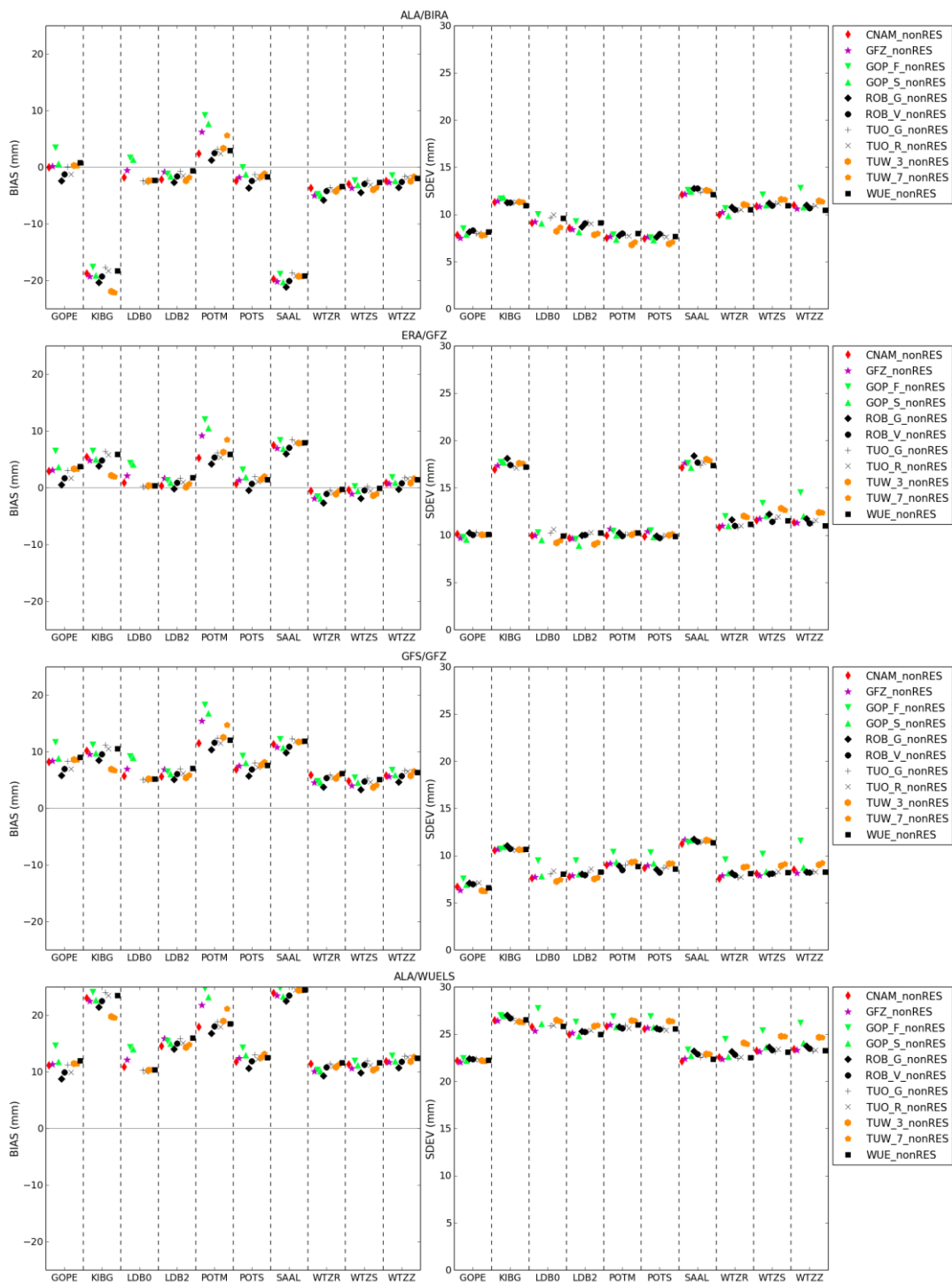
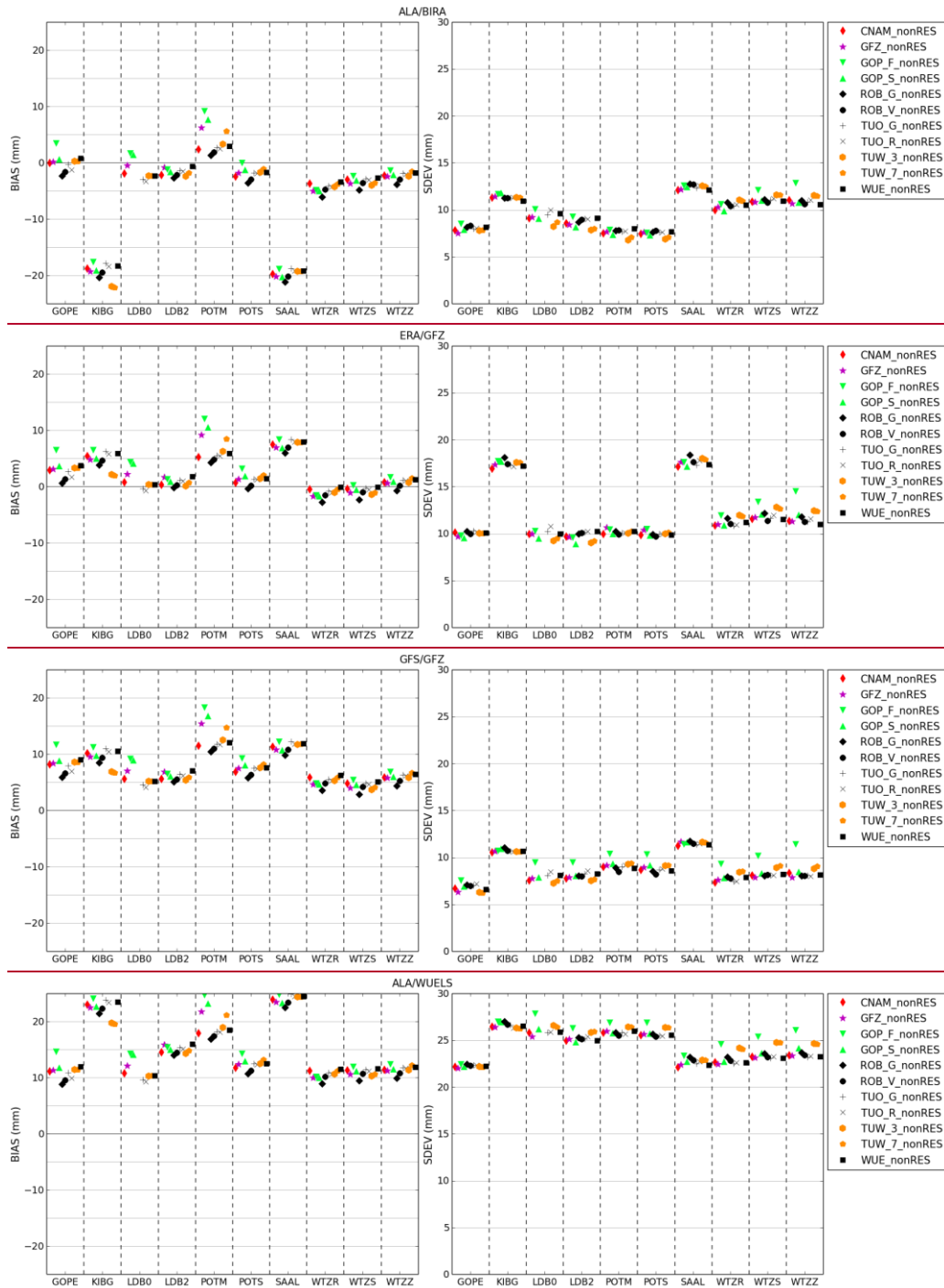


Figure 7: Comparison of individual GNSS STD solutions against GFZ STD solution at station POTS, in slant directions.





5 Figure 8: Comparison of individual GNSS STD solutions without residuals (nonRES) against NWM solutions ALA/BIRA, ERA/GFZ, GFS/GFZ, ALA/WUELS (from top to bottom), projected in the zenith direction: bias (left) and standard deviation (right).

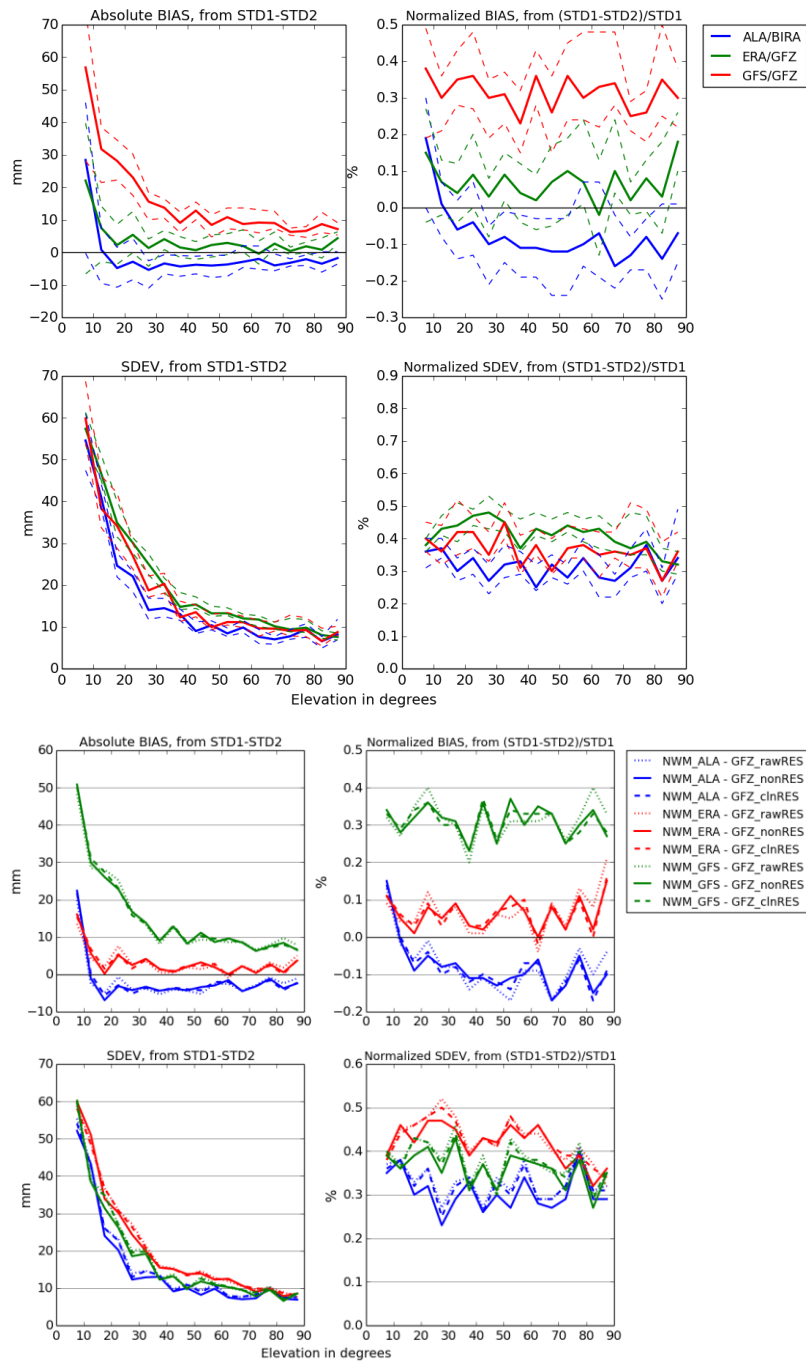


Figure 9: Comparison of NWM-based solutions (ALA/BIRA, ERA/GFZ and GFS/GFZ) against GNSS GFZ solutions at station POTS, in the slant direction; **full line represents a median of all GNSS solutions, dashed lines show minimum/maximum range for GNSS solutions.**

5

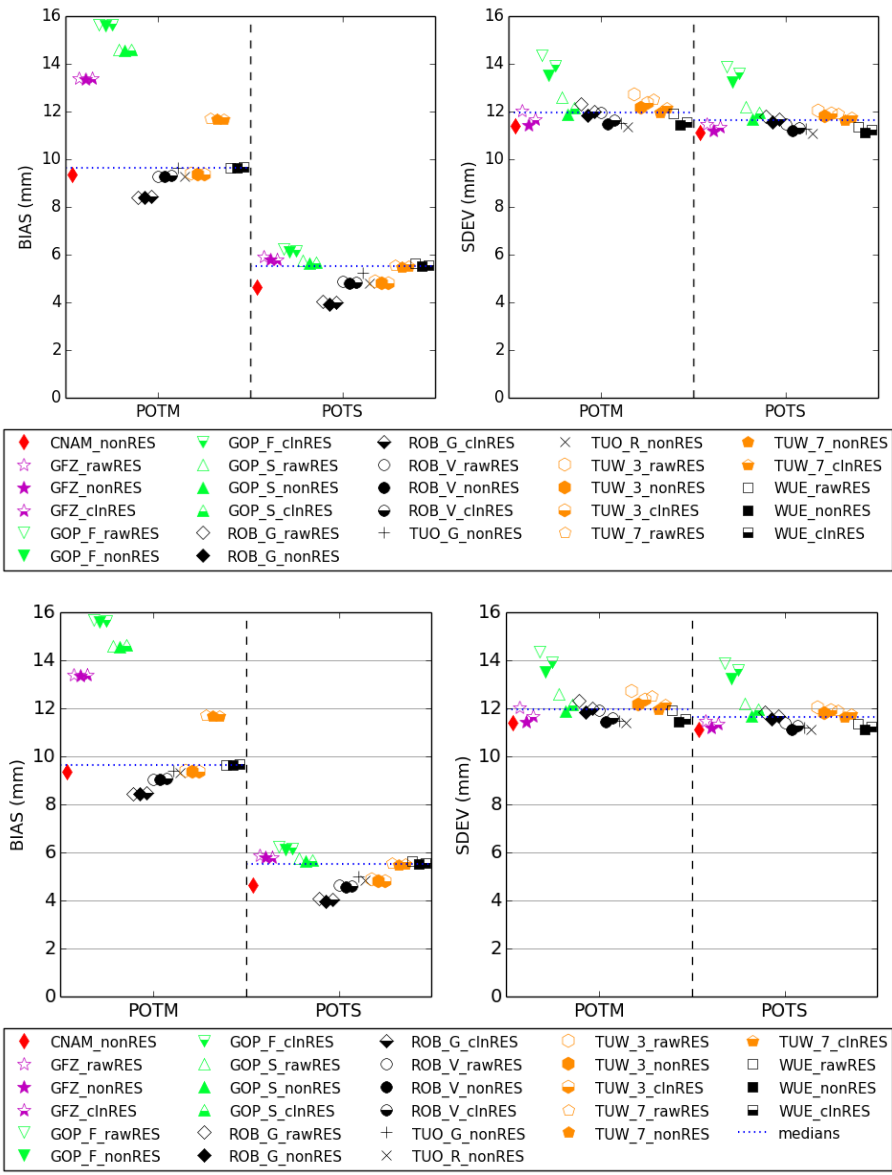


Figure 10: Comparison of individual GNSS STD solutions for stations POTM and POTS versus WVR measurements, expressed in the zenith direction, bias (left) and standard deviation (right). The median value of all solutions at each station is represented by the dotted blue line in each bin.

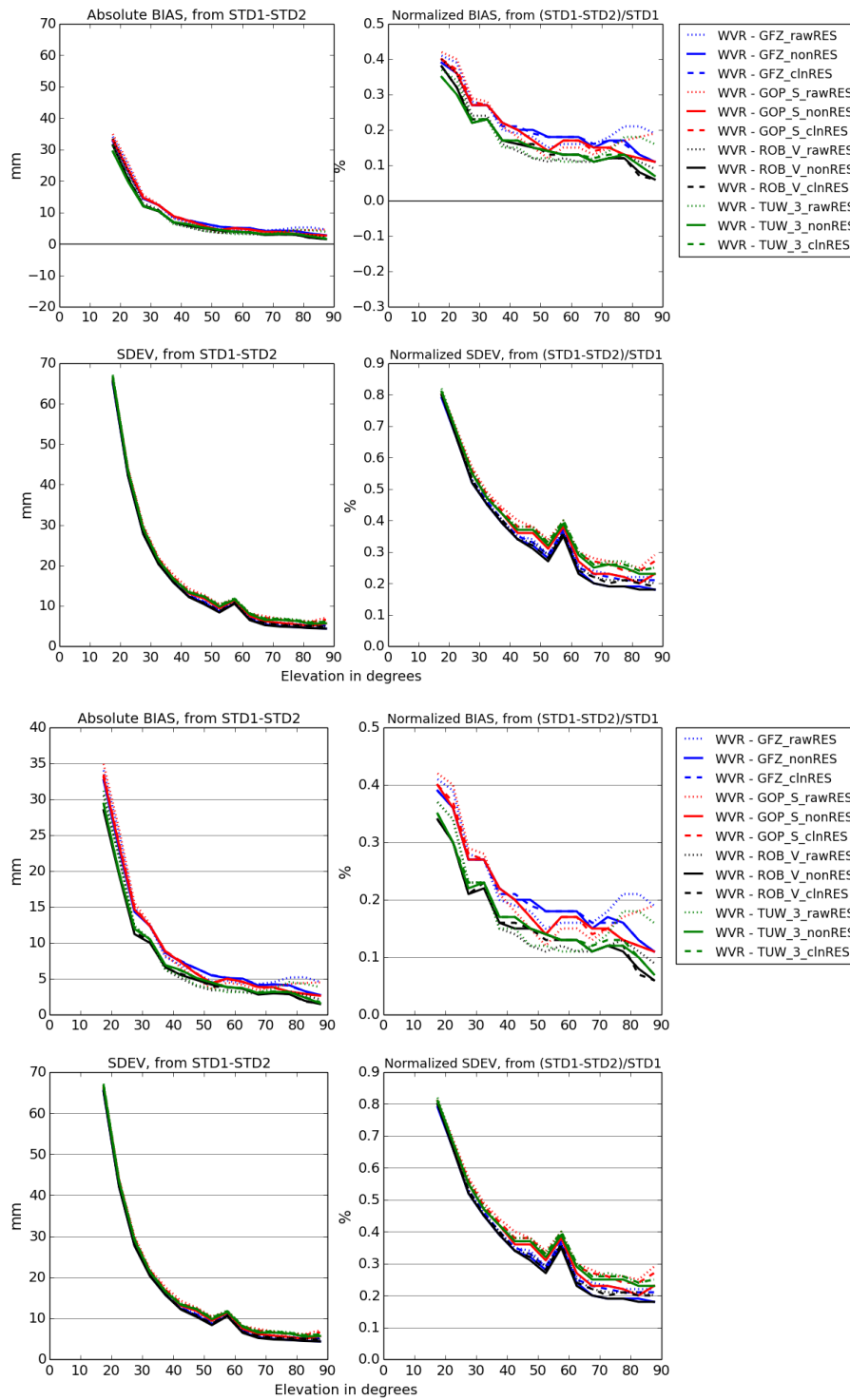
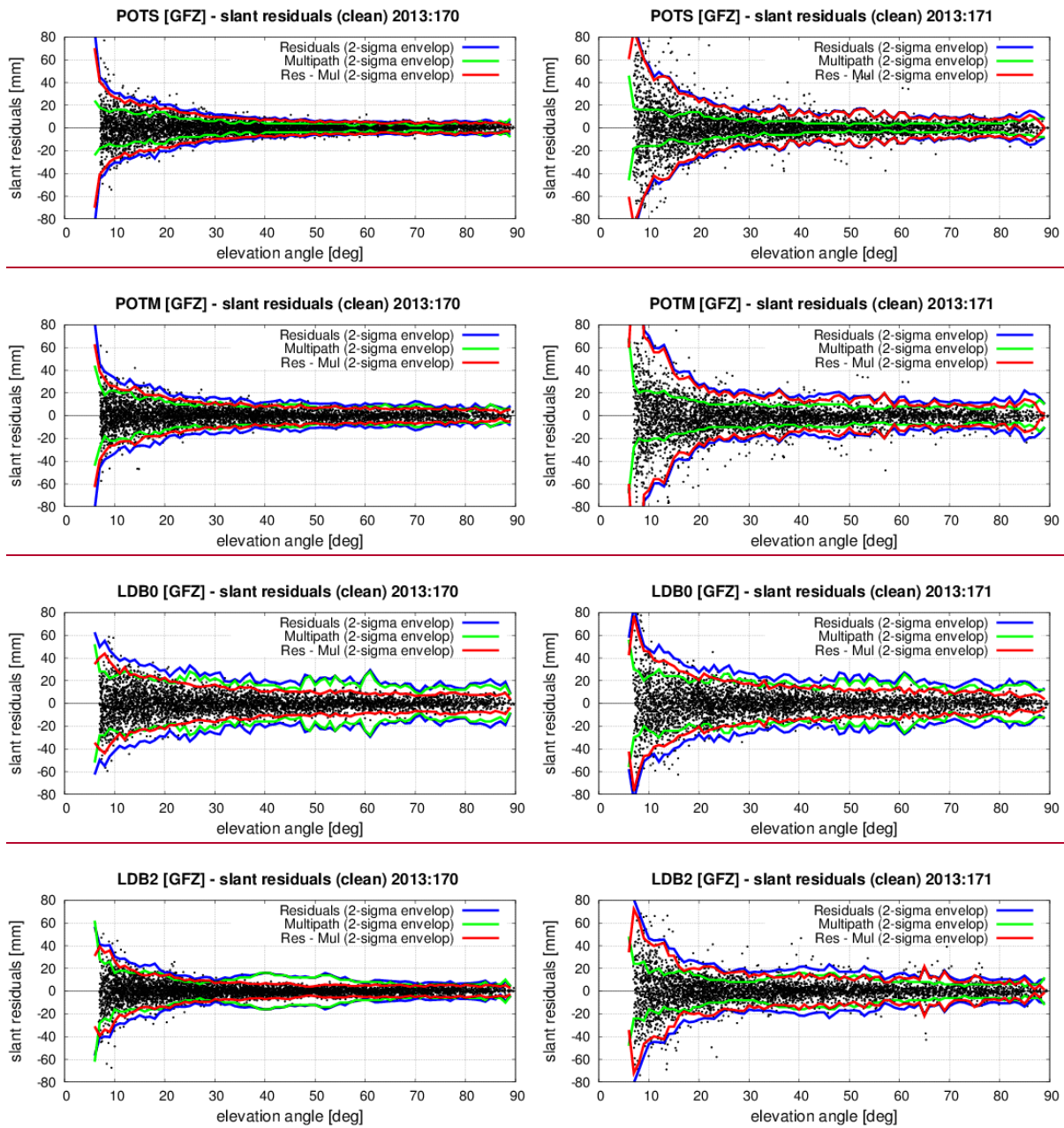


Figure 11: Comparison of WVR against individual GNSS STD solutions at station POTS, in the slant direction.



5 Figure 12: Elevation-dependent variability of clean residuals (black dots) and their 2-sigma envelopes (red curves) are shown for June 19 (DOY 171) and June 20 (DOY 170) and four stations: POTS, POTM, LDB0 and LDB2. Additionally, plots display 2-sigma envelopes for raw residuals (blue curves) and multipath (green curves).

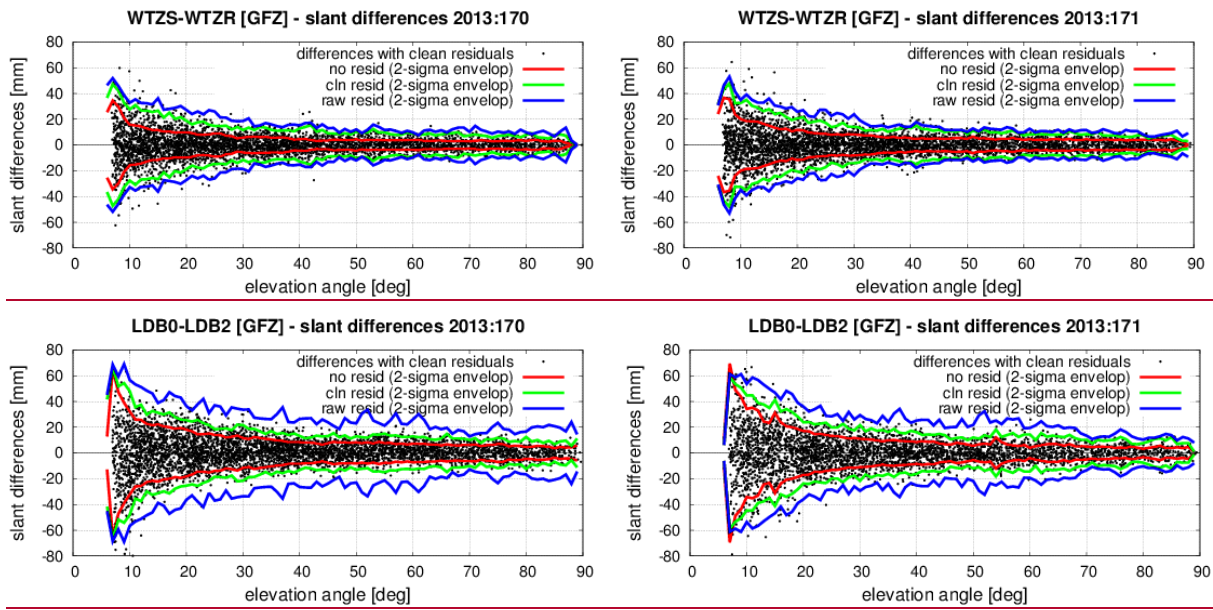


Figure 13: Elevation-dependent variability in STD differences of clean residuals (black dots) and their 2-sigma envelopes (green curves) are showed for June 19 (DOY 171) and June 20 (DOY 170) and two dual-stations: WTZS–WTZR and LDB0–LDB2. Plots also display 2-sigma envelopes for differences of raw residuals (blue curves) and without residuals (red curves).

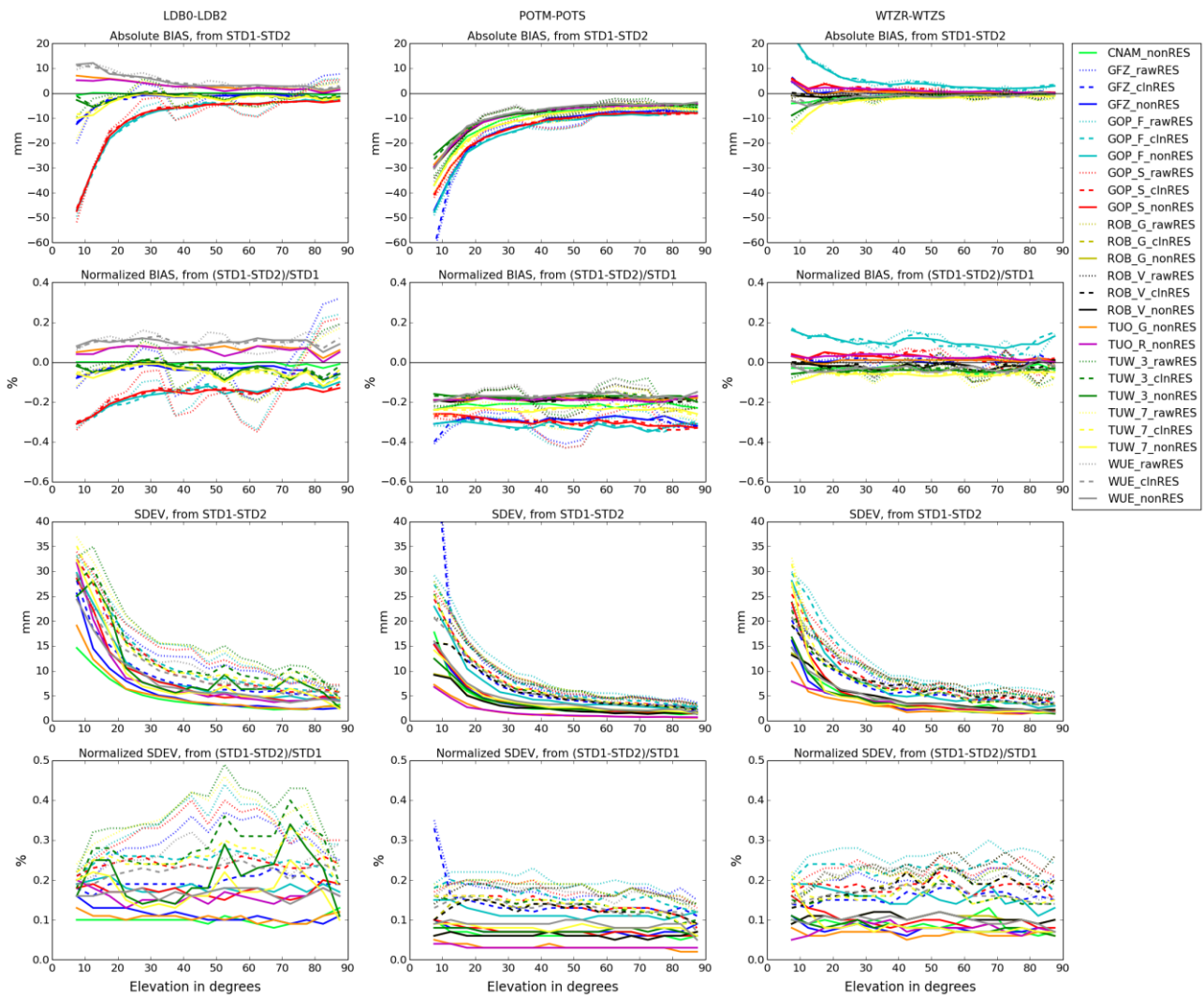


Figure 12: Comparison of GNSS STDs at dual stations from individual GNSS solutions in the slant direction for 'severe weather' days, dual stations from left to right: LDB0-LDB2, POTM-POTS, WTZR-WTZS. Statistical parameters from top to bottom: bias, normalized bias, standard deviation, normalized standard deviation.

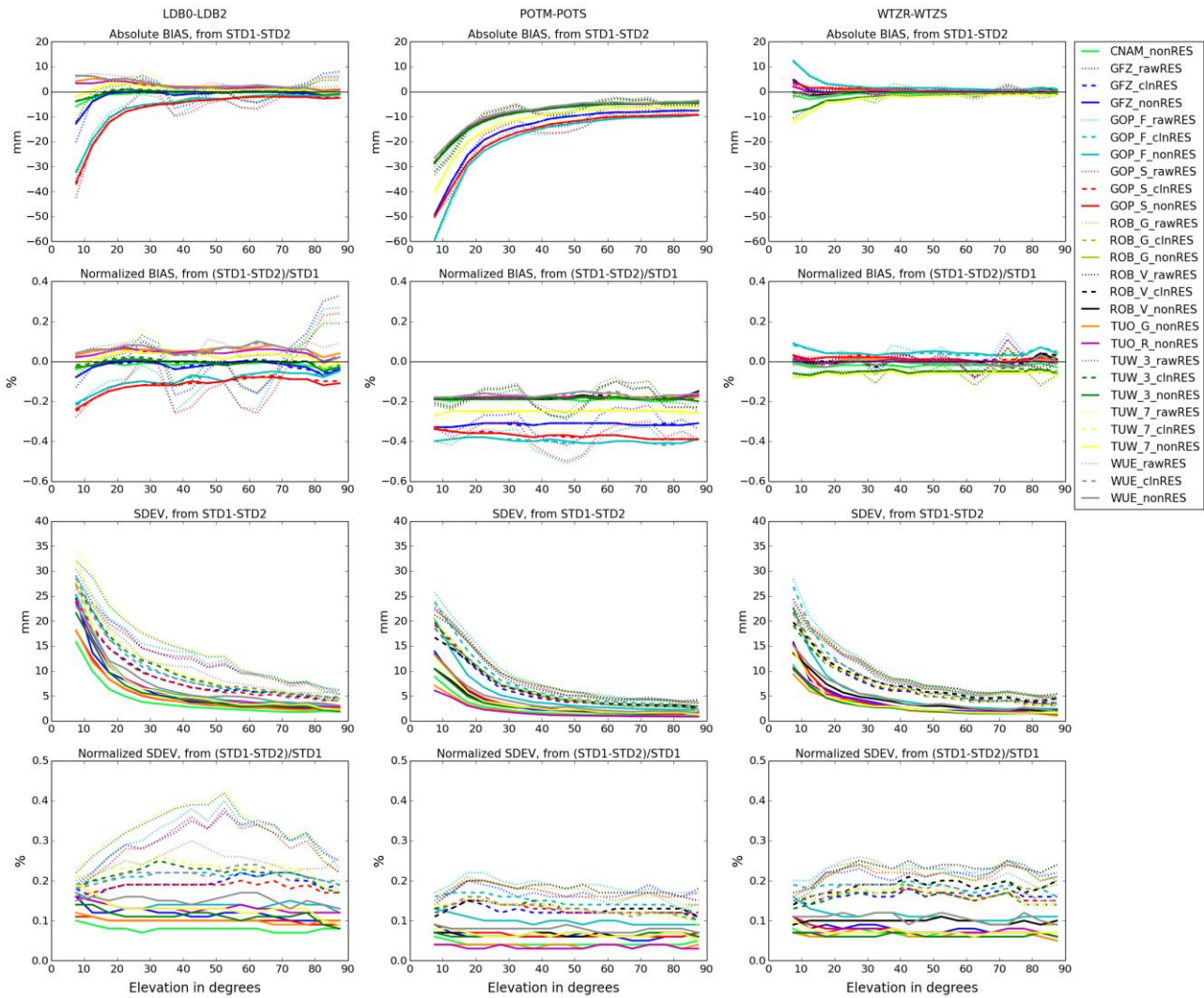


Figure 14: Comparison of GNSS STDs at dual stations computed over whole benchmark period from individual GNSS solutions in the slant direction for dual stations from left to right: LDB0-LDB2, POTM-POTS, WTZR-WTZS. Statistical parameters from top to bottom: bias, normalized bias, standard deviation, normalized standard deviation.